



**LTL-HTL regional model coupling to establish
E2E modeling systems and assessment of the
models skill
Deliverable Nr. 4.4**





Project Full title		Policy-oriented marine Environmental Research in the Southern EUropean Seas	
Project Acronym		PERSEUS	
Grant Agreement No.		287600	
Coordinator		Dr. E. Papathanassiou	
Project start date and duration		1 st January 2012, 48 months	
Project website		www.perseus-net.eu	
Deliverable Nr.	4.4	Deliverable Date	June 2013
Work Package No		4	
Work Package Title		Developing integrated tools for environmental assessment.	
Responsible		Marco Zavatarelli	
Authors & Institutes Acronyms		M. Gregoire, A. Capet (ULG), M. Zavatarelli (CoNISMa-UNIBO) , F. le Loch, C. Albouy (IRD-IFREMER), Claude Estournel (UPS-LA), Javier Ruiz, Laura Prieto, Margarita Rincón, Ignacio Catalán (CSIC), Patricia Reglero (IEO), Libralato S., P. Lazzari , Solidoro C., (OGS) Akoglu E., , Salihoglu B. (METU-IMS) Ballerini T., Banaru D. (UNIVMED) Daskalov G. (IBER-BAS) Kandilarov R. , Staneva J. (DMG-SU) , Tsagarakis K, A.Machias, S.Somarakis, M.Giannoulaki, C. Frangoulis (HCMR)	
Status:		Final (F)	●
		Draft (D)	
		Revised draft (RV)	
Dissemination level:		Public (PU)	●
		Restricted to other program participants (PP)	
		Restricted to a group specified by the consortium (RE)	
		Confidential, only for members of the consortium (CO)	



CONTENTS

ABSTRACT	5
SCOPE.....	5
1. EXECUTIVE SUMMARY	6
2. MAIN DELIVERABLE TEXT (contribution of partners).....	7
2.1 OSMOSE-BFM	7
2.1.1 Description of the tool	7
2.1.2. CASE STUDY : the Adriatic Sea	9
2.2. LAGRANGIAN APPROACHES	16
2.2.1 ICTHYOP.....	16
2.2.1.1 Description of the tool.....	16
2.2.1.2. Case Study: the North-western Mediterranean and the Gulf of Lions.....	16
2.2.2 Particle Tracking.....	23
2.2.2.2 CASE Study: the Catalan Sea	23
2.3 BAYESIAN Approach.....	28
2.3.2 CASE STUDY: The Alboran Sea.....	28
2.4 ECOPATH with ECOSIM	32
2.4.1 Specificity of the tool	33
2.4.1.1 General Approach to E2E modeling with EwE	34
2.4.1.2 Inter-regional comparability.....	35
2.4.1.3 Data requirements	36
2.4.2 Case studies	37
2.4.2.1 Mediterranean basin LTL model	37
2.4.2.2 Adriatic Sea	40
Area description.....	40
Adriatic Sea HTL model.....	41
Extension of the HTL model for the Adriatic E2E model.....	42
2.4.2.3 Gulf of Lions	46
The study area.....	46
Modifications to Ecopath GoL large model to create GoL shelf model	47
Constructing the end-to-end model for the Gulf of Lions	49
GoL shelf mass-balance	49
Results and discussion on the characteristics of the GoL foodweb	50
Structure of the Ecopath GoL shelf model	50
2.4.2.4 Aegean Sea.....	57
North Aegean Sea ecosystem and fisheries	57
Structure of the food web.....	60
Consumption.....	61



PERSEUS Deliverable Nr. 4.4

2.4.2.5 Black Sea global.....	64
2.4.2.6 Black Sea regional	72
2.4.3 A preliminary comparison of “health” indices for Mediterranean areas.....	98



ABSTRACT

Deliverable D4.4 describes the numerical modelling systems assembled and implemented within PERSEUS. The systems are consisting of three main components: 1) a circulation model, 2) a lower trophic level (LTL) model, 3) a higher trophic level (HTL) model. The LTL and HTL components are reciprocally interacting. The following text gives details of each components along with the characteristics of the implementation in the different regional basins that have been selected.

SCOPE

The objective of this modelling effort aimed to couple/link together LTL and HTL models is to achieve the “End to End (E2E)” approach needed to investigate the ecosystem attributes underlying the definition of GES and the MSFD descriptors. With this aim, WP4 develops specific tools, mainly models, in order to reach this E2E approach. In this deliverable, the first tests of coupling between Low Trophic Level (LTL) and High Trophic Level (HTL) models are described.



1. EXECUTIVE SUMMARY

The deliverable has been structured around the different approaches used to assemble and implement the three components modelling systems. For each approach, a description and validation of the LTL models are first presented. Then, the HTL approach is described and tests of coupling LTL-HTL are presented highlighting what has been achieved and the critical points that will deserve further efforts in the following of the project.

Several E2E approach are used.

In the Adriatic Sea (pages 5-13), the two dimensional individual based model (IBM) OSMOSE (Object-oriented Simulator of Marine ecOSystems Exploitation) is used for the 1990s period. The OSMOSE simulations are forced by the vertically integrated contents of 4 planktonic groups provided by a LTL model of the Adriatic Sea. The coupled approach has been used to simulate the fisheries in the Adriatic Sea for the period 1990-2000.

In the Gulf of Lions (pages 14-20), ICHTHYOP (Lett et al., 2008) has been implemented in order to study the trajectories of anchovies. ICHTYOP is a Lagrangian IBM model, coupled with a bioenergetic model. The Gulf of Lions LTL model provides the mesozooplankton, diatoms and microzooplankton abundance to ICHTYOP. Simulations are performed over 2007-2010 and the interannual variability is studied. 2007 and 2008 of enhanced larvae development appear as particular years.

In the Catalan Sea (pages 21-25), the trajectories of bluefin tuna larvae is tracked by advecting larvae in the direction of the geostrophic currents. In this approach the geostrophic current is estimated from the reconstructed gridded field of dynamic height. The comparison of the Lagrangian buoy and the calculated drift trajectories revealed the qualitative good agreement between them.

In the Alboran Sea (pages 25-30), HTL is based on Bayesian methods (Ruiz et al. 2009) where different sources of data can be implemented: environmental records (e.g. kinetic energy, energy of the Atlantic jet and direction of the flow, Ruiz et al., 2013) as covariates and fisheries information for the observational model. The aim is to come with a Bayesian state-space size-structured population dynamics model for anchovy in the Alboran Sea.

ECOPATH with ECOSIM (EwE, pages 30-100) is a mass balanced food web mode, which describe fluxes of mater among an aquatic ecosystem. Food webs EwE models for different subregion of the Mediterranean Sea (Gulf of Lion, Adraitic Sea, Aegean Sea) have been standardized to a common structure, linked to a lower trophic level models (biogeochemical flux model, bfm), and compared. A similar anlysis has been made for the Black Sea.



2. MAIN DELIVERABLE TEXT (contribution of partners)

2.1 OSMOSE-BFM

M. Zavatarelli (CoNISMa-UNIBO), F. le Loch, C. Albouy (IRD-IFREMER)

2.1.1 Description of the tool

The two dimensional individual based model OSMOSE (Object-oriented Simulator of Marine ecOSystems Exploitation) allows to represent in a spatial context all the life cycle of several species and to investigate the dynamics of exploited marine fish communities. The major assumption of this model is the opportunistic and size-based constraint between a predator and its prey (determination of a minimum and a maximum predator to prey size ratio). The basic unit of this IBM is a “super-individual” representing a school of organisms of the same size, in same location and belonging to the same species. These schools interact through opportunistic predation, based on spatio-temporal co-occurrence and size adequacy between a predator and its prey. Because of this opportunism, no *a priori* food-web or diet matrix is set, but they emerge from local trophic interactions. Individual can feed on both plankton and fish according to a feeding size range defined by a maximum and minimum size ratio between a predator and its prey. The model time step was fixed at 15 days and began by the organism spatial distributions, following by the Natural mortality, the predation, the growth, the starvation, the fishing mortality and finally the reproduction process (Figure 1).

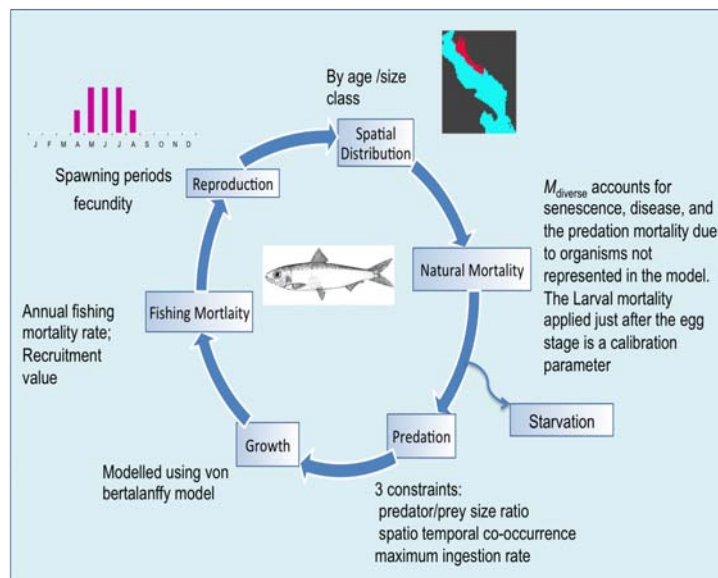


Figure 1. OSMOSE processes during a time step.

The spatial distribution processes in two-dimensional ways, and presence/absence maps provided as input drive the distribution of fish. Schools of species are randomly distributed within the distribution maps computed per species, age and seasons. When the distribution map of the population does not change from one time step to the next, schools move randomly to an adjacent cell of the 2D spatial grid.



The abundance of each school (N_i) is exponentially decreased by a mortality rate M_{nat} corresponding to diseases, senescence, predation by organisms unrepresented in the model (i.e., birds and mammals) (Equation 1).

$$N_{i,t+\Delta t} = N_{i,t} \times e^{-\Delta t \times M_{nat}} \quad (\text{Eq 1})$$

A mortality M_0 is applied to the first stage of fish (corresponding to eggs and first-feeding larvae) in order to take into account the higher mortality undergone compared to other stages.

In OSMOSE the predation is opportunistic and a predator can prey on any organisms present in its own cell provided it displays a suitable size, i.e., comprised between a maximum and minimum size relatively to predator body size. The amount of prey eaten depends on the local relative biomass of prey and on the maximum food edible by the predator. An explicit mortality is applied on prey schools: if enough prey are present the predator feeds upon them uniformly until it reaches satiety, otherwise it depletes all prey available but without reaching satiety. At the end of this process a predation efficiency ξ_i is calculated for each school i as the ratio between the biomass of prey eaten and the maximum food edible.

The predation is considered successful enough to allow growth when the predation efficiency is higher than a critical value ξ_{crit} representing the amount of food required for fulfilling maintenance. In this case, the body size of organisms increases following an adaptation of the von Bertalanffy model. The growth rate in length $\Delta L_{i,t}$ of the school i at time t depends on predation efficiency ξ_i (Equation 2), varying between 0 and twice the mean length increase ΔL calculated from the von Bertalanffy model. The individual weight $W_{i,t}$ is computed from length according to the allometric relationship $W_{i,t} = c L_{i,t}^b$, with b and c two species-specific parameters to be provided in input of the model.

$$\begin{cases} \Delta L_{i,t} = 0 & \text{if } \xi_i < \xi_{crit} \\ \Delta L_{i,t} = \frac{2\Delta L}{1 - \xi_{crit}} (\xi_i - \xi_{crit}) & \text{if } \xi_i > \xi_{crit} \end{cases} \quad (\text{Eq. 2})$$

When the predation efficiency is below the critical value ($\xi_i < \xi_{crit}$), schools have not the food amount required for maintenance and thus undergo a starvation mortality M_ξ , increasing linearly with the decrease of predation efficiency and leading to a decrease of the school abundance (Equation 4).

$$M_\xi = \frac{-M_{\xi_{max}}}{\xi_{crit}} \times \xi_i + M_{\xi_{max}} \quad (\text{Eq. 3})$$

$$N_{i,t+\Delta t} = N_{i,t} \times e^{-\Delta t \times M_\xi} \quad (\text{Eq. 4})$$

The fishing process consists in reducing school abundance by applying a species specific fishing mortality rate F to any school older than a recruitment age specified for each species (Table 3). This mortality is homogeneous spatially but can vary over time following a fishing seasonality provided as input for each species. The amount of fish caught is determined by equation 5.

$$C_{i,t+\Delta t} = N_{i,t} \times (1 - e^{-\Delta t \times F(t)}) \quad (\text{Eq. 5})$$



At the end of the time step, the reproduction process allows to introduce new schools at the egg stage in the model. Following equation 6, the quantity of eggs released $N_{0,t}$ depends on the spawning biomass (with sex-ratio set to 1:1), i.e. the biomass of individuals older than age at maturity (A_{mat}), and the fecundity parameter Φ which varies according to a spawning seasonality provided as input .

$$N_{0,t} = \Phi(t) \times \frac{1}{2} \sum_{a > A_{mat}} A_{a,t} B_{a,t} \quad (\text{Eq. 6})$$

2.1.2. CASE STUDY : the Adriatic Sea

Introduction

The enclosed Adriatic Sea is a very challenging basin for a modelling effort aimed to hindcast and predict (under scenario assumptions) its environmental dynamics.

Its physical and biological oceanographic characteristics shift within a limited space range to truly coastal conditions (northern Adriatic Sea) to almost open ocean conditions (southern Adriatic Sea).

The basin is known to have a large spatial and temporal variability (both seasonal and interannual) depending on its forcing drivers (atmospheric and land based). In addition to that the basin is subject to a strong anthropogenic pressure.

It is therefore quite important to assess both the extent of the changes in the Adriatic Sea in dependence of both the climatic and the (direct) anthropogenic forcing.

Here we describe a numerical modelling system composed by a physical model, a lower trophic level and a higher trophic level models, implemented in the Adriatic Sea. The aim of this effort is to achieve the require “Ecosystem end to end” (E2E) perspective needed to investigate via numerical simulations the ecosystem properties underlying the marine ecosystem states relevant to the MSFD descriptors as required by the PERSEUS Project objectives.

The Adriatic E2E modelling system

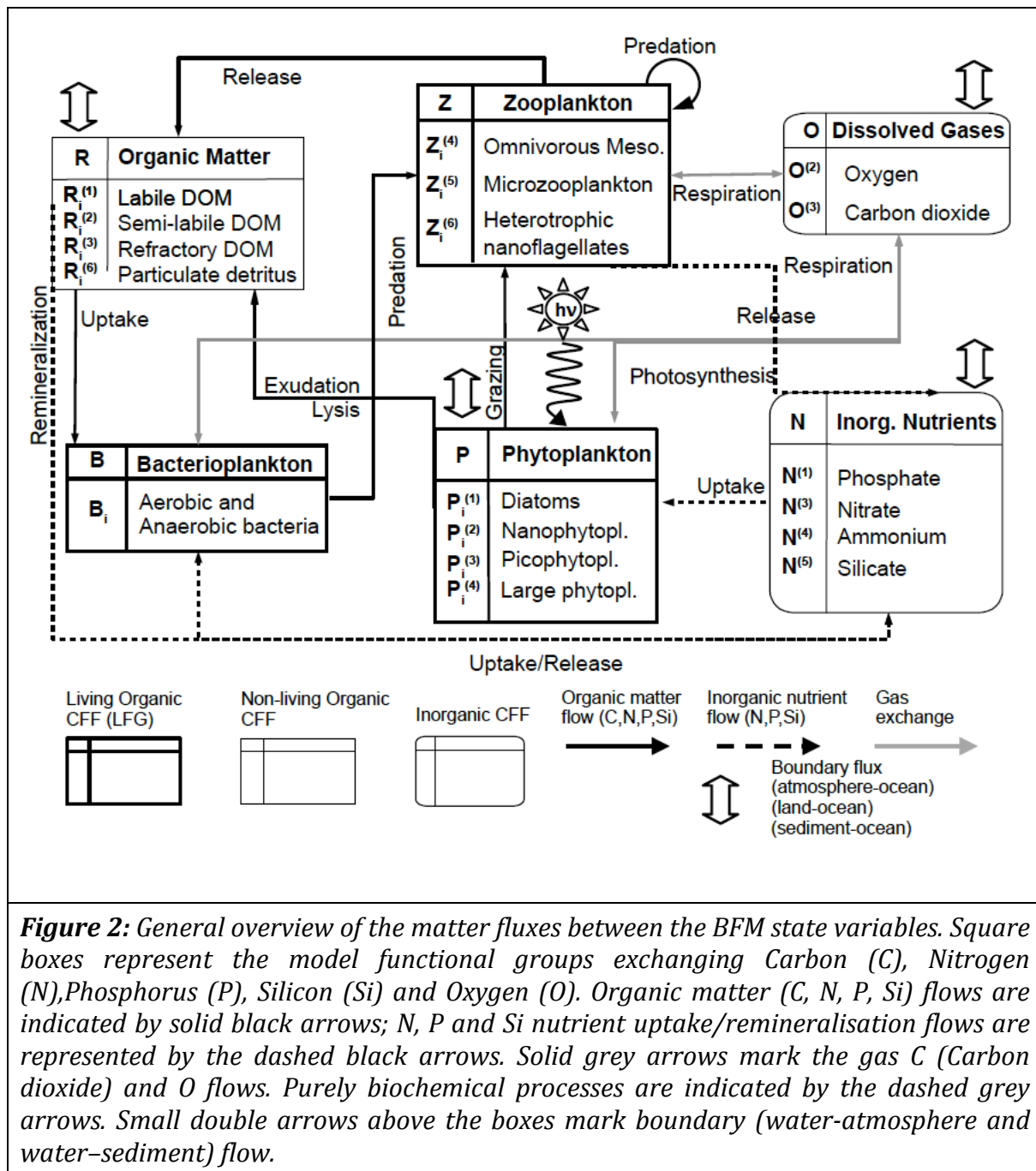
In the following the components of the E2E modelling system are described along with the characteristic of the coupling and of the external forcing.

The coupled Physical-LTL model

The Physical and the LTL biogeochemical model are directly on-line coupled.

The physical model providing the circulation dynamics is constituted by the Princeton Ocean Model , POM (Blumberg and Mellor, 1987). POM is a free surface, finite difference, sigma coordinate general circulation model. It prognostically calculates surface elevation, velocity, temperature, salinity and horizontal and vertical diffusion coefficients; the horizontal diffusion is calculated by a Smagorinsky (Mellor and Blumberg, 1986) formulation, while the vertical diffusion is calculated by the Mellor and Yamada (1982) second order turbulence closure. Previous Adriatic Sea implementations were carried out by Zavatarelli et al. (2002), Zavatarelli and Pinardi (2003) and Oddo et al. (2005).

The LTL Biogeochemical model on-line coupled to POM is the Biogeochemical Flux Model, BFM (Vichi et al., 2007).



BFM (Figure 2) is a biomass and functional group based marine ecosystem model representing the system in Eulerian coordinates by a selection of chemical and biological processes that simulates the pelagic (water column) dynamics in the marine ecosystem. The carbon, nitrogen, phosphorus and silicon biogeochemical cycles are solved independently over a variety of living and non living functional groups (phytoplankton, micro- and mesozooplankton, bacteria, particulate and dissolved organic matter, inorganic nutrients). At the water sediment interface, a simple benthic closure model was applied, that returns a fixed quota of deposited organic matter as nutrients to the water column to parametrise benthic remineralisation.



POM and BFM model are directly on-line coupled utilizing the source splitting coupling method, inserting the biogeochemical rates into the transport tracer integration (Butenschön et al., 2012).

Previous 3d and 1d Adriatic Sea implementations of the POM-BFM modelling system were carried out by Polimene et al (2006, 2007), Butenschön et al. (2012) and Butenschön and Zavatarelli (2012).

LTL-HTL coupling

OSMOSE has been applied to the Adriatic ecosystem for the 1990s period. We selected 11 species of a commercial interest or those that play a key role in the structure of the ecosystem (Table1). Indeed the plankton model used for the coupling only considers copepods as large zooplankton, but euphausiids have been shown to be a major trophic link in ecosystem. The species considered are now composed of one crustacean group: euphausiids (represented by *Euphausia lucens*) and 10 fish species: European pilchard (*Sardina pilchardus*), Round sardinella (*Sardinella aurita*), European anchovy (*Engraulis encrasicolus*), Horse mackerel (*Trachurus trachurus*), Mackerel (*Scomber scombrus*), Chub mackerel (*Scomber japonicus*), Atlantic bonito (*Sarda sarda*), Hake (*Merluccius merluccius*), European sprat (*Sprattus sprattus*), Blue whiting (*Micromesistius poutassou*).

The POM-BFM coupled modelling system served to force an Adriatic OSMOSE model. In order to force this IBM we selected 4 planktonic groups (Diatoms, Dinoflagellates, Micro-zooplankton, Omnivorous meso-zooplankton) that their size allows to be eaten by fish larvae (Fugure 3). We interpolate the 3-dimension data of POM-BFM for these 4 groups along the water column and we obtained a 2-dimension information. Plankton biomass was vertically integrated from 0 meter to 100 meters. Currently the OSMOSE-POM-BFM model works but it suffers of a lack of calibration data that can allow us to produce realistic simulations.

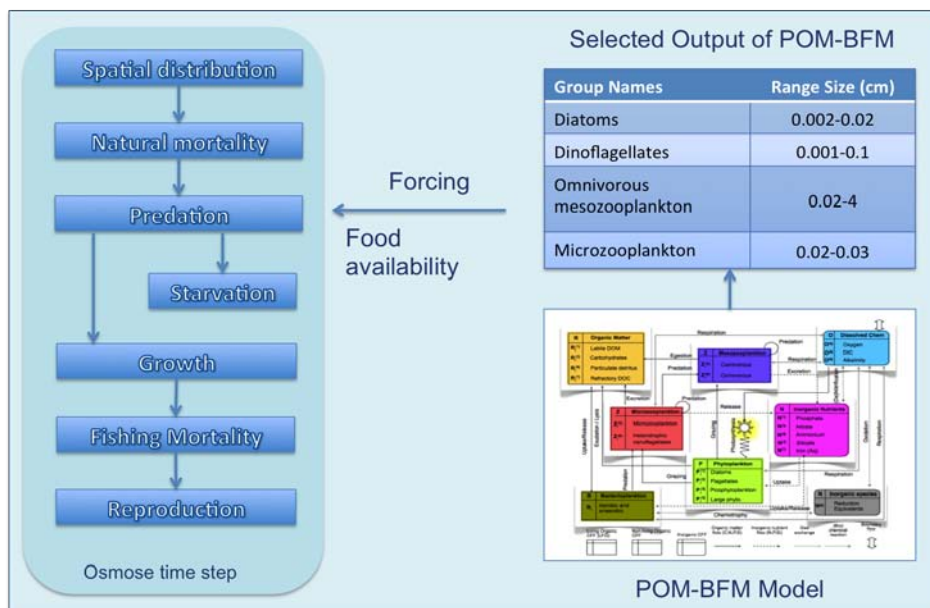


Figure 3: Principle of the forcing between OSMOSE and POM-BFM . At each time step (t) and at each location (x,y), the biomass of phytoplankton and zooplankton is used in OSMOSE for the predation process



The forcing model is considered to be calibrating when species biomasses reach mean values observed in the Adriatic during the 1990-2000 period. To do so, we use a genetic algorithm method applied to a set of 13 unknown parameters, constituted by the 9 larval mortalities (M0) of Adriatic species and 4 availability coefficients for plankton groups. The reference biomasses of HTLs species are associated with valid intervals (within which biomass value is considered acceptable) accounting for variability and uncertainty of biomass estimates over the modelled period

The genetic algorithms method aims at selecting the best set of unknown parameters (called genotype) which allows the simulated biomasses (called phenotype) to be the closest possible to reference biomasses. Based on the Darwinian theory of evolution, this method uses the principles of reproduction (crossover and mutation) and adaptive selection of the best genotypes over the generations. This modelling step is still under evaluation but the last results of the calibration are presented in Figure 4. We are not so far to the equilibrium point but one or two species need to be adjusted especially the hake.

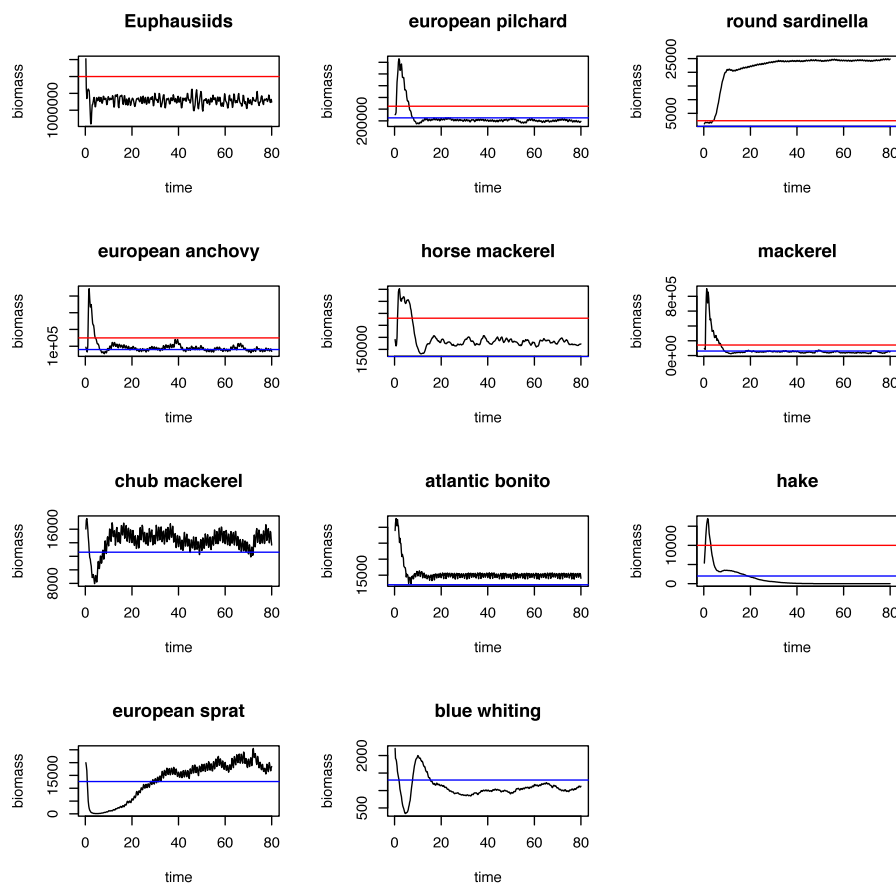


Figure 4. Species Biomass evolution for the Adriatic model in function of time. The red line corresponds to the maximum biomass observed the blue line represents the minimum observed in the Adriatic during the 1990-2000 period.

Model Validation

The coupled POM-BFM system simulations have been objectively validated for



predicted SST and Surface chlorophyll concentrations by comparing with the remotely sensed AVHRR 1985-2007 SST and the SeaWifs 1998-2010 surface pigment concentration. The objective validation has been carried out by compiling Taylor diagrams target plots, model efficiency and reliability index (Jolliff et al., 2009; Stow et al., 2009), at the yearly average time resolution.

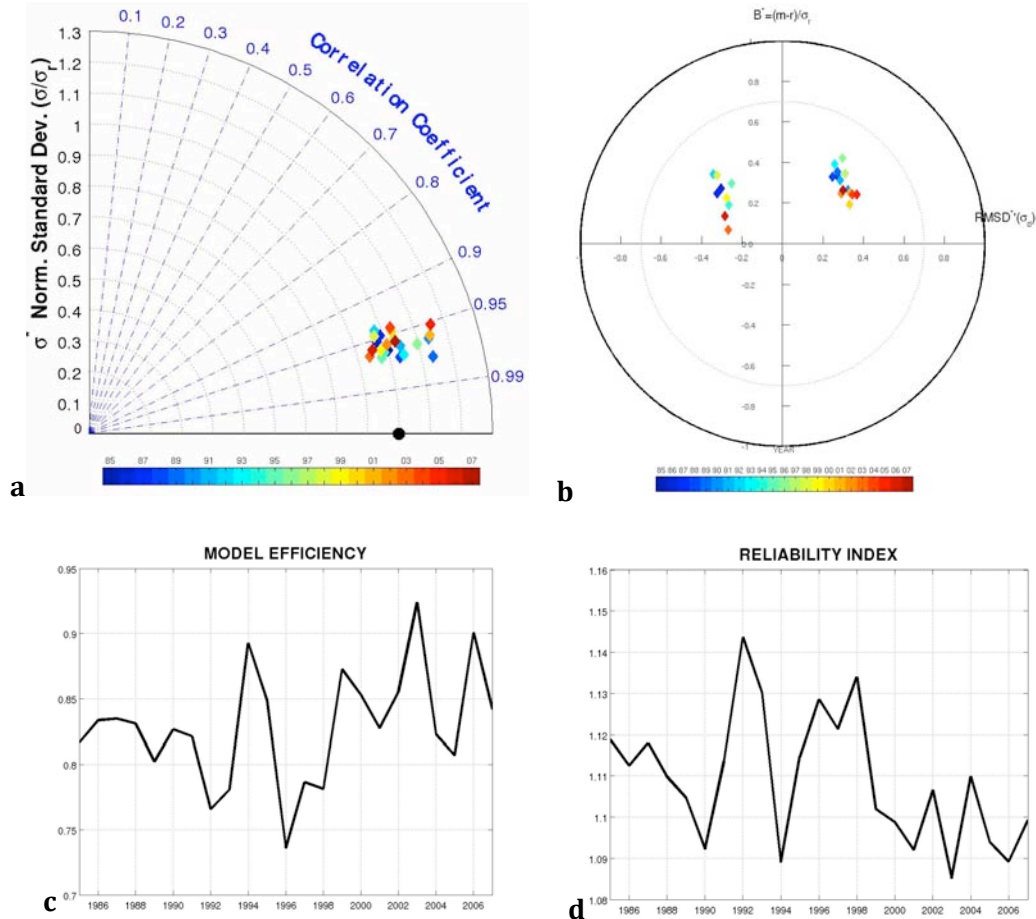


Figure 5: Sea Surface temperature: assessment of the model simulation quality against the 1985-2007 AVHRR observations. a. Taylor Diagram; b. Target plot; c. Model efficiency index. d. Model reliability index.

Figure 5 shows the SST Taylor diagram, the Target plot and the annual values of the Model efficiency and the model reliability indexes computed to obtain an objective assessment of the model simulation quality. The Taylor diagram (Figure 5a) indicates that the model results are highly correlated with the observation and also show a good level of agreement between the observed and the modelled variability. The target plots (Figure 5b) indicates that on the annual scale the model bias and the model RMSD (both normalised by the observation standard deviation) have a value lower than 1, therefore indicating that the model hindcasted fields are better descriptors than the average of the observations. The model efficiency (Nash-Sutcliffe, Figure 5c) index indicates, for each simulated year a value that allows the simulations to be defined as “excellent”. Finally the reliability index (multiplicative factor through which the model predict observation) of Figure 5d, has a value that, through the years varies around the value of 1.09-1.114. This indicates a certain



disagreement between the model and the observations.

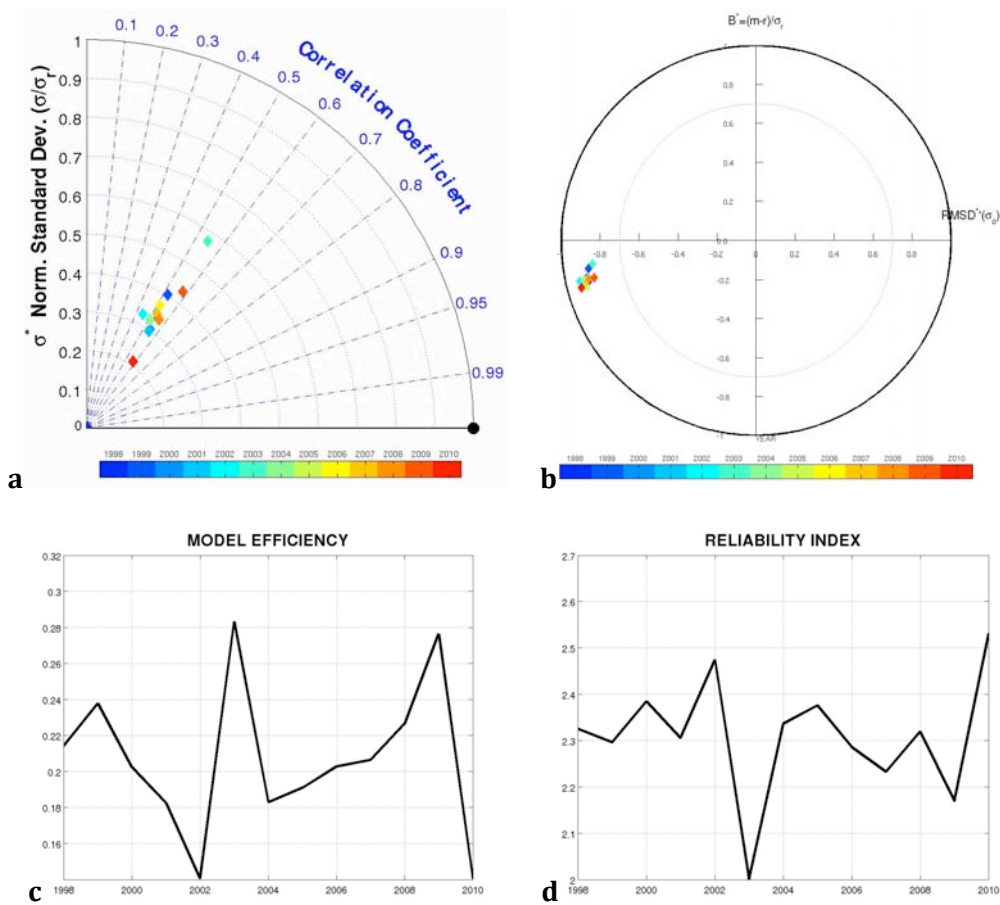


Figure 6: Sea Surface Chlorophyll: assessment of the model simulation quality against the 1998-2010 SeaWiFS surface pigments observations. a. Taylor Diagram; b. Target plot; c. Model efficiency index. d. Model reliability index.

Figure 6 reports the Sea surface chlorophyll Taylor diagram, the Target plot and the annual values of the Model efficiency and the model reliability indexes computed to obtain an objective assessment of the model simulation quality. The Taylor diagram (Figure 6a), report a correlation between hindcasted and simulated data ranging between 0.5 and 0.6 and a modelled variability basically lower than that characterising the observations.

The target plots (Figure 6b) indicates that on the annual scale the model bias and the model RMSD (both normalised by the observation standard deviation) have a value of about 1.09-1.14, therefore indicating that the model hindcasted fields are better descriptors than the average of the observations however, the quality of the chlorophyll predictions is lower than the corresponding SST simulations. This is confirmed also by the model efficiency (Nash-Sutcliffe, Figure 6d) index that achieves lower values than those achieved by the SST validation. However values above zero still indicate a certain model skill. In particular values higher the 0.2 occurring after 2003 and onward, allow to define. Finally the reliability index (multiplicative factor



trough which the model predict observation) of Figure 3d, varying between 2.0 and 2.5 define the disagreement between the modelled and the observed values.

References

- Blumberg, A. F. and Mellor, G. L.: A description of a three-dimensional coastal ocean circulation model. In: Three-dimensional coastal ocean models, (Ed) Heaps, N. S., AGU, 1-16, 1987.
- Butenschön M., Zavatarelli M., Vichi M.: Sensitivity of a marine coupled physical biogeochemical model to time resolution, integration scheme and time splitting method. *Ocean Modelling*, 52-53, 36-53, Doi: 10.1016/j.ocemod.2012.04.008, 2012.
- Butenschön M., Zavatarelli M.: A comparison of different versions of the SEEK Filter for assimilation of biogeochemical data in numerical models of marine ecosystem dynamics. *Ocean Modelling* 54-55, 37-54. 1Doi: 0.1016/j.ocemod.2012.06.003, 2012.
- Duboz, R., Versmisse, D., Travers, M., Ramat, E. & Shin, Y.-J. 2010. Application of an evolutionary algorithm to the inverse parameter estimation of an individual-based model. *Ecological Modelling*, **221**, 840-849.
- Jolliff J.K., Kindle J.C., Shulman I, Penta B., Friedrichs M.A.M. , Helber R., Arnone R.A.: Summary diagrams for coupled hydrodynamic-ecosystem model skill assessment. *Journal of Marine Systems*, 76, 64-82, doi: 10.1016/j.jmarsys.2008.05.0142009, 2009.
- Mellor, G. L. and Blumberg, G.: Modeling vertical and horizontal diffusivities with a sigma coordinate system, *Mon. Weather Rev.*, 113, 1279-1383, 1986.
- Mellor, G. L. and Yamada, T.: Development of a turbulence closure submodel for geophysical fluid problems, *Rev. Geophys. Space Phys.*, 20, 851-875, 1982.
- Polimene, L., N. Pinardi, M. Zavatarelli, and S. Colella: The Adriatic Sea ecosystem seasonal cycle: Validation of a three-dimensional numerical model, *J. Geophys. Res.*, 111, C03S19, doi:10.1029/2005JC003260, 2006.
- Polimene, L., N. Pinardi, M. Zavatarelli, J. I. Allen, M. Giani, and M. Vichi: A numerical simulation study of dissolved organic carbon accumulation in the northern Adriatic Sea, *J. Geophys. Res.*, 112, C03S20, doi:10.1029/2006JC003529, 2007.
- Shin, Y.J. & Cury, P. 2001. Exploring fish community dynamics through size-dependent trophic interactions using a spatialized individual-based model. *Aquatic Living Resources*, **14**, 65-80.
- Shin, Y.J. & Cury, P. 2004. Using an individual-based model of fish assemblages to study the response of size spectra to changes in fishing. *Canadian Journal of Fisheries and Aquatic Sciences*, **61**, 414-431.
- Stow C.A., Jolliff J., McGillicuddy Jr. D.J., Doney S.C., Allen J.I. Friedrichs M.A.M., Rose K.A., Wallhead P.: Skill assessment for coupled biological/physical models of marine systems. *Journal of Marine Systems* 76 4-15, doi: 10.1016/j.jmarsys.2008.03.011, 2009.
- Travers, M. & Shin, Y.J. 2010. Spatio-temporal variability in fish-induced predation mortality on plankton: A simulation approach using a coupled trophic model of the Benguela ecosystem. *Progress in Oceanography*, **84**, 118-120.



Vichi, M., Pinardi, N., Masina, S.: A generalized model of pelagic biogeochemistry for the global ocean ecosystem Part I: Theory. *J. Marine Syst.* 64, (1–4), 89–109, 2007.

2.2. LAGRANGIAN APPROACHES

2.2.1 ICHTYOP

(UPS-LA, Claude Estournel)

2.2.1.1 Description of the tool

ICHTHYOP (Lett et al., 2008) is a free Java tool which has been developed to study how physical (e.g., ocean currents, temperature) and biological (e.g., growth, mortality, larval behaviour) factors affect the spatial and temporal dynamics of ichthyoplankton. The tool uses time series of velocity, temperature and salinity fields archived from oceanic simulations from hydrodynamic models. The larval drift model simulates the following processes that affect individual eggs and larvae: horizontal advection, vertical advection, horizontal dispersion, vertical dispersion, egg buoyancy and larval vertical migration.

2.2.1.2. Case Study: the North-western Mediterranean and the Gulf of Lions

The Gulf of Lions is one of the main spawning areas for European anchovy in the Mediterranean Sea (Garcia and Palomera, 1996). Both temperature and primary production follow annual cycles characterized by strong seasonality. Annual anchovy biomass estimates in the Gulf of Lions have ranged between 19,000 and 118,000 metric tons (PELMED surveys data). The size and structure of stocks have recently shifted with its biomass declining 3-fold since 2001 and its 2009-2011 age-structure dominated by small and young individuals (Palomera et al., 2009; Roos et al., 2011). Our objective here is to understand if and how the environmental conditions can impact this variability.

Our numerical domain is presented in Figure 7. It is a large domain to get the open boundary conditions (especially for the biogeochemical model) far from our place of interest. It will also allow to better understand the connectivity between the different regions of the western basin for transport of larvae. We use a curvilinear grid with a numeric pole to the west of the Gulf of Lion. The horizontal resolution is about 700 m in the west of the Gulf of Lions. It increases to reach 5 km at the outer boundary.

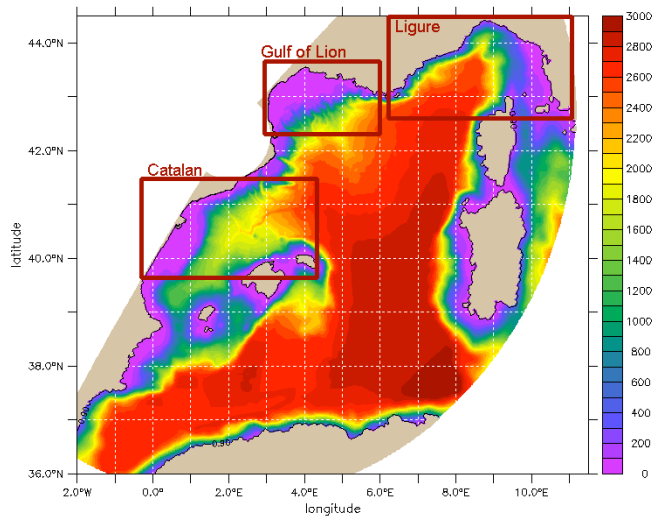


Figure 7: Numerical domain and its bathymetry. The three release areas considered in the following are indicated

The different parts of the HTL-LTL model are described in the following sections. First results are then presented.

Hydrodynamic model

S (or SYMPHONIE) is a Boussinesq hydrostatic ocean circulation model developed by the SIROCCO group. Momentums and tracers are computed on an Arakawa curvilinear C-grid using an energy conserving finite difference method described in Marsaleix et al. (2008). The time stepping method consists of a Leap Frog scheme combined to a Laplacian filter (Marsaleix et al, 2012). A generalized terrain following coordinate preserves the vertical resolution within the bottom boundary layer and ensures the continuity of the fields near the bottom boundary. On the other hand, the well known "sigma coordinate errors" reported in Auclair et al (2000) have been reduced through the use of a suitable pressure gradient scheme (Marsaleix et al, 2009, 2011). Radiative conditions are applied at the lateral open boundaries (Marsaleix et al, 2006).

Biogeochemical model

The biogeochemical model ECO3M-S was previously used to study the Gulf of Lions' pelagic ecosystems impacted by freshwater discharge (Auger et al., 2011) and the pelagic ecosystem dynamics in the offshore areas of the NW Mediterranean basin (Auger et al., submitted). This ecosystem model was built to represent the ecosystem dynamics complexity of the North-Western Mediterranean Sea and includes 34 state variables. This model can be considered as a multi-nutrient and multi-plankton functional types model since the biogeochemical cycle dynamics of several biogenic elements (carbon, nitrogen, phosphorus and silica) and several pelagic plankton groups are simulated.

Three compartments of autotrophs from the smallest to the largest are accounted for: (1) pico- autotrophs, mainly *Synechococcus* (0.7-2 μm), (2) nanophytoplankton (2-20 μm) that dominate the biomass of phytoplankton assemblages for most of the year, this compartment is an assemblage of heterogeneous taxonomic composition (for example autotrophic dinoflagellates) and (3) microphytoplankton community (20-200 μm) largely dominated by phytoplankton silicifiers (mainly diatoms).



Four compartments of heterotrophs from the smallest to the largest ones are considered: (1) picoheterotrophs (mainly bacteria, 0.3-1 μm) that remineralize dissolved organic matter and can compete, in some special circumstances with small phytoplanktons for inorganic nutrients, (2) nanozooplankton (5-20 μm , mainly bacterivorous flagellates and small ciliates) that consume the small phytoplankton group (<2 μm) and bacteria, (3) microzooplankton (20-200 μm , mainly most of ciliates groups and large flagellates) having characteristics (growth, ingestion rates...) close to the previous group but their preys spectrum being wider especially with potential consumption of microphytoplankton, and (4) mesozooplankton (>200 μm , mainly copepod groups but also including amphipods) grazing on the largest categories of plankton (>20 μm , microphytoplankton and microzooplankton) and producing fast-sinking fecal pellets.

Four dissolved inorganic nutrients are considered. For nitrogen, nitrate and ammonium are distinguished owing to their distinct roles in the functioning of pelagic ecosystem (new vs. regenerated production). Dissolved inorganic phosphorus considered as phosphate plays an important role in the control of the primary productivity at some periods of the year. Silicate is also considered as it can punctually (e.g. at the end of bloom) limit the diatoms growth. Dissolved organic matter (DOM, under the forms of C, N and P) is considered in the model as it is consumed by heterotrophic bacteria and for its importance in exported production (e.g. process of seasonal accumulation) in the NW Mediterranean Sea. Particulate organic matter (POM, under the forms of C, N, P, Si and chlorophyll) is divided in two size classes (small and large) differentiated by their sinking velocity.

LTL model Implementation

The hydrodynamic model is initialized and forced at its boundaries by the Mediterranean basin model NEMOMED8 described in Herrmann et al., 2010. We use the same atmospheric forcing than this model i.e the ARPERA dataset (Herrmann and Somot, 2008) which is a dynamic downscaling of the ERA40 climate model reanalysis (1976-2001) and of the ECMWF (European Centre for Medium-Range Weather Forecasts) model reanalysis since 2001. Herrmann et al. (2010) showed that NEMOMED8 (10 km) forced by ARPERA (50 km) is able to reproduce a realistic interannual variability of the Western Mediterranean Deep Water formation.

Our 3D high-resolution hydrodynamic model was run from 1993 to 2011. The atmospheric forcing used pre-calculated fluxes from ARPERA model. This approach which differs from our classical approach based on interactive bulk formulae will have to be assessed in coastal regions through a validation of sea surface temperature. This is all the more important that SST plays an important role in the growth of fish larvae.

The biogeochemical model is first run at the scale of the Mediterranean basin on the NEMO grid. The calculated fields are then used to force our high resolution model at its boundary.

Coupling HTL and LTL

The first part of the study was devoted to the adaptation of ICHTHYOP to the outputs of the S model. This step was done by the development group of ICHTHYOP at



IFREMER-IRD in Sète (France). The goal here is to study the spatial and temporal variation of the larval stage of European anchovies (*Engraulis encrasicolus*) recruitment in the Northwestern Mediterranean and to understand which are the environmental factors (pressures) that impact this recruitment. Indeed, the anchovy stock in the Gulf of Lions and Catalan Sea experiences a very strong variability at the scale of several years.

Bioenergetic model of anchovy larvae: The Lagrangian IBM model ICHTHYOP is coupled to a bioenergetics model (based on the Dynamic Energy Budget theory; Kooijman 2010) calibrated for the European anchovy of the Northwestern Mediterranean (Pethybridge et al., 2013). For this species, bioenergetics models have been successfully implemented to populations of the northern Aegean Sea, Black Sea and Bay of Biscay. The model for the Mediterranean is derived from Pecquerie et al., 2009 developed for the Bay of Biscay by taking into consideration different conditions of temperature, food dynamics and growth data specific to the Gulf of Lions. The model is applied to the two first development stages that are yolk-sac larvae and early-stage larvae. The first one does not feed on external preys while the second one is dependent of food resources. An individual is characterized by three state variables, reserve, structural volume and maturation calculating from differential equations. Food intake is controlled by a scaled functional feeding response curve \times that ranges between 0 (no food intake) and 1 (maximum food intake). It is given by the equation:

$$\times$$

where for a given food type, \times is its density and \times its half-saturation constant (estimated for each food type). Temperature affects metabolic rates including maximum assimilation and somatic maintenance.

The differential equations of the DEB are solved inside ICHTHYOP using a simple Euler scheme.

This study is carried out in close collaboration with an IFREMER group in Sète (S. Bonhommeau and M. Froissart) which are responsible of the “fish” modelling in this study. The IRD group in Sète is also associated to our study.

Our preliminary run was done on the period beginning on April 2006 and ending on December 2011. The year 2006 is considered as a spin-up period and is not considered in the following. As underlined below, early stages of mesozooplankton are suspected to be the basis of the food for the fish larvae. Figure 8 presents the interannual variability of the mesozooplankton concentration at the surface for June from 2007 to 2011. The region of the Gulf of Lion is clearly a favourable area for the development of zooplankton. The signature of the Rhône plume is visible on the zooplankton patterns. Offshore areas of the Northwestern Mediterranean are also characterized by high level of mesozooplankton probably because it is a region of elevated primary production due to intense winter mixing, followed by spring bloom that initiate the development of a long trophic chain. The interannual variability is also important. Further studies are useful to understand the factors responsible of this variability which could also linked to a phase shift in the establishment of the



trophic chain.

Results

10,000 anchovy eggs are released every month from January 2007 and December 2011 in three regions: the Catalan Sea, the Gulf of Lion and the Ligurian Sea (Figure 7). Each larva is followed with its characteristics during 35 days. This is the mean duration of the larval stage before they become able to swim. We did not take into account larval vertical migration as migration of zooplankton which is the food for the fish larvae is not taken into account in the biogeochemical model. The number of eggs introduced in the model and then advected is of the order of 10,000 for the three areas of release defined (Figure 7). Trajectories are plotted on Figure 9 for some of the individuals spawned in the Gulf of Lions and in the Ligurian Sea on January 2007. The larvae spawned in the Gulf of Lions spend more time confined on the shelf than the larvae spawned in the Ligurian Sea that are transported southwest by the powerful Northern Current.

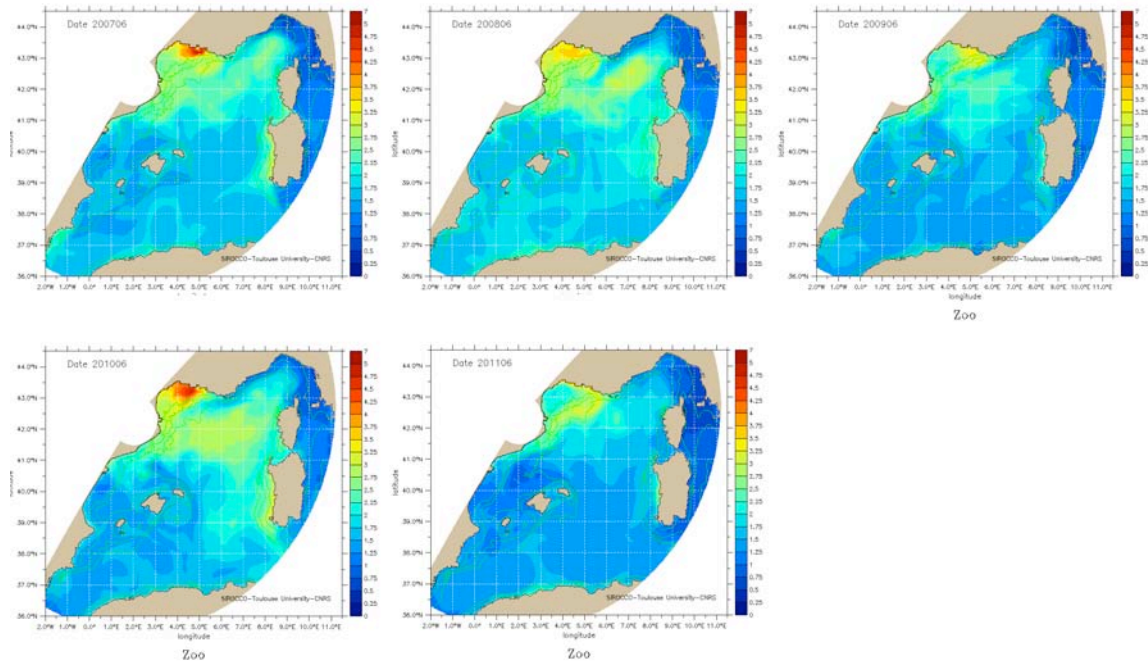


Figure 8: Concentration of mesozooplankton at the surface in June from 2007 to 2011 (mmolC/m^3)

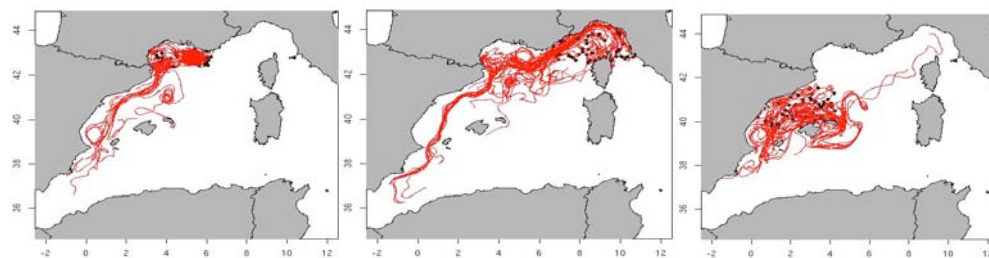


Figure 9: Trajectories of larvae spawned in January 2007, in the Gulf of Lions (left) in the Ligurian Sea (middle) and in the Catalan Sea (right). Black dots represent the initial positions of the particles that were followed over 35 days (random sampling of numerous trajectories).



Three different food types were used for the fish larvae: diatoms, microzooplankton and mesozooplankton. The growth of larvae was compared all along the year for these different diets (Figure 10).

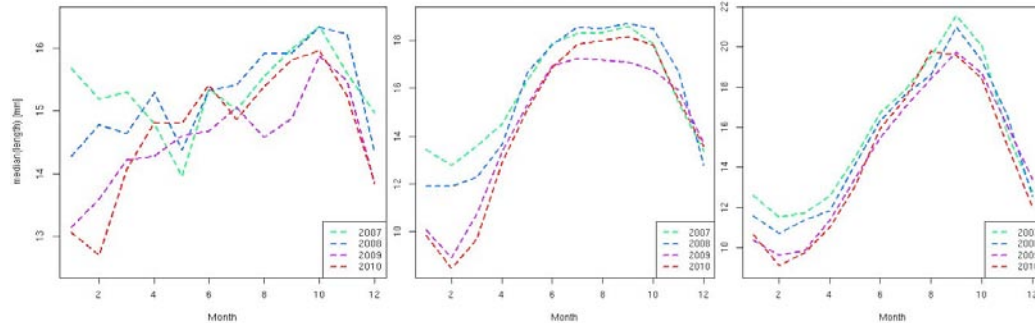


Figure 10: Median size (in mm) of the anchovy larvae released in the Gulf of Lions after 35 days of growth as a function of their spawning month for different years (colours) and different food (diatoms for the left panel, microzooplankton for the middle panel and mesozooplankton for the right panel).

The behaviour of larvae fed with diatoms does not appear coherent with the current knowledge about the most favoured period for spawning between May and August. This is probably due to the fact that temperature and food create tendencies, which are more or less in phase opposition. Spring and fall seasons are relatively favoured compared to the diets based on zooplankton more favourable to summer months. This behaviour is coherent with the studies of different authors (Conway et al. 1998, Tudela et al. 2002, Catalan et al. 2010), which showed the dominance of early stages of copepods (copepodites, nauplii and eggs) in the diet of the larvae.

Another interesting result is the interannual variability appearing on Figure 10. For example, years 2007 and 2008 allow a more important development of larvae than the other years and this is true for a major part of the year. This variability will be studied considering the interannual variability of food and SST. As an example, Figure 11 presents the mean SST for June. A strong variability impacts the Gulf of Lions along the coast as well as in the region of the Rhône river discharge.

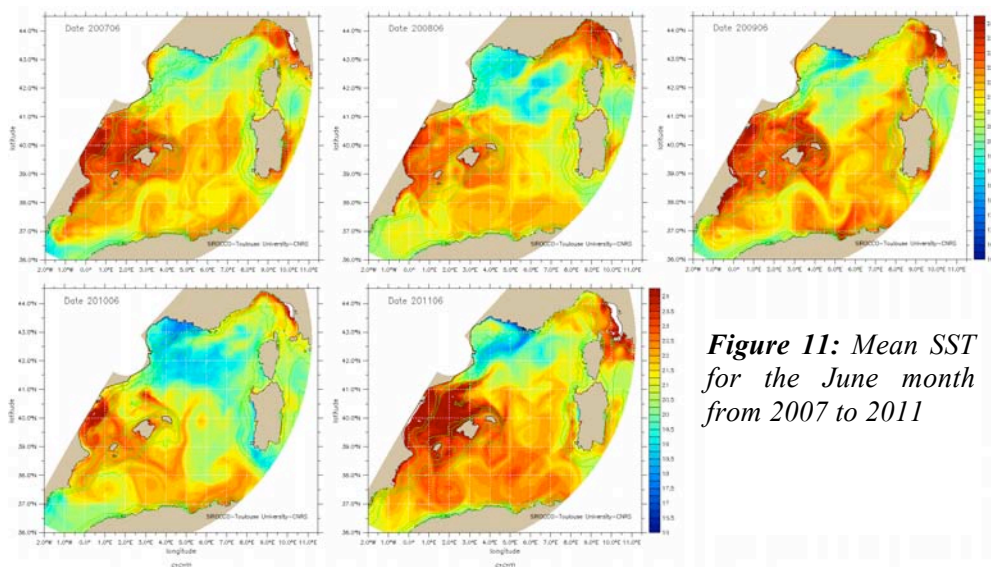


Figure 11: Mean SST for the June month from 2007 to 2011



Further work

The results presented in this report are preliminary. Other simulations are needed to explore the variability of the ecosystem in response to the different natural pressures. Water temperature and food availability (zooplankton) are the two direct pressures for anchovy larvae growth. These two pressures are themselves function of oceanic and climatic variability.

The variability of the complete system will be analysed starting from the climatic pressure: air/sea fluxes, rivers discharge, long-term evolution of the stratification to their consequences on the marine ecosystem. Besides, an effort has to be done to validate and possibly calibrate the zooplankton behaviour in the biogeochemical model. This is the compartment for which few data are available (especially time series) but it is of major importance for the coupling of low and high trophic levels.

References

- Auclair F., Casitas S., Marsaleix P., 2000. Application of an inverse method to coastal modelling. *Journal of Atmospheric and Oceanic Technology*. 17, 1368-1391. [http://dx.doi.org/10.1175/1520-0426\(2000\)017<1368:AOAIMT>2.0.CO;2](http://dx.doi.org/10.1175/1520-0426(2000)017<1368:AOAIMT>2.0.CO;2)
- Auger P.A., Diaz F., Ulses C., Estournel C., Neveux J., Joux F., Pujo-Pay M., and J. J. Naudin J.J., 2011. Functioning of the planktonic ecosystem of the Rhone River plume (NW Mediterranean) during spring and its impact on the carbon export: a field data and 3-D modelling combined approach. *Biogeosciences*, 8, 3231-3261. <http://dx.doi.org/10.5194/bg-8-3231-2011>.
- Catalán I.A., Folkvord A., Palomera I., Quílez-Badía G., Kallianotid F., Tselepides A., Kallianotis A., 2010. Growth and feeding patterns of European anchovy (*Engraulis encrasicolus*) early life stages in the Aegean Sea (NE Mediterranean). 86, Issue 2, 299–312.
- Conway D.V.P., Coombs S.H., Smith C., 1998. Feeding of anchovy *Engraulis encrasicolus* larvae in the northwestern Adriatic Sea in response to changing hydrobiological conditions. *Mar Ecol Prog Ser.*, Vol. 175: 35-49.
- García A., Palomera, I., 1996. Anchovy early life history and its relation to its surrounding environment in the Western Mediterranean Basin. *Scientia Marina* 60, 155–166.
- Herrmann M., Somot, S., 2008. Relevance of ERA40 dynamical downscaling for modeling deep convection in the Mediterranean Sea. *Geophys. Res. Lett.* 35.
- Herrmann M., Sevault, F., Beuvier, J., Somot, S., 2010. What induced the exceptional 2005 convection event in the northwestern Mediterranean basin? Answers from a modeling study. *J. Geophys. Res.* 115.
- Kooijman S.A.L.M. (2010) *Dynamic Energy Budget theory for metabolic organisation*. Cambridge University Press, Great Britain. 532 pp. ISBN 9780521131919.
- Lett C., Verley P., Mullon C., Parada C., Brochier T., Penven P., and B. Blanke. A lagrangian tool for modelling ichthyoplankton dynamics. *Environmental Modelling & Software*, 23(9) :1210–1214, 2008.
- Marsaleix P., Auclair F., Estournel C., 2006, Considerations on Open Boundary Conditions for Regional and Coastal Ocean Models. *Journal of Atmospheric and Oceanic Technology*, 23,1604-1613, <http://dx.doi.org/10.1175/JTECH1930.1>



- Marsaleix P., Auclair F., Floor J. W., Herrmann M. J., Estournel C., Pairaud I., Ulses C., 2008. Energy conservation issues in sigma-coordinate free-surface ocean models. *Ocean Modelling*, 20, 61-89. <http://dx.doi.org/10.1016/j.ocemod.2007.07.005>
- Marsaleix P., Auclair F., Estournel C., 2009. Low-order pressure gradient schemes in sigma coordinate models: The seamount test revisited. *Ocean Modelling*, 30, 169-177. <http://dx.doi.org/10.1016/j.ocemod.2009.06.011>
- Marsaleix P., Auclair F., Estournel C., Nguyen C., Ulses C., 2011. An accurate implementation of the compressibility terms in the equation of state in a low order pressure gradient scheme for sigma coordinate ocean models. *Ocean Modelling*, 40, 1-13 <http://dx.doi.org/10.1016/j.ocemod.2011.07.004>
- Marsaleix P., Auclair F., Duhaut T., Estournel C., Nguyen C., Ulses C., 2012. Alternatives to the Robert-Asselin filter. *Ocean Modelling*, 41, 53-66 <http://dx.doi.org/10.1016/j.ocemod.2011.11.002>
- Palomera I., Recasens, L., Mol, B., Libori, P., 2009. Spawning stock biomass of the North Western Mediterranean anchovy in 2007 and 2008 GSA 6 and GSA 7. *Biomass, (ICM)*, 37-49.
- Pecquerie L., Petitgas, P., Kooijman, S.A.L.M., 2009. Modeling fish growth and reproduction in the context of the Dynamic Energy Budget theory to predict environmental impact on anchovy spawning duration. *Journal of Sea Research*, 62, 93-105.
- Pethybridge H., Roos D., Loizeau V., Pecquerie L., Bacher C., 2013. Responses of European anchovy vital rates and population growth to environmental fluctuations: An individual-based modeling approach. *Ecological Modelling* 250 (2013) 370-383.
- Roos D., Bigot, J.L., Le Corre, G., Bourdeix, J.H., 2011. Diagnostic des populations d'Anchois et de Sardine du Golfe du Lion. Rapport d'avancement, May 2010. Partenariat scientifique Ifremer/Amop pour une gestion de la ressource en petits pélagiques.
- Tudela S., Palomera I. and Quílez G., 2002. Feeding of anchovy *Engraulis encrasicolus* larvae in the north-west Mediterranean. *Journal of the Marine Biological Association of the UK*, 82, 2, pp 349-350

2.2.2 Particle Tracking

(IEO, Patricia Reglero)

2.2.2.1 Description of the tool:

Estimate forward tracking by advecting recently-hatched bluefin tuna larvae in the direction of the geostrophic currents.

2.2.2.2 CASE Study: the Catalan Sea

Material and methods

Salinity, temperature and dynamic height distributions recorded from in-situ stations



by means of Sbe25 CTD, were interpolated onto a uniform grid of $1/15^\circ \times 1/15^\circ$ (4 nmi x 4 nmi, 1 nmi \sim 1852 m) by using minimum error variance methods with a correlation length of 0.3° (18 nmi) and a maximum allowed rms error for the interpolated field of 20%. The correlation length specifies how far away the observed information influences the values determined over the model grid. It does not depend on the way a variable is sampled but on the size of the dominant mesoscale structures. At the same time, the correlation length determines the degree of smoothing of the output fields. By smoothing the structures with scales shorter than 18 nmi we sought to reduce the bias due to the smaller not measured scales. The geostrophic currents were estimated by first differencing the interpolated dynamic height field using finite differences.

Estimated geostrophic currents at 15 m depth were interpolated into a regular grid of $1/60^\circ \times 1/60^\circ$ (1 nmi x 1 nmi). The geostrophic currents obtained in this way, $v_g(r) = (u_g(r), v_g(r))$, were used to evaluate an order of magnitude of the distance that a passive drifter would be advected in a given time (that could emulate the larvae displacement). Diffusion effects were not considered and the velocity fields are assumed to be constant during the integration time. The position of a particle at time step $(n+1)$, $r(n+1) = (x(n+1), y(n+1))$, was estimated from its position at time step (n) , $r(n) = (x(n), y(n))$ as:

$$x(n+1) = u_g(r(n)) \cdot \Delta t + x(n)$$

$$y(n+1) = v_g(r(n)) \cdot \Delta t + y(n)$$

being Δt , the time step that is set to 3600 seconds to satisfy the Courant–Friedrich–Lewy stability criterion: $c\delta t \leq 1 \delta x$.

Sensitivity tests on the reference level of no motion and the correlation length were done to assure the robustness of the calculated geostrophic currents. One set of initial positions were defined at a distance of 0.05° around the initial position of the lagrangian buoy in order to guess the performance of the 15 m depth geostrophic currents used to estimate the passive drifters progress. Other three sets of initial positions for passive drifters were defined at distances of 0.05° , 0.10° and 0.15° (3 nmi, 6 nmi, 9 nmi) around the cage position to take into account the possible drift of the cage with currents.

Three possible drift paths of one particle released in an initial point determined by the evidence of the presence of spawning adults and bluefin tuna eggs (Figure 12). The spatial distribution of age-dependent bluefin tuna larvae surveyed around the initial point was compared to the estimated trajectories. A lagrangian buoy equipped with a drogue so it was drifting at 8-15 m depth was deployed at the same location. The position of the buoy was recorded every 10 minutes during the next 2 days.

Results

Sensitivity tests on the reference level of no motion and the correlation length were done to assure the robustness of the calculated geostrophic currents. Figure 13 shows three possible drift paths of one particle released close to the initial lagrangian buoy position and left to travel alone during 10 days. Geostrophic currents for the different paths were calculated for three different cases: with the standard reference level of



no motion at 350 m (red line), using a reference level of no motion of 600 m (black line) and considering a correlation length of 8 nmi as deduced from data correlation statistics plus an anti-aliasing filter calculated by convolving the weight functions of the interpolation scheme with a normal error filter.

The calculated geostrophic currents and deduced drift paths of the passive drifters released at 15 m depth and at a distance of 0.05° around the lagrangian buoy were in agreement with the trajectory of the buoy for which inertial oscillations were clearly identified (Figure 14). The local wind at 10 m above the surface reanalyzed by the HIRLAM model every 12 hours shows that the shift in surface wind from the SW at day 1 to the SE at day 1.5 is clearly observed in the abrupt change of the lagrangian buoy path at that time.

The drift paths of the pseudo-particles released from the cage followed different trajectories depending on the initial distance to the cage. When the particles were released closer to the cage, at 0.05° from its position, the particles were transported out of the sampling area towards the east in 3 to 7 days. Some of the particles released at a distance of 0.10° and 0.15° from the cage position are transported westwards following the main geostrophic patterns remaining in the area for 7 to 18 days (Figures 15).

Conclusion and Summary

The comparison of the lagrangian buoy and the calculated drift trajectories revealed the qualitative good agreement between them. It is necessary to observe that the lagrangian buoy drifts on surface and is very sensitive to wind strength and direction while calculated trajectories consider geostrophic velocities at 15 m depth and in any case cannot reflect changes in wind faster than the time necessary for CTD sampling, since the geostrophic computations assume stationary. Further scenarios using the model including wind sensitivity will improve lagrangian trajectories.



Figura 1

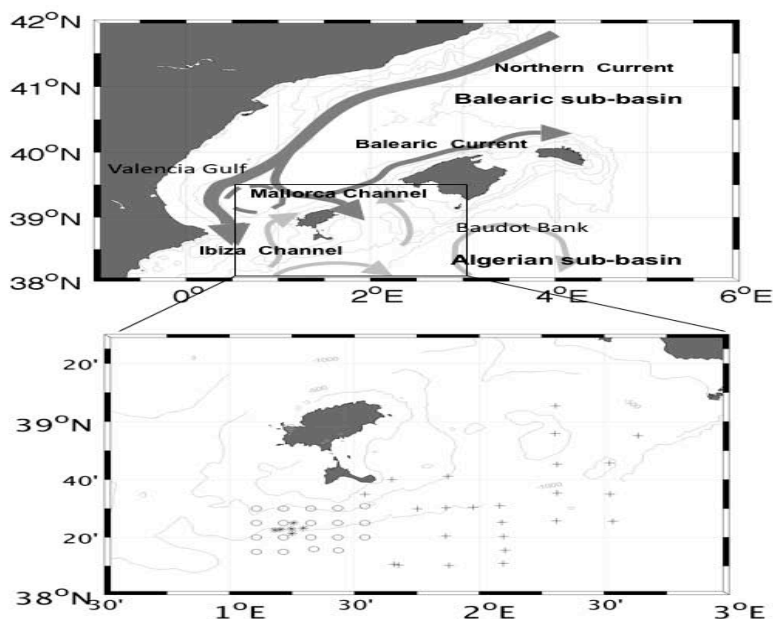


Figure 12. Main hydrographic features in the area of study (top) and sampling area with the three blocks of stations designed in the sampling strategy (bottom).

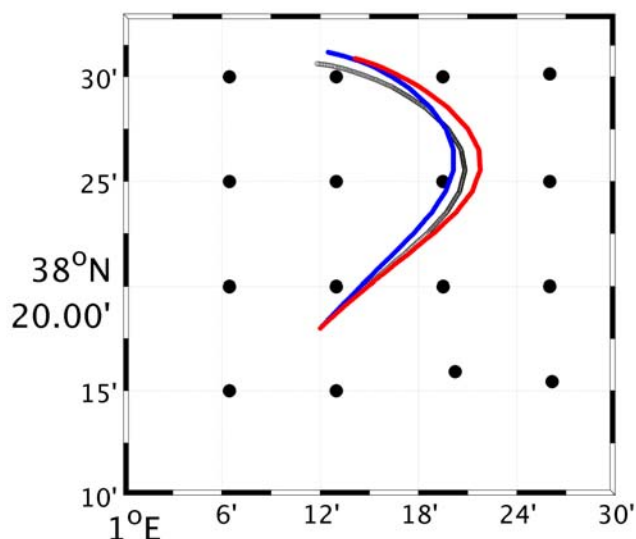


Figure 13: Possible drift paths of one particle released close to the initial lagrangian buoy position and left to travel alone during 10 days. Geostrophic currents calculated with the standard reference level of no motion at 350 m (red line), using a reference level of no motion of 600 m (black line) and considering a correlation length of 8 nmi plus an anti-aliasing filter (blue line).

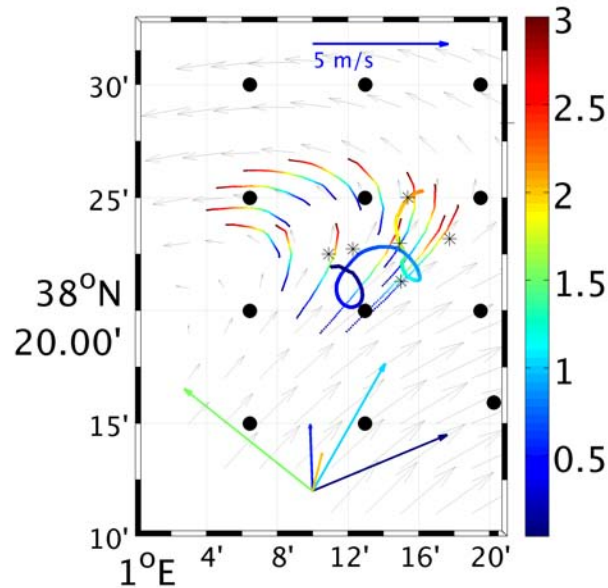


Figure 14: Drift patterns of the passive drifters released at 15 m depth and at a distance of 0.05° around the lagrangian buoy. Color bars indicate the time elapsed since particles were released in days. The trajectory of the buoy is also shown using the same color criteria. The local wind at 10 m above the surface reanalyzed by the HIRLAM model every 12 hours are shown at the bottom of the Figure for day 0, 0.5, 1, 1.5 and 2. Black dots correspond to CTD sampling stations. Red circle correspond to initial cage position. Stars correspond to sampled stations.

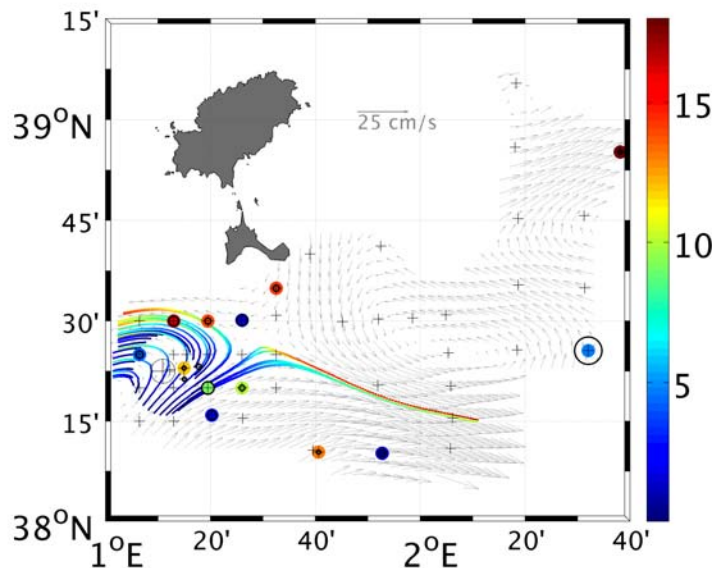


Figure 15: Geostrophic velocities in grey and drift paths of the pseudo-particles released from the cage at 0.10° along 18 days. Color bar indicates number of days since initial time. Color dots indicate the mean age of larvae if there is any. Black circles within or around color dots indicate larvae density (larvae. 100 m^3).



2.3 BAYESIAN Approach

(CSIC: Javier Ruiz, Laura Prieto, Margarita Rincón, Ignacio Catalán)

2.3.1 Description of the tool

The HTL modeling is based on Bayesian methods where different sources of data can be implemented: environmental records as covariates and fisheries information for the observational model. This approach has been validated in the Gulf of Cadiz (Ruiz et al. 2009) and it's being adapted for the Alboran Sea for PERSEUS.

2.3.2 CASE STUDY: The Alboran Sea

LTL model

The LTL is based on the recently published paper (Oguz et al. 2013) in the framework of PERSEUS and is based in a N2P2Z2D compartments with an *ad hoc* parameterization for the zooplankton mortality valid for the Gulf of Cadiz and Alboran Sea areas.

We have developed a running LTL model of two compartments that has been coupled with a 3D high resolution Regional Ocean Modeling System model (Peliz et al. 2013) forced with climatologies for the Gulf of Cadiz and Alboran Sea basins.

Specifically, the hydrodynamical model consisting of a ROMS (Shchepetkin, McWilliams 2005) based numerical simulation at 5 km resolution forced with realistic winds (ASCAT) and heat fluxes from ERA-Interim (Dee et al. 2011). The ocean model domain has been chosen in order to include the coupling of the inflow/outflow and the development of the Gulf of Cadiz slope Current (GCC; Peliz et al. 2007) on the east, and the recurrent mesoscale features on the Alboran side: the Western Alboran Gyre (WAG) and Eastern Alboran Gyre (EAG), the Almeria-Oran front, and the beginning of the Algerian Current where occasionally a third Gyre is observed (Tintoré et al. 1988 and Millot 1999). The extension of the domain to the east is associated with the occurrence of strong mesoscale activity in the transition between the Alboran Sea and the Algerian–Balearic basin.

In a first approach, the simulations were performed using the ROMS coupled to a Fasham type biological module. The single compartment (NPZD) ecosystem consists of four state variables: nitrate, phytoplankton, zooplankton and detritus. The model was forced with climatologic conditions and tested for different setups of the biological module in order to determine the biological parameters values and equations more adequate to represent the first trophic levels of the region. The setup validation was performed by comparing total chlorophyll output from the model with climatologic satellite data in eight control points at both sides of the strait. The higher correlation coefficient for the overall eight points ($R=0.66$) was obtained by using the standard Fasham's equations and only changing four parameters to site-specific values: maximum grazing rate, zooplankton mortality to detritus, phytoplankton mortality to detritus rate and light attenuation by chlorophyll. However, the individual analysis of the control points confirmed that each modification in the biological module affects in a distinct way to each region. Also, the consequences of



using different expressions of zooplankton mortality and predation by higher trophic levels in the Gulf of Cadiz (SW Iberian Peninsula) had been explored. These analyses showed that the best fit with observations is obtained when zooplankton mortality was simulated by a quadratic (i.e., density-dependent) expression and when predation by higher trophic levels (i.e., fish) was explicitly included in the model formulation. These results clearly indicated that using a more complex biogeochemical code was a reasonable option to better represent the ecosystems in the vicinity of the Strait of Gibraltar.

Therefore, in a second approach the N2P2Z2D model was implemented (Oguz et al. 2013). Based on available observations (Rodríguez et al. 2001), the phytoplankton community was represented by large (microphytoplankton) and small (nanophytoplankton) groups with cell sizes larger and smaller than 20 μm that generally typify diatoms and flagellates, respectively. The availability of coccolithophores and dinoflagellates was considered as much less critical than the other major groups within the annual phytoplankton community structure, although this assumption may not be strictly true for 1997–2002 in the NW Alboran Sea (Mercado et al. 2007). The zooplankton community was represented by microzooplankton (nominally <0.2 mm) and mesozooplankton (0.2–2 mm). The microzooplankton category included heterotrophic flagellates, ciliates and juvenile copepods. The mesozooplankton category essentially consisted of adult copepods. The link to higher predators was parameterized by the quadratic predation term (as the default setting) in the zooplankton equations. This term represented fish predation pressure as a continuous loss from the lower trophic food web structure (i.e., no recycling within the food web). Apart from its role in the closure of the model, it may further act as stabilizer of the model (Gibson et al. 2005). The model neglected the role of bacterioplankton and other components of the microbial food web because of the lack of data and also to keep the model as simple as possible for its 3-D implementation. The model thus preferentially sets the energy flow to the higher predators through (i) the small plankton size community structure (the nanophytoplankton and microzooplankton groups), and (ii) the large plankton size community structure (the microphytoplankton and mesozooplankton groups). These two primary food chains were interconnected with each other by additional energy flows among their members. Within the Alboran and Balearic Sea ecosystems, nitrogen is the most limiting nutrient for phytoplankton growth (Dafner et al. 2003, Ramírez et al. 2005 and Mercado et al. 2007). The plankton dynamics are therefore complemented by the nitrogen cycle, which involves ammonium, nitrate, and particulate organic nitrogen components. In the absence of bacterioplankton and dissolved organic nitrogen pool, detritus is remineralized directly to ammonium at a constant rate.

Coupling HTL-LTL

A Bayesian state-space size-structured population dynamics model for anchovy in the Alboran Sea is being under development as HTL. In fishery research, state-space models coupling with bayesian Monte Carlo Markov Chains (MCMC) methods provide accurate estimates for abundance while measuring the uncertainty pervasive in all the life-cycle. State-space models separates the problem into two stochastic models



(Meyer and Millar, 1999; Rivot et al., 2004). The first one, the process model, accounts for the unobservable stochastic variations that govern the internal population dynamics. The second one, the observational model, describes how the population state is observed and with what uncertainty. The linking of these two stochastic models provides consistent simulation of stock-dynamics and computes uncertainty as a natural output (Millar and Meyer, 2000; Punt and Hilborn, 1997).

We define two modules for the process model in order to integrate an environmentally forced recruitment with the size-structured stock dynamics. The first one is dependent on the particular environmental conditions in the Alboran Sea considering that recruitment is forced by the environment in the earliest life stages. The second one describes growth and mortality processes. The observational model is defined with data from catch in numbers, some acoustic surveys and LTL model outputs.

For the first part of the process model we are developing a mathematical structure that includes kinetic energy, which has been identified as a relevant covariate in the recruitment process (Ruiz et al. 2013). The second part assumes a von-Bertalanffy growth function to model the length frequency evolution and the mortality forces are defined following the Baranov equations. The software we are using is R 2.14.1 (R Development Core Team, 2011) and JAGS 3.3.0 (Plummer, 2013) and the code is being written in R linked with the MCMC sampler through the rjags package.

Skill assessment: comparison of first test with data

On one hand, the functioning of the biological model for LTL has been contrasted with data from the Gulf of Cadiz and Alboran Sea data while functioning in 0 and 1 dimensions. These results are already published as a PERSEUS product (Oguz et al. 2013). The performance of the physical model has already been validated and published (Peliz et al. 2013). The performance of the coupled functioning with climatological forcings has already been tested with Taylor diagrams as well as with the contrasting with the ecological regions diagnosed by Navarro and Ruiz (2006) and Macias et al. (2007) for both basins (east and west of the Strait of Gibraltar). This model is an outstanding improvement with respect to the one-compartment SESAME version.

On the other hand, the HTL model has been developed in a Bayesian framework for the Gulf of Cadiz and it's being adapted to the Alboran Sea by replacing the environmental drivers of the system. Whereas in Cadiz the drivers are wind and temperature, in Alboran the main driver of the pelagic system is the energy of the Atlantic Jet and the direction of the flow. We showed this year that changes in Kinetic Energy of the jet are able to explain the main fluctuations in anchovy fisheries in the area as published in a PERSEUS paper (Ruiz et al. 2013). This Skill was actually tested within the time-frame of 1988-2012. We therefore will link the 3D LTL model, already tested, with the HTL model, already tested, through the forcing parameters of the Bayesian model, substituting the wind by the kinetic energy and its biogeochemical consequences, which will be derived from the 3DROMS model. On the other hand, we have already coupled the ROMS with an IBM in the area (Catalán et al. 2013). This exercise will provide recruits to the nursery zone, and this magnitude will be both feed-backed by the Bayesian model and be used as an input to it.



Advantage and limitations of the method

The LTL model represents a first feasible capacity to simulate the dynamics of the biogeochemical cycles and the LTL in the connection of the Mediterranean with the world ocean. The model is capable to simulate different food web structures in response to different combinations of fish predation and resource availability.

The innovative coupling of LTL with Bayesian HTL allows a very realistic simulation of exploited species as forced by LTL, including in the simulations real human pressure as mortality generated catches in the fishing fleet.

Conclusion

A LTL is available to simulate the time slices of PERSEUS, its dynamics realistically reproduce the diversity of oceanographic conditions that characterize both adjacent basins of the Strait and Gibraltar and the exchanges associated to the connection between Mediterranean and Atlantic waters.

A HTL based on the Bayesian approach is ready to connect with the LTL model in an innovative coupling able to merge the physical forcing and its biogeochemical consequences with real landing data from the fishing fleet.

References

- Catalán, I.A., Macías, D., Solé, J., Ospina-Alvarez, A., Ruiz, J. Stay off the motorway: Resolving the pre-recruitment life history dynamics of the European anchovy in the SW Mediterranean through a spatially-explicit individual-based model (SEIBM). *Progress Oceanogr.* 111 (2013), 140-153.
- Dafner, E.V., Boscolo, R., Bryden, H.L. The N:Si:P molar ratio in the Strait of Gibraltar. *Geophys. Res. Lett.* 30 (10) (2003), 13.1–13.4.
- Dee, D.P. *et al.* The ERA-Interim reanalysis: configuration and performance of the data assimilation system. *Q.J.R. Meteorol. Soc.* 137 (2011), 553-597, doi: 10.1002/qj.828.
- Gibson, G.A., Musgrave, D.L., Hinckley, S. Non-linear dynamics of a pelagic ecosystem model with multiple predator and prey types. *J. Plankton Res.* 27 (5) (2005) 427-447. ing. R Foundation for Statistical Computing, Vienna, Austria. ISBN 3-900051-07-0.
- Macías, D., Navarro, G., Echevarría, F., García, C.M., Cueto, J.L. Phytoplankton pigment distribution in the northwestern Alboran Sea and meteorological forcing: A remote sensing study. *J. Mar. Sys.* 65 (2007), 523-543.
- Mercado, J.M., Cortés, D., García, A., Ramírez, T. Seasonal and inter-annual changes in the planktonic communities of the northwest Alboran Sea (Mediterranean Sea). *Progress Oceanogr.* 74 (2007), 273-293.
- Meyer, R., Millar, R. B. BUGS in bayesian stock assessments. *Can. J. Fish. Aquat. Sci.* 56 (1999), 1078-1087.
- Millar, R. B., Meyer, R. Bayesian state-space modeling of age-structured data : fitting a model is just the beginning. *Can. J. Fish. Aquat. Sci.* 57 (2000), 43-50.



- Millot, C. Circulation in the Western Mediterranean Sea. *J. Mar. Sys.* 20 (1-4) (1999), 423-442.
- Navarro, G., Ruiz, J. Spatial and temporal variability of phytoplankton in the Gulf of Cadiz through remote sensing images. *Deep-Sea Res. II* 53 (2006), 1241-260. doi:10.1016/j.dsr2.2006.04.014
- Oguz, T., Macías, D., Renault, L., Ruiz, J., Tintoré, J. Controls of plankton production by pelagic fish predation and resource availability in the Alboran and Balearic Seas. *Progress Oceanogr.* In press (2013), doi: <http://dx.doi.org/10.1016/j.pocean.2013.03.001>.
- on Cancer.
- Peliz, A., Boutov, D., Cardoso, R., Delgado, J. & Soares, P.M.M. The Gulf of Cadiz-Alboran Sea sub-basin: Model setup, exchange and seasonal variability. *Ocean Model.* 61 (2013), 49-67, doi: <http://dx.doi.org/10.1016/j.oceanmod.2012.10.007>.
- Peliz, A., Dubert, J., Marchesiello, P., Teles-Machado, A. Circulation in the Gulf of Cadiz: model and mean flow structure. *J. Geophys. Res.* 112 (2007), p. C11015
- Plummer, M. (2013). JAGS version 3.3. 0 user manual. International Agency for Research
- Punt, A. E., Hilborn, R. Fisheries stock assessment and decision analysis : the bayesian approach. *Rev. Fish. Biol. Fisher.* 7 (1997), 35-63.
- R Development Core Team (2011). R: A Language and Environment for Statistical Comput-
- Ramírez, T., Cortés, D., Mercado, J.M., Vargas-Yáñez, M., Sebastián, M., Liger, E. Seasonal dynamics of inorganic nutrients and phytoplankton biomass in the NW Alboran Sea. *Estuarine Coastal Shelf Sci.* 65 (2005), 654-670.
- Rivot, E., Prévost, E., Parent, E., Baglinière, J. A bayesian state-space modelling framework for fitting a salmon stage-structured population dynamic model to multiple time series of field data. *Ecol. Modell.* 179 (2004), 463-485.
- Rodríguez, J., Tintoré, J., Allen, J.T., Blanco, J.M., Gomis, D., Reul, A., Ruíz, J., Rodríguez, V., Echevarría, F., Jiménez-Gómez F. Mesoscale vertical motion and the size structure of phytoplankton in the ocean. *Nature* 410 (2001), 360-363.
- Ruiz, J., González-Quirós, R., Prieto, L., Navarro, G. A bayesian model for anchovy: the combined pressure of man and environment. *Fish. Oceanogr.* 18 (2009), 62-76.
- Ruiz, J., Macías, D., Rincón, M.M., Pascual, A., Catalán. I.A., Navarro, G. Recruiting at the Edge: Kinetic Energy Inhibits Anchovy Populations in the Western Mediterranean. *PLoS ONE* 8(2) (2013), e55523. doi:10.1371/journal.pone.0055523
- Shchepetkin, A.F., McWilliams, J.C. The regional oceanic modeling system (roms): a split-explicit, free-surface, topography-following-coordinate oceanic model. *Ocean Model.* 9 (2005), 347-404.
- Tintoré, J., La Violette, P.E., Blade, I., Cruzado, A. A study of an intense density front in the eastern Alboran sea: the Almeria-Oran front. *J. Phys. Oceanogr.*, 18 (1988), 1384-1397.

2.4 ECOPATH with ECOSIM

Libralato S.¹, Solidoro C.¹, Akoglu E. ², Ballerini T.³, Banaru D.³, Capet A.⁴, Daskalov G.⁵,



Gregoire M.⁴ , Kandilarov R.⁶ , P. Lazzari ¹ , Salihoglu B.² , Staneva J. ⁶ , Tsagarakis K.⁷

1) OGS; 2) METU-IMS; 3)UNIVMED; 4) Ulg;5) IBER-BAS; 6)DMG-SU;7)HCMR

2.4.1 Specificity of the tool

Ecopath with Ecosim (EwE) is a software package developed for analysing energy flows in marine food webs under the assumption of mass-balance. Some of the Ecological Network Analysis algorithms in NETWRK (Ulanowicz, 1999; Heymans and Baird, 2000) was reprogrammed into Ecopath 2 (Christensen and Pauly, 1992) and have been updated in the Ecopath with Ecosim version 6 (www.ecopath.org). Ecopath with Ecosim (EwE) is a quantitative tool used to analyse aquatic ecosystems. EwE combines software for ecosystem trophic mass balance analysis (Ecopath) with a dynamic modelling capability (Ecosim), and also includes a space-time dynamic routine (Ecospace) which can be used to explore past and future impacts of fishing activities on marine ecosystems (Christensen et al., 2005).

The modelled ecosystem is represented by functional groups (i), which can be composed of single species, groups of species with ecological similarities, or part of a population (i.e., ontogenetic fractions, like juveniles or adults, of a species). Ecopath uses two master equations to describe balance of flows (as nutrients, carbon, mass or energy) in the ecosystem: one equation describes the predator-prey interactions in the modelled food web and the second one describes the balance at the level of each individual trophic group (Christensen et al., 2005). The first equation estimates the production of each trophic group considered in the model as:

Production =
 catch + predation mortality + biomass accumulation + net migration + other mortality
 (Eq. 7)

or,

$$P_i = Y_i + \sum_j M_{ji} + E_i + P_i(1 - EE_i) \tag{Eq. 8}$$

where P_i is the total production of group i, Y_i is the total fishery catch rate of i, M_{ji} is the instantaneous predation rate for group i, E_i the net migration rate (emigration - immigration), BA_i is the biomass accumulation rate for i, and $P_i(1 - EE_i)$ is the 'other mortality' rate for i (Christensen et al., 2005). Equation (8) can be re-written as:

$$P/B_i = Z_i + \sum_j Q_j/B_j + DC_{ji} \tag{Eq. 9}$$

where P/B_i is the production/biomass ratio for i and under most conditions corresponds to the total mortality rate, Z , commonly estimated as part of fishery stock assessment. EE_i is the ecotrophic efficiency of group i, describing the proportion of the production that is utilised in the system, Q_j/B_j is the consumption/biomass ratio of the predator j and DC_{ji} is the fraction of prey i in the average diet of predator j (Christensen et al., 2005).

The second equation assure that the balance within each group is respected by setting consumption by group i equals the production by i, plus respiration by i and unassimilated food by i. The units of the model are expressed in terms of nutrient or energy related currencies, and by a unit of surface. Frequently biomass is expressed



in t·ww km⁻² (ww = wet weight) and production and consumption are expressed in t·ww km⁻²·yr⁻¹. Nevertheless, although yearly rates are dominating, energy, nutrient and carbon units can also be used. Ecosim is the dynamic expression of the ecosystem over time and is defined by a series of differential equations:

$$\boxed{\text{[Red X]}} \tag{Eq. 10}$$

where dB_i/dt is the growth rate during time t of group i in terms of its biomass B_i ; g_i is the net growth efficiency of group i ; M_i is the non-predation ‘other’ mortality rate; F_i is the fishing mortality rate; e_i is the emigration and I_i is immigration rate (Christensen et al., 2005). The ΣQ_{ji} expresses the total consumption by group i and is calculated based on the foraging arena concept, where B_i ’s are divided into vulnerable and invulnerable components (Walters et al., 1997). ΣQ_{ij} indicates the predation by all predators of group i (Christensen et al., 2005). The transfer rate (v_{ij}) between the vulnerable and invulnerable components sets the top-down or bottom-up control of each interaction (Christensen et al., 2005). For each predator-prey interaction the consumption rate C_{ij} is calculated by:

$$\boxed{\text{[Red X]}} \tag{Eq. 11}$$

where, a_{ij} is the effective search rate for predator i feeding on a prey j , v_{ij} is the base vulnerability expressing the rate with which prey move between being vulnerable and not-vulnerable, B_i is prey biomass, P_j is predator abundance, T_i represents prey relative feeding time, T_j predator relative feeding time, S_{ij} user-defined seasonal or long term forcing effects, M_{ij} mediation forcing effects, and D_j represents handling time as a limit to consumption rate (Walters et al., 2000; Christensen et al., 2005).

Ecopath with Ecosim requires three of the following four parameters for each trophic group considered in the model:

- Biomass (B , t·km⁻²) for the year under consideration;
- Production/Biomass ratio (P/B , year⁻¹);
- Consumption/Biomass ratio (Q/B , year⁻¹);
- Ecotrophic Efficiency (proportion). This parameter indicates the unexplained mortality for each group, it is difficult to estimate and usually is obtained as an output from the model. In addition, Ecopath with Ecosim requires also the specification of the diet composition for each trophic group (i.e. percent contribution in mass of the prey group to the diet of the predator group), as well as the landings and discards (both are expressed in t·km⁻²·year⁻¹) for each fishery included in the model and for each the trophic group that is fished. To run the dynamic simulations in Ecosim yearly estimates of biomass, fishing mortality, and catch by species and/or gear are required inputs.

2.4.1.1 General Approach to E2E modeling with EwE

The integration of the biogeochemical (low trophic level; LTL) and EwE food web (High Trophic Level, HTL) models followed the procedure described in Libralato and Solidoro (2009). The central idea is that the HTL model will be extended to provide a first, rough, description of also the LTL compartments (extended HTL model) and then an adjustment will be done for the extended HTL model to represent better the



LTL dynamics. The limiting nutrient will be used to drive the food web from the bottom: given the current knowledge and models results P (phosphorous) was defined for the Mediterranean sea and the NorthWestern Shelf of the Black Sea, whereas N (nitrogen) was instead considered more appropriate for the inner basin of the Black sea (see Black Sea State of the Environment Report 2001-2006/7 page 43). Moreover, since zooplankton groups are usually poorly represented in both LTL and HTL models, it was decided that the two models will be linked at the nutrients level (Libralato and Solidoro, 2009). The effects of the 3D results from the biogeochemical models reparametrized into 0D EwE HTL model will need to be accounted (Solidoro et al., 2010b), through a residual function that will be estimated by the E2E model (EwE extended): this adjusting function will be estimated by comparing E2E and LTL model outputs for nutrient dynamics over time.

In a first step, thus, the HTL models were converted in P and N units. The biomasses, immigration rates, catches and discards of all functional groups in the food web model (HTL functional groups) was converted in phosphorous and nitrogen units, by using conversion factor obtained by assuming an average C:N:P ratio of 88.5:15.7:1 (Sterner and George, 2000; Hjerne and Hansson, 2002) and a general value of 9 gww/gC (Pauly and Christensen, 1995).

Moreover, unassimilated ratio ($UN = Q - P - R$) for HTL groups was adjusted in order to have zero respiration thus allowing complete conservation of the nutrient (while production and consumption rates were kept untouched). This was accomplished by setting $UN = 1 - P/Q$. When aggregating groups, the Q/B values derived from the gross growth efficiency for the model groups that have very wide range of Q/B values (e.g. benthic invertebrates) in order to represent the respiration processes more precisely, i.e. the representation of mass-balance for the model groups on the level of consumption, assimilation and respiratory processes that forms the energy budget of the each group.

The comparison of EE estimates for all functional groups allowed checking the consistency of the food web model in nutrient units with the original one in wet weight units.

2.4.1.2 Inter-regional comparability

Different structures seem to better grasp ecological features typical of different areas, and allows to keep areas specificity and the optimal complexity based on local experts as the best representation of reality. Nevertheless, although it is always possible to compare models with different structure, previous works (Angelini & Agostinho, 2003) highlighted the influence of HTL model structure, i.e. number and composition of functional groups, on results and in particular on indicators. Actual models have different groups parametrized into multistanza functional groups, and given the peculiarity of this representation was accepted the suggestion to consider model structure without multistanza groups in the HTL-EwE models.

Given that PERSEUS WP4 needs to compare scenarios and models in terms of vigor, organization and resilience, there is a need for standardization of the models structure. In order to define a common structure, an overview of existing structures were considered, including: A) the structure of models for Adriatic, Catalan and Aegean somewhat similar (40 functional groups; e.g. Coll et al. 2006, 2007; 2009; Tsagarakis et al., 2010); B) the general structure used by Christensen et al., 2009; C)



the simplified structure (16 Functional groups) used by Libralato et al. 2010; D) the least complex among structure for subsystems embedding each and every regional structure; E) the most complex among subregional structures common to all regional systems.

Overall, the structure needs to be ecologically sound for the Mediterranean but also “fishery oriented” and useful to produce results linked with the MSFD. For instance, benthopelagic fish group, usually a poorly defined group, will be included in the standard structure because of its importance for fisheries, especially in the Northern Aegean Sea. Moreover, macrozooplankton group (krill and other invertebrates > 2 mm) from the HTL model that would also be represented in the standardized models. Therefore, it was decided a standardized structure for the extended EwE model (E2E) including 28 living groups and 6 non-living groups as described in the following Table 1.

#	Group name	Description
1	Phytoplankton	mainly large diatoms
2	Picophytoplankton	
3	Bacteria	eterotrophic bacterioplankton
4	Nano-Microzooplankton	ciliates, fine filter feeders and metazoa
5	Mesozooplankton	carnivorous, mixed filter feeders and herbivorous
6	Macrozooplankton	
7	Gelatinous zooplankton	
8	Anellids	
9	Bivalves and gastropods	
10	Benthic cephalopods	
11	Benthopelagic cephalopods	
12	Small benthic crustaceans	
13	Decapods	
14	Other invertebrates	
15	Sardine	
16	Anchovy	
17	Other small pelagic fish	
18	Medium pelagic fish	
19	Benthopelagic fish	
20	Large pelagic fish	
21	Red mullets	
22	Medium benthodemersal	
23	Hake	
24	Anglerfish	
25	Benthodemersal elasmobranch	
26	Large benthodemersal fish	
27	Seabirds	
28	Dolphins and other +marine mammals	
29	Input P	Input of phosphorous
30	PO4	Phosphate (inorganic phosphorous)
31	DOP	Dissolved Organic Phosphorous
32	POP	Particulate Organic Phosphorous
33	Discards	
34	Detritus	

Table 1: Standardized food web structure for the Mediterranean Sea E2E models.

Aggregation of HTL groups from original models was done by taking their average of rates (P/B and Q/B), using biomass as a weighting factor. Similarly, aggregation of diet was done by considering both the consumption rate and biomass.

2.4.1.3 Data requirements

For the linking with LTL model, the food web model (EwE) will have some additional



boxes (HTL model extension to LTL groups), namely: diatoms [Phytoplankton] and small phytoplankton [Picoplankton]; two groups of zooplankton: ciliates, fine filter feeders and metazoa [microzooplankton], and carnivorous, mixed filter feeders and herbivorous [mesozooplankton]; heterotrophic bacteria [bac], inorganic nutrient [DIN or PO₄], dissolved organic matter and particulate organic matter, in terms of phosphorus [DOP] and [POP] or nitrogen [DON] and [PON].

In order to represent these groups in the extended HTL model, all information regarding average concentrations and flows between these additional groups are taken as average values from BGC simulations. Spatially averaged, vertical integrated values are estimated from outputs regarding the specific part of the LTL model representing the HTL model domains. Other than average concentrations of LTL compartments, diet composition for the zooplankton groups in the extended EwE model are estimated from LTL model run as average yearly proportions. Flows to detritus in the extended EwE model for LTL groups were set to represent average yearly flows in the biogeochemical model, to represent flows of excretion, mortality, bacterial degradation, organic matter decay, alkaline phosphatase, and sinking. These flows are set using average proportions from BGC model runs.

For the PERSEUS case study areas in the Mediterranean Sea: Gulf of Lions, Adriatic Sea, Northern Aegean Sea, results from the BFM model will be used by the participants. Concerning the Black Sea case study areas; northwestern shelf of the Black Sea and the inner basin and the eastern Black Sea, results from GHERECO, BIMS-ECO, BIOGEN respectively will be used by different partners.

2.4.2 Case studies

2.4.2.1 Mediterranean basin LTL model

Lazzari P., Libralato S., Solidoro C. (OGS)

The OPATM-BFM is a computer code, developed to describe in a 3D space the dynamics of major biogeochemical processes occurring in the Mediterranean marine system. The OPATM-BFM simulates the cycles of nitrogen, phosphorus, silica, carbon, and oxygen in the water inorganic and organic dissolved phase, as well as in the plankton and particulates. Plankton dynamics are parameterized by introducing a number of plankton functional groups, each representing a class of taxa (functional groups). BFM plankton functional groups are classified as producers (phytoplankton), consumers (zooplankton), and decomposers (bacteria). These broad functional classifications are further divided into functional subgroups, Figure 16, to create a planktonic food web (e.g. diatoms, picophytoplankton, microzooplankton, etc.).

The 3D transport component is resolved using the eulerian formalism, the advection of matter is forced using the stored-on-disk output of an ocean general circulation model (OGCM). The simulations for the entire Mediterranean basin considered in this document are analogous to the one presented in Lazzari et al. (2012), the forcing fields are obtained by the MED16 OGCM (Beranger et al., 2010) and upscaled to 1/8 of degree of horizontal resolution (approximately 12 km x 12 km boxes). The vertical discretization presents 43 levels with 14 levels in the upper 200 m of the water column, and a coarser discretization for the deeper levels. The period considered in the simulation spans from 1998 to 2005, we skipped the first year of simulation for



the E2E application. The model saves the outputs as monthly averages NetCDF files to reduce the space occupied by the data.

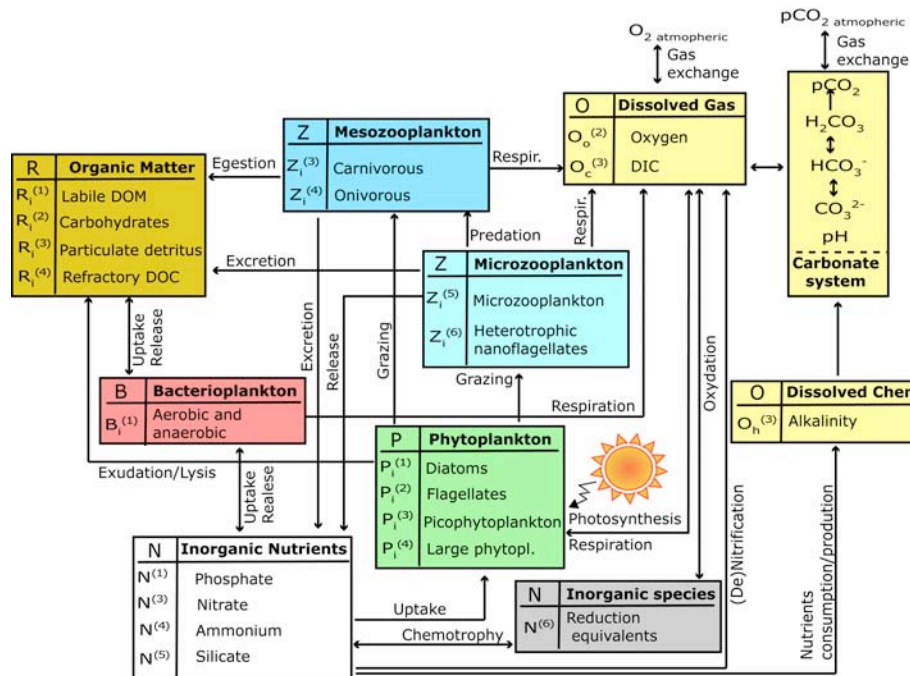


Figure 16. Scheme of the BFM model version used in the present document, general info about the BFM model can be found at <http://bfm-community.eu/>

Input data from LTL model to HTL models in the Mediterranean Sea

For the Mediterranean areas where P is considered the limiting nutrient, in a second step the main biogeochemical P pools have been added to the food web model to describe inorganic phosphorous as phosphate (PO₄), Dissolved and Particulate Organic Phosphorous (DOP and POP, respectively). An additional pool, named InputP was added in the HTL extended model to represent the input of nutrient and set as a primary producer to force it over time.

The data have been horizontally aggregated averaging on the poligons defined for each local area Adriatic Sea, Gulf of Lions and North Aegean Sea (see Figure 17) and then integrated along the water column. We prepared a specific configuration of the OPATM-BFM model (E2E 1.5) that stores on disk all the carbon fluxes required by the Ecopath model in particular to calculate the diet matrix.

Monthly outputs from the BFM from 1999 to 2004 for the Mediterranean case study areas were used to reparametrize and extend HTL model. The LTL variables (flows and biomasses) from the biogeochemical model were grouped depending on plankton functional types in order to be used in the E2E modeling scheme. For example, the BFM results for different copepods (Z3 and Z4) were lumped into a single functional group (Mesozooplankton), and groups Z5 and Z6 were lumped together under another functional group, denominated [Nano-microzooplankton]. Diatoms, dinoflagellates and nanoflagellates (P1, P2 and P4) in BFM were grouped together into Phytoplankton group, while Picoplankton (P3) and Bacteria (Bact) were represented as separate functional groups (Figure 18).



Figure 17: Domains of the case study sites in the Mediterranean sea: Adriatic Sea, Northern Aegean Sea and Gulf of Lyon.

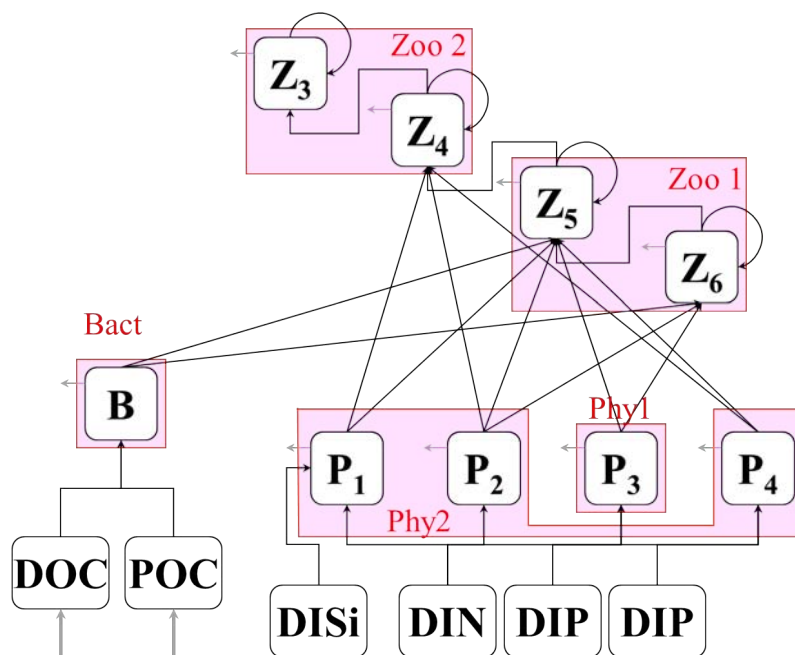


Figure 18: Variables from the OPATM-BFM aggregated for re-parametrizing biomasses and flows in the HTL extended model.

LTL model outputs were prepared in order to calculate the actual consumption and production rates and average biomasses of the LTL variables in the biogeochemical model to be used in the E2E model.

All information regarding average concentrations and flows between these additional groups used to extend the HTL model for the Mediterranean areas, were taken from average values of OPATM-BFM simulation (Lazzari et al., 2012) taking outputs for the specific model domains: Gulf of Lyon, Aegean Sea and Adriatic Sea. Other than



average concentrations, diet composition for the two zooplankton groups in the extended EwE model was set as the yearly proportions estimated from the BFM run. Flows to detritus in the extended EwE model for LTL groups were set to represent average yearly flows in the biogeochemical model, i.e. flows of excretion (flows to DOP), mortality (flows to POP), bacterial degradation (from Bacteria to inorganic nutrient), decay (from particulate and dissolved nutrient), alkaline phosphatase (from DOP to PO₄), and sinking (from POP to detritus) were set using average proportions from the BFM or when not available from the run of a BGC model representing a Mediterranean water column (Cossarini and Solidoro, 2009).

2.4.2.2 Adriatic Sea

Libralato S., Solidoro C. (OGS)

Area description

The northern and central Adriatic Sea, or NC Adriatic (with the south limit in Vieste harbor) constitutes the widest continental shelf in the Mediterranean Sea (Pinardi et al. 2006). The substrate is prevalently muddy in the western part of the basin and prevalently sandy bottoms occur in the eastern part (Brambati et al. 1983). Due to the influence of the river runoff and the oceanographic conditions the region exhibits a decreasing trend of nutrient concentration and production from north to south and from west to east (Fonda Umani 1996; Zavatarelli et al. 1998). The Adriatic, being an important area for dense water formation, is an area of overwhelming importance for the Mediterranean circulation.

Phytoplankton annual cycle is generally characterized by two intense Diatom blooms triggered by nutrient input from Po river: one in late-winter and early spring (mainly *Skeletonema marinoi*) and one in fall (Pugnetti et al., 2008, Mozetic et al., 2009; Cabrini et al, 2012, Bernardi Aubry et al. 2012). Further minor and variable peaks of small size phytoplankton are observed in spring and summer periods (Mozetic et al., 2009, Bernardi Aubry et al. 2006, Pugnetti et al., 2008).

Diatoms spring blooms are followed, with a delay of about 1 month, by copepods peak. In particular calanoids (mainly *Acartia clausi* and *Paracalanus parvus*), are the dominant components of mesozooplankton community (Fonda Umani et al., 1992). Other relevant mesozooplankton groups are Cladocerans that attain their highest abundance in summer with occasional blooms of *Penilia avirostris* (Camatti et al. 2002, Pugnetti et al., 2008). Microzooplanktons (ciliates, tintinnids and metazoans) are present during the whole year, with maxima in summer, feeding on both small phytoplankton and bacterioplankton (Mozetic et al., 1998; Cataletto et al., 1995; Fonda Umani and Beran, 2003).

Heterotrophic bacteria exert important role by channeling energy from dissolved organic matter to higher trophic levels via protozoan grazing processes (Pugnetti et al., 2008; Fonda Umani and Beran, 2003), by recycling nutrients and by competing with phytoplankton for nutrients (Solidoro et al, 2005, Cossarini et al. 2012).

The area presents a high diversity of environmental conditions. It is an important area for the reproduction of small pelagic fish, especially anchovy *Engraulis encrasicolus*, and sardine *Sardina pilchardus* (Morello and Arneri, 2009), a strategic



region for marine vertebrate conservation (e.g., Groombridge 1990; Bearzi et al. 2004) and for other goods and services such as aquaculture products (e.g. Solidoro et al., 2010a).

This area is of great value for fishing within the Italian and the European context (Cataudella and Spagnolo, 2012), and includes the fishing harbours from Trieste to Vieste. Small pelagics and demersal resources are targeted by local fisheries since historical times (Fortibuoni et al., 2010). Small pelagic fish are important in the catch and are mainly caught by purse seines and mid water trawlers (Arneri, 1996; Mannini and Massa, 2000). The demersal fishery mainly comprises juveniles of several target species, e.g. hake (*Merluccius merluccius*), red mullet (*Mullus barbatus*), but also invertebrates such as mantis shrimp (*Squilla mantis*) and squids (*Sepia officinalis*) constitute an important proportion of the catch.

Important changes in landings have been registered in the NC Adriatic, with a dramatic increase from the mid 1970s to the mid 1980s, mainly due to the increase of small pelagic fish in the catch. The progressively decline from late 1980s to the present is primarily because of the decrease in biomass of small pelagic fish (anchovy and sardine) populations (Cingolani et al., 1996; Azzali et al., 2002; Santojanni et al., 2003, 2005). Other target demersal species have also been reported as overexploited (e.g. Jukic-Peladic et al., 2001; Vrgoc et al., 2004). Important amounts of discards produced (Pranovi et al., 2000, 2001), and long terms analyses of community structure (e.g. Fortibuoni et al., 2010) are supporting the considerations that NCA ecosystem is exploited under a non-sustainable regime (Coll et al. 2009). All the above highlight the physical, biological and economic potential impacts that climatic changes might induce on this ecosystem (Giani et al. 2012).

Adriatic Sea HTL model

The model represented the NCA ecosystem in the 1990s (Coll et al., 2007; Libralato et al., 2010) and represents the system after the collapse of the anchovy stock and the decrease of other small pelagic fish species in the area. The area within 3 nm from the coast, or down to 10 m depth, where the artisanal fleets mainly operate and trawling activity is banned, was excluded from the western part; the area within 12 nm from the coast, where the rocky archipelagos occur, was excluded from the eastern part. A total of 40 functional groups were used for the food-web model. The definition of functional groups included in the model was based on similarities in their ecological and biological features (e.g. feeding, habitat, growth) and on the importance of the species in terms of the fisheries, by application of Factorial Correspondence Analysis (FCA) and Hierarchical Cluster Analysis (Coll et al. 2007). Input parameters for the food-web model were mainly compiled from available published and non published information of the Istituto di Scienze Marine – Sede di Ancona (CNR-ISMAR, Italy) and are explain in detail in Coll et al. (2007). Biomass values (B_i) were obtained from data collection using the swept area method, sediment cores, bottom dredge sampling, acoustic surveys and information available in the literature. Production/biomass ratios $(P/B)_i$ and consumption/biomass ratios $(Q/B)_i$ were taken from the literature or obtained from the application of empirical equations using length, weight and growth data (Pauly, 1980; Pauly et al., 1990; Christensen et al., 2005). Diet composition (DC_{ij}) and assimilation rates were compiled from published information. The microbial food web was initially partially included in the original



model, by taking into account available data, in two different ways: a) through zooplankton consumption by considering detritus as a proportion of zooplankton diet, b) through zooplankton feeding as imported to the system (Coll et al. 2007).

Principal fishing activities in the area were included in the model (Bombace, 1992): bottom trawling (named Strascico), beam trawling (Rapido), mid-water trawling (Volante), purse seine (Lampara) and tuna fisheries (including purse seines, troll bait and recreational fleets). Official landings statistics from the 1990s were obtained from the governmental statistical institute (ISTAT). These data were corrected by considering discard information drawn from the literature, including by-catch of cetaceans and turtles and estimates of illegal, unregulated or unreported landings (Coll et al. 2007).

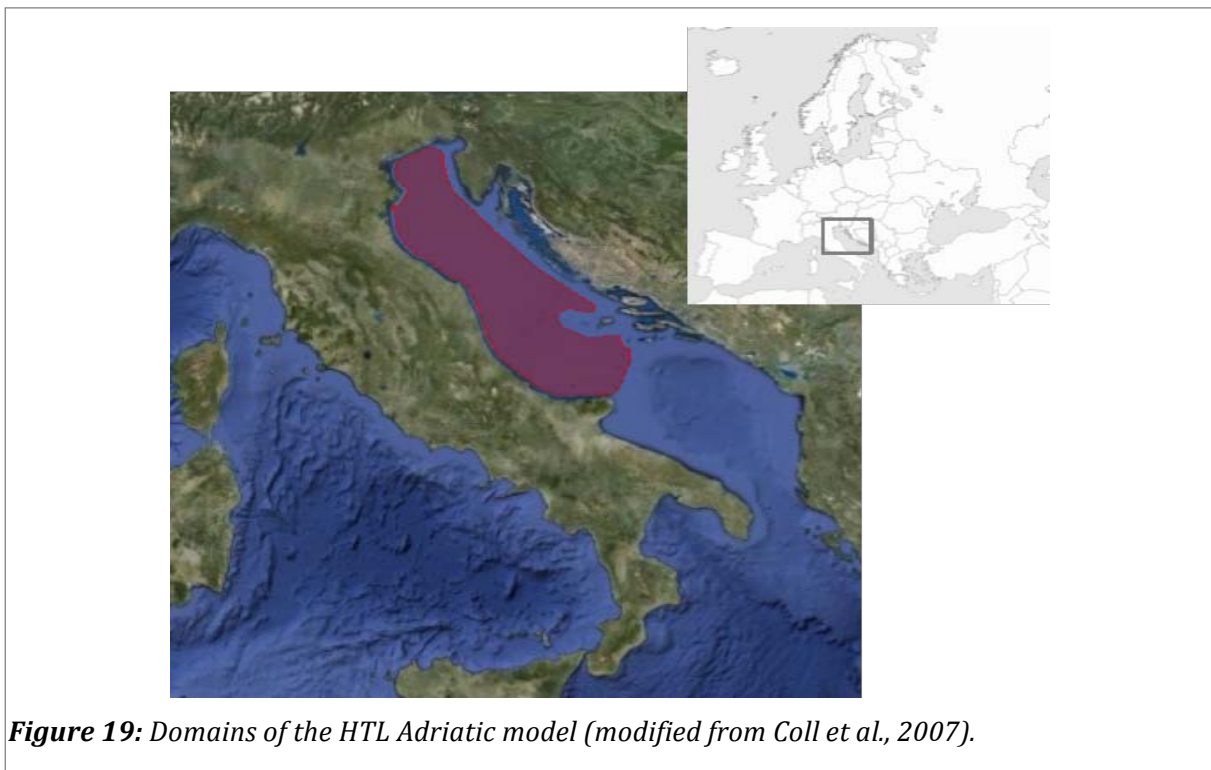


Figure 19: Domains of the HTL Adriatic model (modified from Coll et al., 2007).

Extension of the HTL model for the Adriatic E2E model

In the extension of the HTL model to comprise BFM outputs for the Adriatic domain data from 199 to 2004 were spatially and temporally averaged in order to obtain average yearly fluxes between LTL compartments ($\text{mgP m}^{-2} \text{ year}^{-1}$) and average concentrations (mgP m^{-2}). The diet composition of LTL groups were calculated using average consumption flows. Moreover exchanges between non living compartments representing degradation, excretion, faeces, remineralization, were taken from previous analyses (Libralato et al. in prep) using results from a BGC model from the Northern Adriatic Sea (Cossarini and Solidoro, 2009). The extended EwE model, however, needed for:

- modification of diet of mesozooplankton, by reducing cannibalism estimates from BFM (29%) too high to be sustained by the system; 20% of it was,



instead, set to come to from POP.

- input of P to the system were calculated from average values of Po and Adige rivers (2.69 ktonnes/year of PO4 and 5.38 ktonnes/year of total P). Assuming this to distribute to the whole Adriatic domain (about 120 000 squared km), it resulted in an imposed P inflow of 44.83 kgP m⁻² year⁻¹, equal to 44.83 mgP m⁻² year⁻¹).
- This inflow of PO4 was assumed to flow to PO4 (50%) and to equal parts in DOP and POP.
- modification of the flows from living plankton groups to non-living groups. In fact, in order to balance the PO4 consumption, it was necessary to represent the flow from DOP to PO4 (remineralization) that was represented implicitly by redirecting the 36% of the flow from living planktoners to DOP to PO4.
- the balance from input and consumptions on detritus group is usually set as export from the model, thus implicitly assuming non complete balance of the system. In the case of the ADR extended model, the surplus of detritus was set to contribute to PO4 (representing thus the release from bottom sediments).

with these modification the model is balanced with minimal outputs from all forms of non-living groups (including detritus), and complete use of PO

The detritus fate matrix for the full and standardized Adriatic models was thus defined as in the following Table 2

	Source / fate	PO4	DOP	POP	Discards	Detritus
1	Phytoplankton	0.1	0.18	0.72	0	0
2	Picophytoplankton	0.21	0.38	0.41	0	0
3	Bacteria	1	0	0	0	0
4	Nano-Microzooplankton	0.26	0.46	0.28	0	0
5	Mesozooplankton	0.054	0.096	0.850	0	0
....	all other groups of the web	0	0	0	0	1
41	Input P	0.5	0.25	0.25	0	0
42	PO4	1	0	0	0	0
43	DOP	1	0	0	0	0
44	POP	0	0.88	0	0	0.12
45	Discards	0	0	0	0	1
46	Detritus	1	0	0	0	0

Table 2: Definition of main flows from living to non-living and among non living functional groups.

Extended HTL model representing LTL groups for both initial (46 functional groups) and standardized (34 functional groups) models are represented in Figures 20 and 21 respectively. A comparison of some global indices from original and standardized food webs (Table 3 and Table 4) highlighted that the majority of them are not sensitive to structure of the model. Nevertheless, some like System Omnivory Index,



Connectance index, that are possibly related to organization are deeply affected by aggregation.

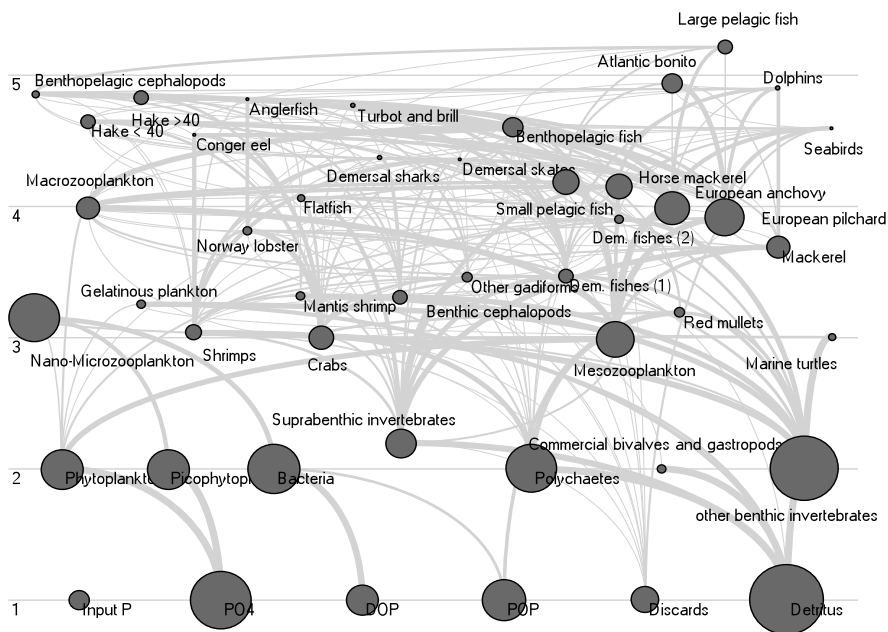


Figure 20: Food web structure of the extended model for the ADR domain (47 FG)

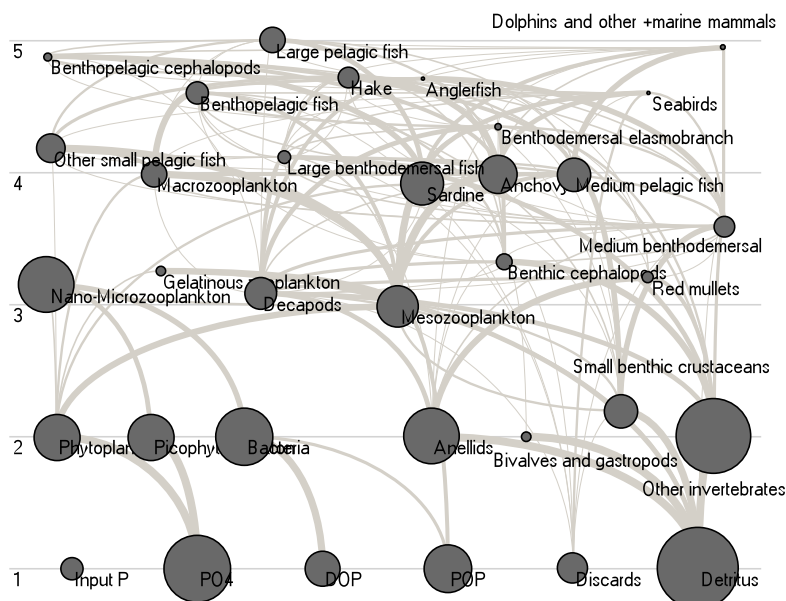


Figure 21: Food web structure of the extended model for the ADR domain standardized (34 FG)



Global indicator	Full extended model	Standardized model	Units
	46 FG	34 FG	
Sum of all consumption	11238.24	11237.99	mg P/m ² /year
Sum of all exports	7.536942	7.524261	mg P/m ² /year
Sum of all respiratory flows	-0.005499236	-0.005551111	mg P/m ² /year
Sum of all flows into detritus	9735.271	9735.26	mg P/m ² /year
Total system throughput	20981.04	20980.77	mg P/m ² /year
Sum of all production	6604.91	6604.89	mg P/m ² /year
Gross efficiency (catch/net p.p.)	0.17	0.17	
Calculated total net primary production	44.83	44.83	mg P/m ² /year
Total primary production/total respiration			
Net system production	44.84	44.84	
Total primary production/total biomass	0.11	0.11	mg P/m ²
Total biomass/total throughput	0.02	0.02	mg P/m ² /year
Total biomass (excluding detritus)	424.27	424.17	
Total catch	7.67	7.66	
Connectance Index	0.17	0.20	
System Omnivory Index	0.27	0.25	

Table 3. Ecological indicators related to community energetic, structure, flows and information theory for the Adriatic Sea extended Ecopath models (initial and standardized).

Source	Ascendency (flowbits)	Ascendency (%)	Overhead (flowbits)	Overhead (%)	Capacity (flowbits)	Capacity (%)
Full extended model (46 FG)						
Import	24.3	0.0	4.1	0.0	28.5	0.0
Internal flow	45211.7	46.3	52273.5	53.5	97485.1	99.9
Export	49.4	0.1	64.5	0.1	113.9	0.1
Respiration	0.0	0.0	0.0	0.0	0.1	0.0
Total	45285.4	46.4	52342.1	53.6	97627.5	100.0

Standardized model (34 FG)						
Import	24.3	0.0	2.8	0.0	27.2	0.0
Internal flow	45189.7	46.3	52202.1	53.5	97391.8	99.9
Export	48.5	0.0	61.9	0.1	110.4	0.1
Respiration	0.0	0.0	0.0	0.0	0.1	0.0
Total	45262.5	46.4	52266.8	53.6	97529.4	100.0

Table 4. Ascendency and other network analysis indicators for the Adriatic Sea extended Ecopath models (initial and standardized).



2.4.2.3 Gulf of Lions

Banaru D., Ballarini T. (UNIVMED)

Introduction

The Gulf of Lions (GOL), in the Northwestern Mediterranean Sea, is an important feeding area for many resident and migratory fish, seabird and marine mammal species. It is a highly productive system because of large nutrient inputs coming from the Rhone River, the coastal upwelling activity, bottom morphology and water circulation (Agostini and Bakun, 2002; Hu et al., 2009; Lefevre et al., 1997; Petrenko et al., 2005). The 20% of the French fishing fleet operates in the the GOL and 90% of the French Mediterranean landings come from this area. Many fish species of commercial interest have been intensively exploited on the GOL continental shelf for decades by the French fleets using multispecific artisanal gear such as trawlers, purse seines, gillnets and other gear (Farrugio et al., 1993; Sacchi, 2008). Current analyses on the status of Mediterranean marine ecosystems suggest that most demersal and pelagic fish stocks are fully exploited or overexploited (Aldebert and Recasens, 1996; Bas et al., 2003; FAO, 2009; Papaconstantinou and Farrugio, 2000; Sardà, 1998).

Both low trophic level (LTL) and high trophic level (HTL) models have been developed for several regions in the Mediterranean Sea. Among LTL models, Baklouti et al. (2006) developed a coupled physical-biogeochemical model for the Northwestern Mediterranean Sea while Lazzari et al. (2012) developed a coupled physical-biogeochimical model for the whole Mediterranean basin. In both these models, the highest trophic level was represented by a mesozooplankton group (Eisenhauer et al., 2009; Lazzari et al., 2012).

Among the HTL models, a mass-balance EwE model was developed by Banaru et al. (2013) for the Gulf of Lions. This model was parameterized for the period 2000-2009 and comprised an area of 20 400 km², from 0 up to 2 500 m depth. This initial model (**Ecopath GOL large**) had 40 trophic groups, including 5 groups of primary producers, detritus and discards, 12 groups of invertebrates, 18 groups of fish, 1 group of seabirds and 2 groups of marine mammals; the model units were wet weight tonnes km⁻². Other mass-balance EwE models were developed for the Adriatic Sea and the Aegean Sea (Coll et al., 2007; Tsagarakis et al., 2010). **Ecopath GOL large** model was not directly comparable with the other Mediterranean models because of differences in model spatial domain (i.e. bathymetry), different trophic groups included in the models and differences in the parameterization of trophic groups (cfr. Coll et al. 2007; Tsagarakis et al. 2010; Banaru et al. 2013).

The study area

The Gulf of Lions is located in the Northwestern Mediterranean Sea (42°26.3 N, 3°9.9 E; 43°12.6 N, 5°27.5 E). The Ecopath model represents an average annual situation over the last decade (1998–2009) of the Gulf of Lions ecosystem covering a total area of 11 000 km² and with a bathymetry between 20 and 200 m (Figure 22).

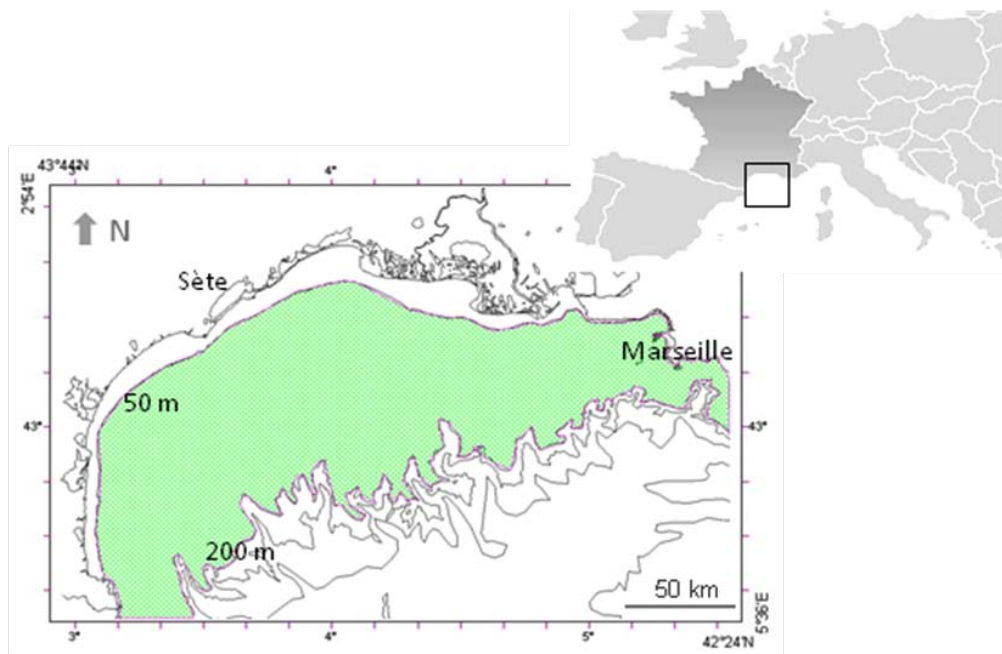


Figure 22. Study area situated on the continental shelf of the Gulf of Lions (north-western Mediterranean Sea).

The continental slope constitutes a long open boundary to the South-East of the Gulf of Lions. Along this boundary, the main mesoscale circulation feature is a strong geostrophic current, the Northern Current, which generally flows along the continental slope of the Gulf of Lions (Millot, 1999). The dominant forcing drivers in the area are the strong North-western (Tramontane) and Northern (Mistral) winds which induce strong coastal upwelling activity (Agostini and Bakun, 2002; Millot, 1999), the western Mediterranean mesoscale circulation, and the freshwater input from the Rhone River (Petrenko et al., 2005). These drivers generate important primary and secondary production and the Rhone River is an important source of dissolved and particulate organic matter in this system (Gaudy et al., 2003; Harmelin-Vivien et al., 2008; Lefevre et al., 1997). The Gulf of Lions shows a decreasing trend in nutrient concentration and production from east to west and from the continental shelf to deeper waters. The substrate is characterized by muddy and sandy bottoms. The area presents a high diversity of organisms and many aspects of their ecology and biology have been investigated over the past decades (Beaubrun, 1995; Hermand et al., 2008; Labruno et al., 2007; Mellon-Duval et al., 2009).

Modifications to Ecopath GoL large model to create GoL shelf model

Input parameters of the **GoL large** model were : B (biomass), P/B (production/biomass ratio), Q/B (consumption/biomass ratio), EE (ecotrophic efficiency) for some groups, U/Q (assimilation rate estimated from the ratio unassimilated/consumed food), catch and discards, diet composition and net migration rate (estimated as “imports” in the diet). Biomass and fisheries data come from Ifremer MEDITS and PELMED scientific campaigns onboard on the oceanographic vessel Europe and from Fisheries Information System (IFREMER). Detailed description of the other data sources for **GoL large** model are described in



Banaru et al. (2013). The initial **Ecopath GoL large** model was reduced in term of covered area and in term of number of groups to be standardized with the other models in the Mediterranean Sea. Some groups from the **Ecopath GoL large** model were removed (benthic primary producers like microphytobenthos, *Posidonia*, benthic macrophytes that were very close to the coast mainly less than 20 m depth, whales that do not come on the shelf) while some groups were lumped together.

Annelids in **GoL shelf** model correspond to worms in **GoL large**. Bivalves and gastropods remained the same as before. In the **GoL large** model, there were two cephalopods groups: octopus and cuttlefish and squids. These two groups were reorganized in benthic cephalopods (including octopus and squids) and benthopelagic cephalopods (including squids only). Small benthic crustaceans (all small crustaceans like isopods and amphipods, excepting decapods) in **GoL shelf** represent one part of benthic crustaceans in **GoL large**. Decapods in **GoL shelf** comprise pagurids, shrimps, brachiurids and lobsters. Other benthic invertebrates in **GoL shelf** comprise echinoderms and all the groups in other benthic invertebrates in **GoL large**. Fish feeding on plants in **GoL large** becomes part of benthic-demersal medium in GOL-shelf (*Boops boops*) (while *Salpa salpa* feeding mainly on benthic primary producers and being present mainly between 0 and 20 m depth was no longer represented in **GoL shelf**). For the other groups that were feeding partly on the benthic primary producers, their diet has been changed and it was apportioned on the detritus group. Benthic-pelagic medium in **GoL shelf** comprises Atlantic mackerel, Mediterranean horse mackerel, Atlantic horse -mackerel and *Scomber colias* (which was a part of pelagic fish feeding on fish in **GoL large**). Benthopelagic fish in GOL-shelf comprises bluewithing, that was alone in **GoL large**. Large pelagic fish in GOL-shelf comprises of Atlantic bluefin tuna, swordfish (before, swordfish was part of pelagic fish feeding on fish in **GoL large**). Red mullets have a low biomass in the Gulf of Lions ecosystems and in the GOL large model were comprised in fish feeding on benthos group; in the **GoL shelf**, however, model they are considered as a group on its own because they are important in terms of biomass in the other Mediterranean ecosystems. Benthic-demersal medium in **GoL shelf** comprises poor cod, fish feeding on benthic crustaceans, seabream and fish feeding on polychetes from **GoL large**. Hake and anglerfish remained unchanged. Benthic-demersal elasmobranch were a part of benthic-demersal fish feeding on fish in **GoL large** but are now a separate group in **GoL shelf** model. Even if their biomass is rather low this separation was made for conservation purposes and to allow with modeling tools the evaluation of their role in the foodweb. Large benthic-demersal fish in **GoL shelf** comprises large benthic-demersal fish from benthic-demersal fish feeding on fish in **GoL large** plus conger that was alone before.

The biomass of each trophic group included in Gol shelf model was recalculated to correspond to the smaller spatial model domain in respect to Gol large. The other model input parameters were scaled to take into account the different species / taxonomic groups included in each model group. The P/B and Q/B ratios were weighted by the biomass of the species included in the model groups. The P/B value for the dolphins group was recalculated to 0.06. The Q/B values for the invertebrate groups were reconstructed considering the gross growth efficiency (Towsend et al. 2003). Diets were aggregated on the basis of group biomass. Compared to **GoLlarge**, in **GoLshelf** diets were improved for cephalopods, mackerels and horse mackerels using with recent results from the Gulf of Lions (Banaru et al., pers. comm.). Landings



and discards were recalculated by gear for the **GoL shelf** area.

Units of the model are initially expressed in $t\ km^{-2}\ y^{-1}$ wet weight organic matter for flows and $t\ km^{-2}$ for biomasses. Then this units were transformed into wet weight carbon and finally into mg phosphorous using the ratio C:N:P of 88.5:1 (Sterner and George, 2000; Hjerne and Hansson, 2002).

Constructing the end-to-end model for the Gulf of Lions

The end-to-end model for the Gulf of Lions (**end-to-end GoL**) was built linking the HTL **GoL shelf** model with the LTL OPATM-BFM model (Lazzari et al., 2012). The **E2E GoL** model comprises 5 new groups that come from the LTL model: Input PO₄, PO₄, DOP (Dissolved Organic Phosphorus) and POP (Particulate Organic Phosphorus) and bacteria. In the E2E model, the Input PO₄ group is considered as the only “producer” in the system; PO₄, DOP and POP are considered as “detritus” groups; the bacteria are a “consumer” group. Phytoplankton and zooplankton groups, which were represented also in the HTL model, were reparameterised with the data from the OPATM-BFM model corresponding to the **GoL shelf** area model and both of these groups are considered as “consumers” in the E2E model. Treating the phytoplankton groups as “consumers” require a recalculation of the trophic level for the all the consumer groups in the E2E model (not treated in the results).

Gol shelf mass-balance

The Gol shelf model was mass-balanced following the same strategy used by Banaru et al. (2013) to mass-balance the Gol large model. The Automatic Mass Balance Procedure (Kavanagh et al., 2004) was used after having modified some data with higher uncertainty in terms of biomass. These changes concerned some invertebrates (cuttlefish-squids and echinoderms) and fish species (other planctono- phagous fish, blue whiting, Atlantic horse mackerel and European conger). For the majority of these groups initial biomass was assessed by the swept area method applied to experimental trawl survey data. In these cases the alternative input of EE taken from other studies in similar areas in the literature was used to estimate the biomass of species/groups from the food demands of the upper levels and fisheries.

The model was considered balanced when: (1) realistic estimates of the missing parameters were obtained ($EE < 1$); (2) values of production/consumption ratios (P/Q, or gross efficiency of food conversion) for functional groups were between 0.10 and 0.35 with the exception of fast growing groups with higher values and top predators with lower values; (3) values of respiration/biomass ratios (R/B) were consistent with the group's activities with high values for small organisms and top predators; (4) values of respiration/food assimilation ratios (R/A) were < 1 and values for top predators were higher; (5) values of net efficiency of food conversion were < 1 for all the functional groups (Christensen et al., 2005). The “pedigree” of input data was recorded, identifying whether it was taken from a model of a similar system, or based on a rough or precise estimate from local data. These values were then used to assess model quality (Pauly et al., 2000; Christensen and Walters, 2004; Christensen et al., 2005).



Results and discussion on the characteristics of the GoL foodweb

Structure of the Ecopath GoL shelf model

The structure of the **Ecopath GoL shelf** high trophic level model includes 29 groups: 2 primary producers, 4 zooplankton groups, 7 invertebrates groups, 12 fish groups, 1 seabirds, 1 dolphins and 2 detritus groups (detritus and discards) (Figure 23). It also includes 9 fishing gears represented here at their mean trophic level of exploitation. This model, as well as the **GoL large** model, represents more than 99% of the biomass of the exploited fish and invertebrate species in the Gulf of Lions. The structure of the **end-to-end GoL** model includes 34 groups, considering the 5 supplementary groups from the LTL model: bacteria, Input PO4, PO4, DOP and POP. All the trophic links between groups were represented in Figure 24.

Flows of predation, consumption, flows to detritus, catchers and export are represented in Figure 25. Biomass, consumption and flows to detritus decrease with increasing trophic level. The highest catches occur at the 4th trophic level corresponding to the 3th one in the initial HTL model and mainly to small pelagic fish. The same flows were represented for the Ecopath GoL large model in Banaru et al. (2013). However they are not comparable because of high differences in covered areas, model groups and units.

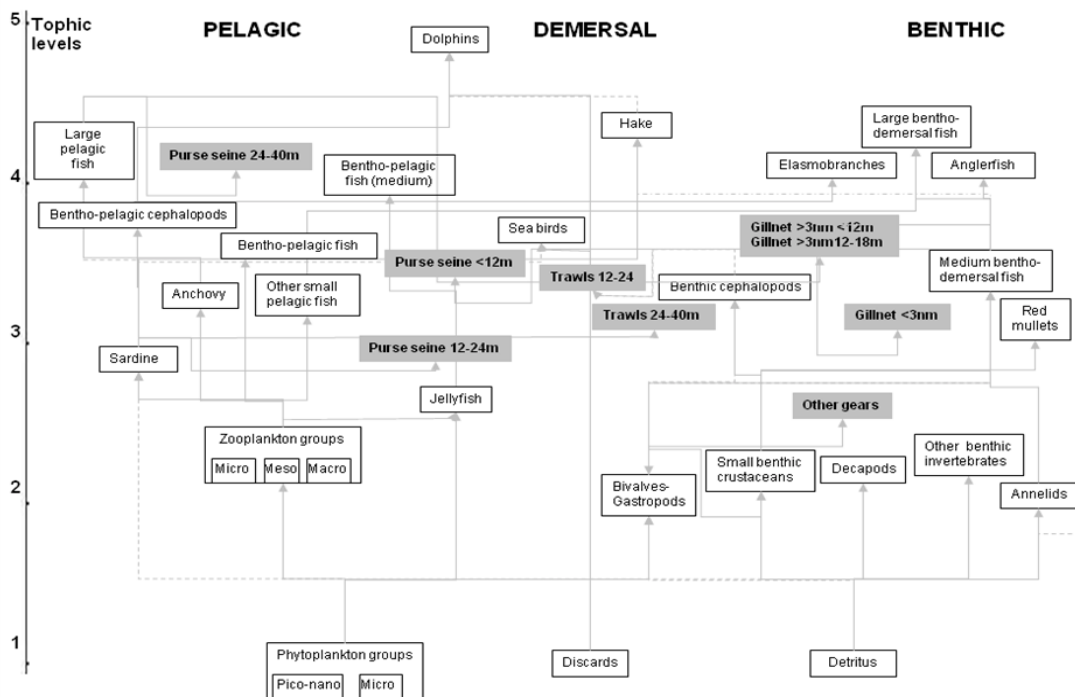


Figure 23. Structure of the pelagic, demersal and benthic food web in the **Ecopath GoL shelf** model. The links between the different compartments show the trophic flows. Continuous arrows indicate main flows and dotted arrows indicate less important flows.

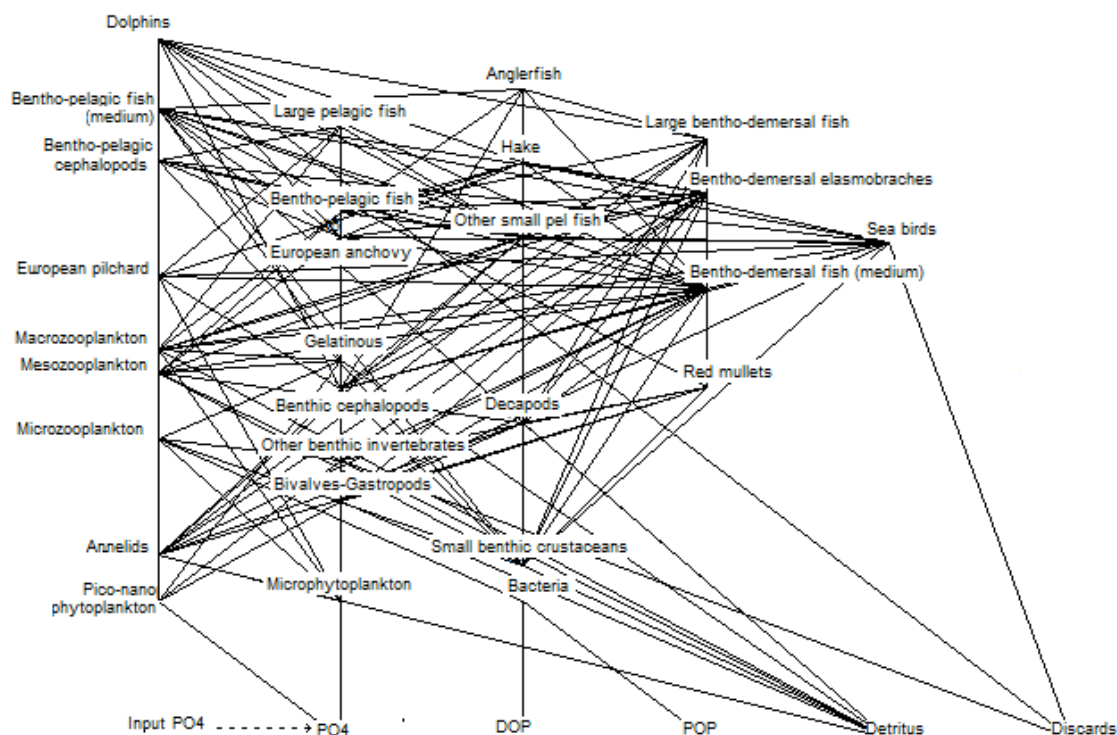


Figure 24: Structure of the foodweb in the end-to-end *Ecopath GoL shelf* model. The links between the different compartments show the trophic flows.

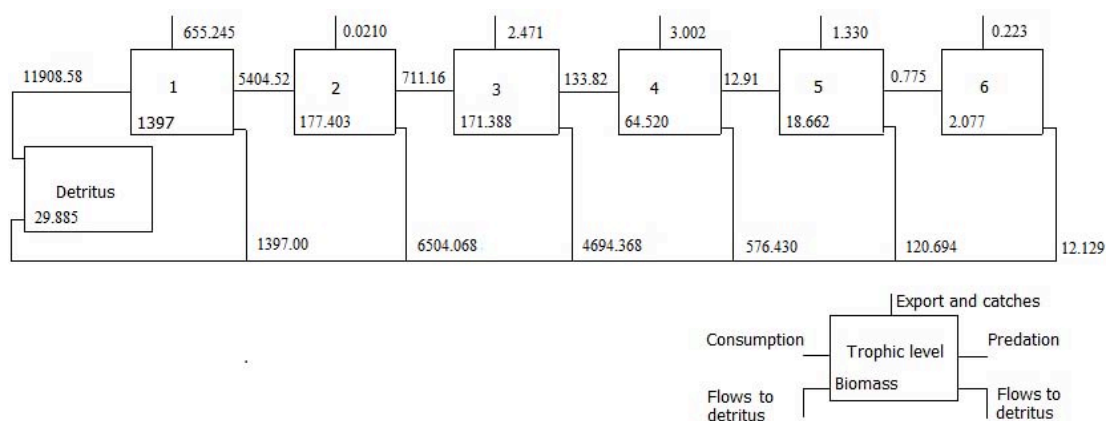


Figure 25: Lindeman spine of the end-to-end *Ecopath GoLshelf* model: flows between trophic levels ($mg P m^{-2}$).

The highest biomass in the end-to-end GoL shelf model is represented by the detritus groups (82.2%) (Table 5). Excluding detritus, benthic invertebrates present the highest biomass (38.8%) followed by small pelagic fish (19.7%), zooplankton and bacteria groups. Excluding plankton and bacteria, the majority of the biomass is represented by benthic invertebrates (59.2%) and small pelagic fish (30.0%). When benthic demersal invertebrates are also excluded, the percentage of biomass of small pelagic fish increase to (73.6%), followed by medium benthic demersal fish (16.8%). Keystone groups like seabirds and dolphins (Banaru et al., 2013) represented less than 0.1% in biomass and large predator fish represented 1.3% in the benthic-



demersal compartment and 0.5% in the pelagic one.

This composition of biomass indicate a highly exploited system with low level of predators, dominated by small pelagic fish and controlled mainly bottom-up by plankton and microorganisms of low trophic level. As indicated by Banaru et al. (2013), small pelagic fish play an important role in energy transfer in the the Gulf of Lions ecosystem, being a link between the plankton groups and the top predators and between the pelagic and benthodemersal compartments.

Consumption

Detritus represents the most consumed groups in the model (Table 6). Excluding detritus, phytoplankton, zooplankton and bacteria groups presented the highest values in term of consumption (between 26 and 32.3%). When excluding these groups, benthic invertebrates become the most important ones (66.8%), followed by small pelagic fish (25.5%). Among fish groups, the most consumed in the food web are the small pelagic fish (76.8%) followed by medium benthodemersal fish groups (14.9%).

Mortality

In the end-to-end GoL model / Ecopath GoL shelf model, predation is the main cause of mortality for phytoplankton groups, bacteria, most of the invertebrates groups (excepting jellyfish, microphytoplankton and microzooplankton. This was also the case for small pelagic fish groups, benthopelagic fish, red mullets and benthodemersal fish (medium). Other fish groups die mainly because of fisheries, with the exception of benthopelagic fish (medium) and benthodemersal elasmobranchs that who died in large percentage by natural causes. For the European pilchard and European anchovy, which are the two fish species with the highest landings in GoL area, the first cause of mortality is predation (60.2-93.5%).

Table 5. Percentages of the biomass in the end-to-end GoL shelf model. The trophic groups of the model were aggregated to simplify the interpretation.

Biomass	% of the total biomass	% excluding detritus	% excluding plankton and bacteria	% excluding plankton, bacteria and benthic invertebrates
Phytoplankton	1.3	7.5		
Bacteria	2.2	12.2		
Zooplankton	2.6	14.8		
Benthic invertebrates	6.9	38.8	59.2	
Small pelagic fish	3.5	19.7	30.0	73.6
Medium benthopelagic fish	0.4	2.1	3.2	7.8
Large pelagic fish	0.0	0.1	0.2	0.5
Medium benthodemersal fish	0.8	4.5	6.9	16.8
Large benthodemersal fish	0.1	0.3	0.5	1.3
Sea birds	0.0	0.0	0.0	0.0
Dolphins	0.0	0.0	0.0	0.0
Detritus groups	82.2			



Table 6. Percentages of the biomass consumed in the end-to-end GoL shelf model. The trophic groups of the model were aggregated to simplify the interpretation.

Consumption	% of the total biomass	% excluding detritus	% excluding plankton and bacteria	% excluding plankton and invertebrates	% excluding bacteria and benthic
Phytoplankton	14.7	26.0			
Bacteria	16.2	28.7			
Zooplankton	18.3	32.3			
Benthic invertebrates	4.9	8.7	66.8		
Small pelagic fish	1.9	3.3	25.5		76.8
Medium benthopelagic fish	0.2	0.3	2.5		7.4
Large pelagic fish	0.0	0.0	0.1		0.3
Medium benthodemersal fish	0.4	0.6	5.0		14.9
Large benthodemersal fish	0.0	0.0	0.2		0.5
Sea birds	0.0	0.0	0.0		0.1
Dolphins	0.0	0.0	0.0		0.0
Detritus groups	43.4				

Mixing trophic impact

Direct and indirect interactions between trophic groups were analyzed using the mixed trophic impact (MTI) routine and are shown in Figures 26 and 27a. These analyses describe increases or decreases in the biomass of a group that are to be expected if hypothetical changes in the biomass of another group occur. Direct impact resulting from trophic interactions can be underlined but also indirect impact due to prey availability and niche overlapping as well as to cascade effects. The mixing trophic impact analysis showed that the PO₄, detritus, plankton groups such mesozooplankton, microphytoplankton, macrozooplankton, European pilchard and small benthic crustaceans had highest positive impact on the entire system. They represent the main food sources in the system, while some of their predators like benthopelagic fish, bacteria, decapods etc had the highest negative impacts in the system.

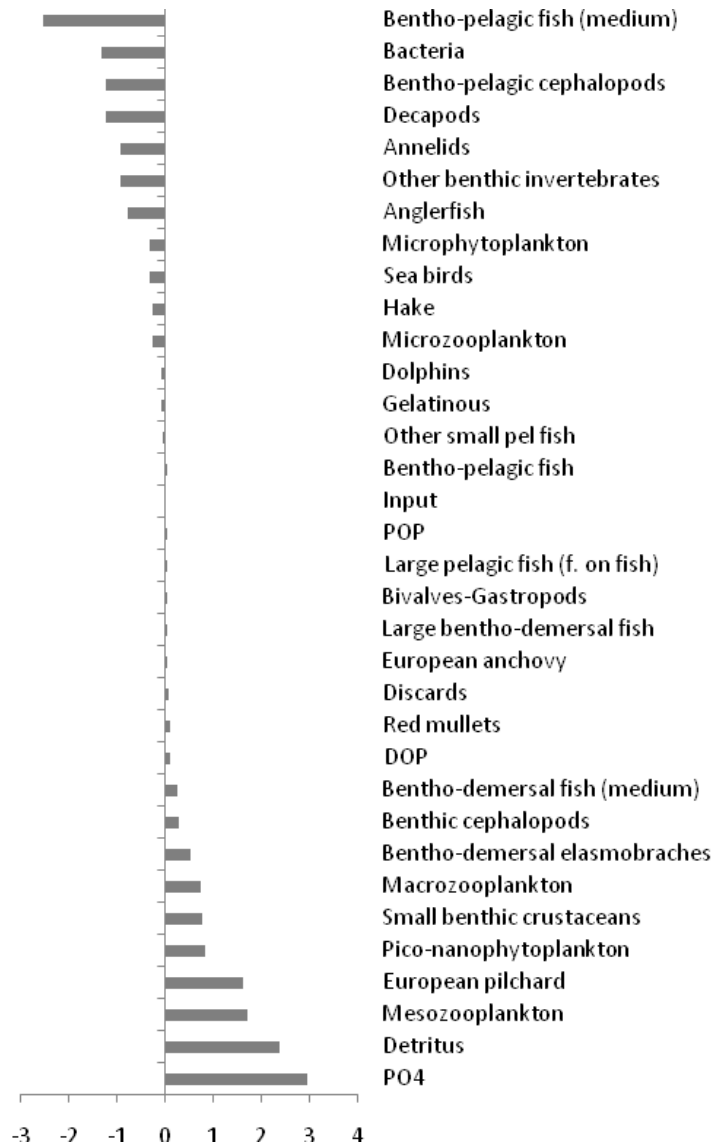


Figure 26. Graphic representation of the mixed trophic impact of each functional group on the other groups.

Fisheries catches and impact

Fisheries are represented by 9 gears in the end-to-end GoL shelf model. Large trawls (24-40 m) represent 71% of total catches (landings and discards), followed by trawls (12-24 m) (17%) and purse seine (12-24 m) (4%).

These gears target different species and they all have negative mixing trophic impact on the entire GoLshelf system (Figure 27b). Some fisheries, such as the trawls (both 24-40 m and 12-24 m) catch many species, while other fisheries are more selective, such as the purse seine (< 24 m). Purse seine gears (< 24 m) have lower negative mixing trophic impact on the ecosystem than nets with higher landings but less selective. Purse seine (24-40 m) is the most selective fishery targeting only large pelagic fish and in rather low quantities compared to other gears, but its negative impact is high (Figure 27a). This negative impact may be explained by cascade effects through the food web because the large pelagic predators consume small pelagic fish,



which in turn consume zooplankton and these groups represent highly important food resource in the GoL system.

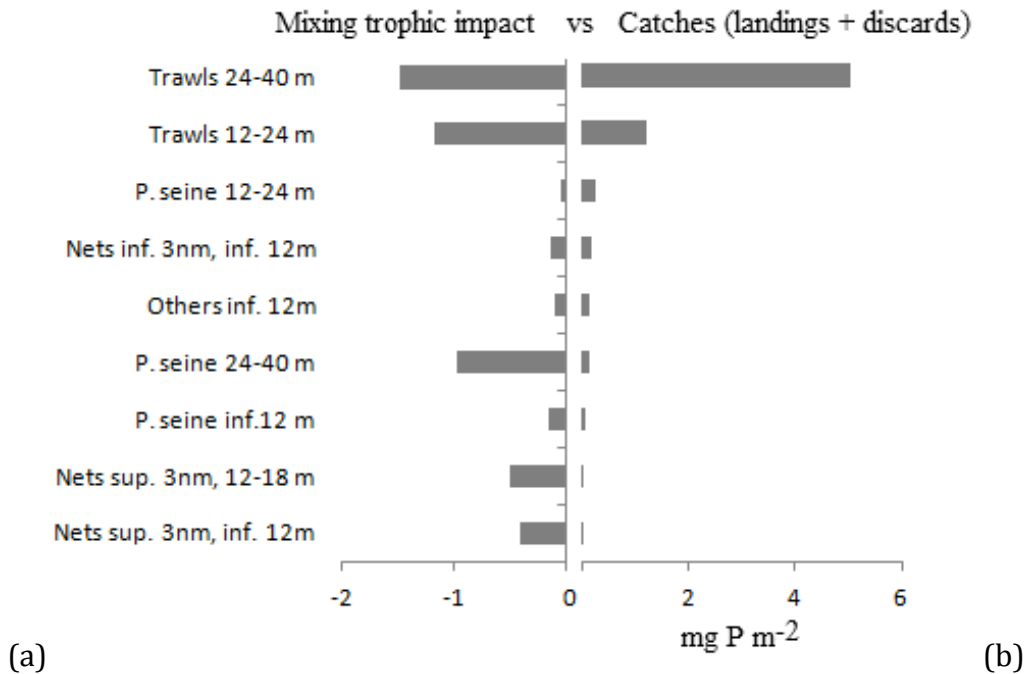


Figure 27. Graphic representation of (a) the cumulated mixed trophic impact of each gear on the other groups and (b) catches (where catches represent the sum of landings and discards) by gear.

Summary statistics and indicators

Results from the ecological Ecopath GoL shelf model in terms of aggregated summary statistics, network flows and information indices are shown in Table 7. The same indicators were represented for the Ecopath GoL large model (see Banaru et al., 2013). However they are not comparable because of high differences in covered areas, model groups and units.

Table 7 shows the indicators of marine ecosystem state estimated from the end-to-end GoL model; these indicators can be considered as being representative of the “health” of the Gulf of Lions as proposed by Costanza and Mageau (1999). Total system throughput is related to vigor, capacity is related to the organization, overhead is related to resilience, and ascendancy is related both to vigor and organization. These indicators combined together might be used to characterize the “health” of marine ecosystems (Costanza and Mageau; 1999).

The indicators are not absolute measures of ecosystem state, they are relative values that can be used to compare one marine ecosystem over time or to compare several marine ecosystems one in respect to the other (see final discussion on the comparison between Gulf of Lions, Adriatic and Aegean seas).



Table 7. Ecological indicators related to community energetic, structure, flows and information theory. Bold characters indicated results of the Ecopath GoL shelf model related to vigor, organization and resilience.

Global indices	index	Unit
Sum of all consumption	18995.8	mg P/m ² /year
Sum of all exports	662.307	mg P/m ² /year
Sum of all respiratory flows	0	mg P/m ² /year
Sum of all flows into detritus	14563.72	mg P/m ² /year
Total system throughput	34222	mg P/m²/year
Sum of all production	12801	mg P/m ² /year
Gross efficiency (catch/net p.p.)	0.005055	
Calculated total net primary production	1397	mg P/m ² /year
Total primary production/total biomass	0.763	
Total biomass/total throughput	0.054	
Total biomass (excluding detritus)	1831.201	mg P/m ²
Total catches	7.062	mg P/m ² /year
Connectance Index	0.187	
System Omnivory Index	0.237	
Ascendency	77544.1	(flowbits)
Ascendency	46.8	(%)
Overhead	87981.2	(flowbits)
Overhead	53.2	(%)
Capacity	165525.3	(flowbits)
Throughput cycled (excluding detritus)	0	mg P/m ² /year
Predatory cycling index	0	% of throughput w/o detritus
Throughput cycled (including detritus)	25867.75	mg P/m ² /year
Finn's cycling index	75.59	% of total throughput
Finn's mean path length	51.67	-
Finn's straight-through path length	10.711	without detritus
Finn's straight-through path length	12.613	with detritus

The end-to-end GoL shelf model was built following a standardized model structure that allows comparison with end-to-end models developed for the Adriatic Sea and the Aegean Sea marine ecosystems. The present work might be considered as first step into the development of a large end-to-end modeling approach in the Mediterranean Sea. Important datasets and ecological knowledge are necessary to



construct an end-to-end model from nutrients and bacteria up to fish and fisheries. Both Ecopath Gol large and shelf models were constructed using Ifremer scientific databases from this area. The comprehension of a complex marine ecosystem cannot be done with ecological data from other areas as it is currently done in many studied due to data gaps. Scientific field campaigns, new methods of biomass estimation for some species, laboratory studies of organisms' diets and integration of local data into foodweb model are essential in order to improve them and to be able to provide information for the management of these ecosystems.

The results of the present work contribute to characterize the descriptors D4 marine food webs and D3 exploited species of the MSFD in the Gulf of Lions (Northwestern Mediterranean Sea) and to estimate and compare the "health" of Mediterranean foodwebs.

In spite of a good pedigree of the model (0.67), and high quantities of data available for the Gulf of Lions, we should continue to consider the limits of this modeling approach (see "Improvements and limits of the data sources" in Banaru et al. (2013)) and continue efforts to improve field ecological knowledge of this area. Complementary methods of modeling (spatial, individual-based models) are recommended to be used in order to bring a better comprehension of the system.

2.4.2.4 Aegean Sea

K. Tsagarakis, A.Machias, S.Somarakis, M.Giannoulaki, C. Frangoulis (HCMR)

North Aegean Sea ecosystem and fisheries

The North Aegean Sea ecosystem (N. Aegean Sea; Thracian Sea and Strymonikos Gulf; Figure 28) is among the most productive areas in the otherwise oligotrophic Eastern Mediterranean Sea (Lykousis *et al.*, 2002; Bosc *et al.*, 2004). This feature is due to (a) the influence of nutrient rich, low saline, Black Sea water occupying the surface water layers (Stergiou *et al.*, 1997; Lykousis *et al.*, 2002), (b) river flows that locally enhance the productivity of the coastal zone (Karageorgis *et al.*, 2003), and (c) the extended continental shelf. Wide *Posidonia oceanica* meadows extend up to a maximum depth of 25 m while other macrophytes are also found to slightly deeper bottoms (Orfanidis *et al.*, 2005). Sand (approximately with 40-90% content) and mud (approximately with 10-60% content) dominate the surface sediments in the area (Karageorgis *et al.*, 2005). Several parts of the area have been identified as important habitats, spawning and nursery grounds for small pelagic (Giannoulaki *et al.*, 2011; Tugores *et al.*, 2011; Giannoulaki *et al.*, 2013) and demersal fish (Politou, 2007; Katsanevakis *et al.*, 2009). The invasive ctenophore, *Mnemiopsis leidyi* a species associated with the collapse of pelagic fish resources in the Black Sea during the early 90's, has recently entered the N. Aegean Sea (Shiganova *et al.*, 2001).

The N. Aegean Sea fisheries catches represent 30% of total Greek landings (El.Stat., 2011) despite the fact that the local continental shelf accounts for less than 15% of the country's continental shelf. More than 60 bottom trawlers, 40 purse-seiners and 1080 artisanal boats operate in the area, while pelagic trawls are banned according to Greek legislation. Small pelagic fish (anchovy, *Engraulis encrasicolus*, and sardine, *Sardina pilchardus*) dominate landings and are mainly caught by purse seiners. Trawls primarily target European hake (*Merluccius merluccius*), red mullets (*Mullus*



barbatus), commercial shrimps (*Parapenaeus longirostris*), and cephalopods (such as *Octopus vulgaris* and *Eledone spp.*) (Stergiou *et al.*, 2003). Artisanal boats use several fishing gears targeting different species: long lines target mostly hake and large pelagic fish (e.g., bluefin tuna *Thynnus thynnus*), while static nets target a large number of demersal and pelagic species (e.g., cephalopods, medium pelagic fish, mullets). An important pot fishery targeting octopuses also exists in the area and operates exclusively in shallow waters (<40m). Thus, fishing activities can be characterized as dynamic and intense in the study area.

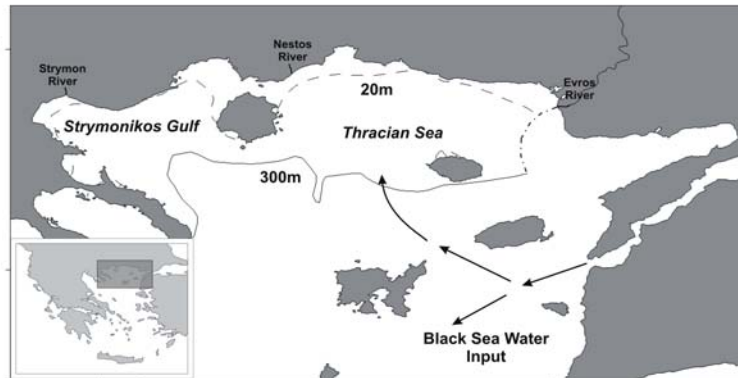


Figure 28. North Aegean Sea (Strymonikos Gulf and Thracian Sea). Isobaths of 20m and 300m which define the model area are shown, as well as the most important rivers of the area. Arrows indicate the direction of Black Sea Water Input.

North Aegean Sea HTL model

The model area is defined by the 20 m and 300 m isobaths (Figure 1) covering 8374 km² in total. This is mainly the area where trawlers, purse seiners and the biggest fraction of artisanal fleets operate. The coastal zone (<20 m deep) where *Posidonia oceanica* seabeds are mainly found was excluded from the modelling exercise since species composition is very different in seabeds dominated by seagrasses compared to the rest of the ecosystem. Moreover, quantitative information concerning species composition and their biomasses was limited over the seagrass meadows in the area. The HTL model is based on the previously developed ecopath model in the area for the period 2003-2006 (Tsagarakis *et al.*, 2010). This model was adjusted to input data from the 1990s, averaging data from separate years. The 1990s model has a slightly modified structure in comparison to the 2003-2006 model. Specifically, no multi-stanza groups are considered in the '90s model, while "Blue whiting" and "Gastropods & Bivalves" are described as explicit groups in the '90s model (see Table 1), which was not the case for the 2000s one.

Input data for the 1990s model included bottom trawl surveys (Bertrand *et al.*, 2002; Labropoulou and Papaconstantinou, 2004), fisheries (El.Stat., 2011) and discards (Anon, 2008) data and other sources of information described in detail in Tsagarakis *et al.* (2010). For each species, production and consumption values were retrieved from the literature (Froese and Pauly, 2012) or estimated based on empirical equations (Pauly, 1980; Pauly *et al.*, 1990), while for multispecies functional groups (FG) these values were weighted with the relative biomass of each species in the FG. Input for diet composition was also based on a literature review. Finally, several small modifications were also made based on updated literature information (e.g. for



sardine diet, Nikolioudakis *et al.*, 2012).

In a next step, the FGs of this 1990s model were aggregated based on a common structure, as defined within the PERSEUS project meetings. Specifically, the aggregated standardized model structure included 11 FGs less than the extended model (Table 8), while it didn't take into account Loggerhead turtles which were excluded from the common structure.

Towards constructing an end-to-end model, the previously described models were coupled with LTL groups, using data outcomes of the BFM biogeochemical model (Lazzari *et al.*, 2010), following the methodology of Libralato and Solidoro (2009). The BFM outcomes included biomass, production, consumption and diets of five plankton groups (Phytoplankton, Picophytoplankton, Bacteria, Nano-microzooplankton and Mesozooplankton) and four detritus groups (Input PO₄, PO₄, DOP and POP), while the parameterization proposed by Libralato and Solidoro (2009) was followed. Since the originally developed HTL models were in wet weight while LTL model outputs were in mg P m⁻², standard conversion factors from WW to C and from C to P were used to develop the model in the finally required format.

Table 8. Functional groups of the aggregated model corresponding to the extended model

Extended model	Aggregated model	Extended model (cont.)	Aggregated model (cont.)
Phytoplankton	Phytoplankton	Blue whiting	Benthopelagic fish
Picophytoplankton	Picophytoplankton	BepeFish	
Nano-microzooplankton	Nano-microzooplankton	Medium pelagic fish	Large pelagic fish
Mesozooplankton	Mesozooplankton	Large pelagic fishes	
Macrozooplankton	Macrozooplankton	Mulletts	Red mulletts
Gelatinous zooplankton	Gelatinous zooplankton	Flatfishes	Medium benthodemersal fish
Annelids	Annelids	Other gadiforms	
Bivalves and gastropods	Bivalves and gastropods	DemeFish1	
Benthic cephalopods	Benthic cephalopods	DemeFish3	
Benthopelagic cephalopods	Benthopelagic cephalopods	DemeFish4	
Suprabenthos	Small benthic crustaceans	Hake	Hake
Shrimps	Decapods	Anglerfish	Anglerfish
Crabs		sharks	Benthodemersal elasmobranches
Norway lobster		rays & skates	
Other invertebrates	Other invertebrates	DemeFish2	Large benthodemersal fish
Sardine	Sardine	Sea birds	Seabirds
Anchovy	Anchovy	dolphins	Dolphins and other marine mammals
picarels and bogue	Other small pelagic fish	Discards	Discards
Other Small pelagic fishes		Detritus	Detritus
Horse mackerel	Medium pelagic fish	Loggerhead turtle	/
Mackerel			



Structure of the food web

The flow diagrams of the coupled extended and aggregated models are shown in Figures 29 and 30 respectively. Large pelagic fish and dolphins were the top predators in both models. The Trophic Level (TL) of all FG are shifted by approximately one unit due to the parameterization of primary producers as consumers, preying upon detritus groups.

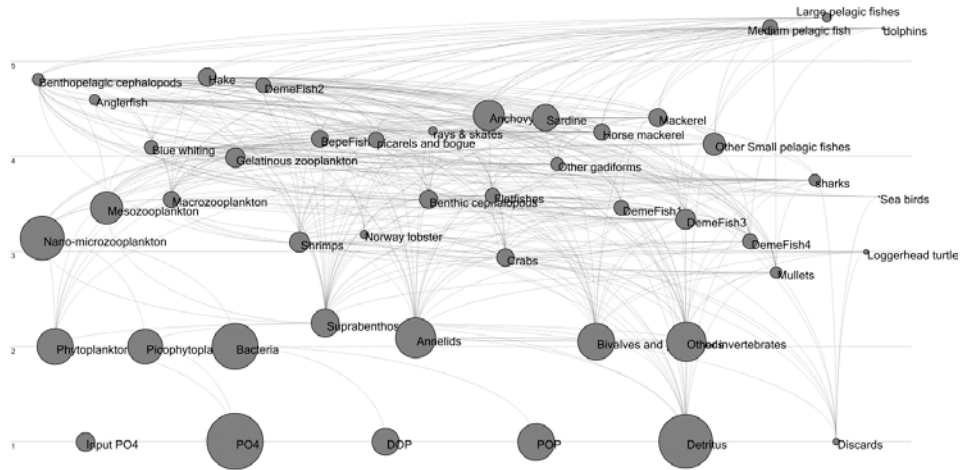


Figure 29. Food web structure of the extended model

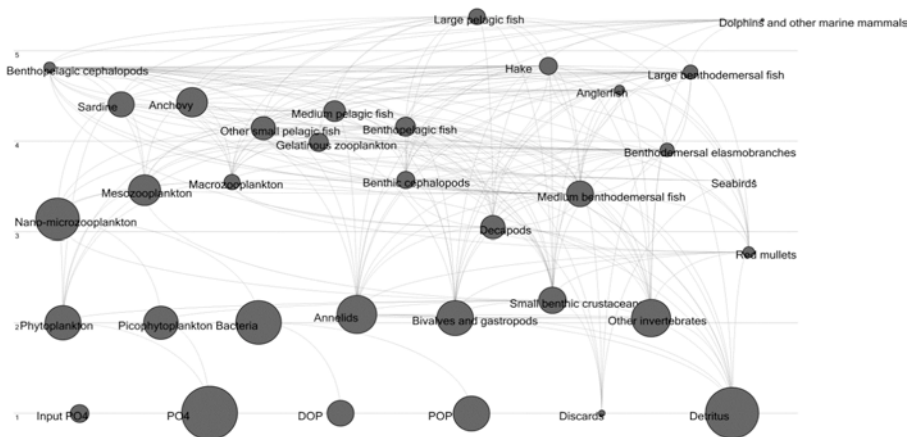


Figure 30. Food web structure of the aggregated model

The highest biomass correspond to the detritus groups (60.6%), while the of planktonic groups dominate in terms of biomass among the living organisms (~57%, excluding detritus; Table 9). The groups of benthic invertebrates followed in terms of biomass while among the vertebrates, small pelagic fish species had the highest biomass (51.8% among vertebrates; Table 9). Small pelagic fish constitute a link between the plankton and top predators and in a lesser extent between benthic and pelagic groups. For these reasons, they have been shown to have high keystone



values in the N. Aegean Sea ecosystem (Tsagarakis et al., 2010).

FG	% of the total biomass	% excluding detritus	% excluding plankton and bacteria	% excluding plankton, bacteria and benthic invertebrates
Phytoplankton	4.7%	11.9%		
Bacteria	8.8%	22.3%		
Zooplankton	8.9%	22.6%		
Benthic invertebrates	12.3%	31.2%	72.2%	
Small pelagic fish	2.5%	6.2%	14.4%	51.8%
Medium benthic-pelagic fish	0.4%	1.0%	2.3%	8.1%
Large pelagic fish	0.2%	0.5%	1.1%	3.9%
Medium benthic-demersal fish	1.2%	3.0%	6.9%	24.7%
Large benthic-demersal fish	0.5%	1.4%	3.1%	11.3%
Sea birds	0.0%	0.0%	0.0%	0.0%
Dolphins	0.0%	0.0%	0.0%	0.2%
Detritus groups	60.6%			

Table 9. Percentages of the biomass in the end-to-end North Aegean Sea 1990s model. The trophic groups of the model were aggregated to simplify the interpretation.

Consumption

Detritus groups were the most consumed groups (Table 10), followed by the planktonic groups. As in the allocation of biomass, the importance of benthic invertebrate groups was shown when excluding detritus and plankton, while again, small pelagic fish was the most important prey among vertebrates (Table 10), in line with their high keystoneess.

FG	% of the total biomass	% excluding detritus	% excluding plankton and bacteria	% excluding plankton, bacteria and benthic invertebrates
Phytoplankton	17.3%	30.6%		
Bacteria	18.9%	33.3%		
Zooplankton	16.9%	29.9%		
Benthic invertebrates	2.6%	4.6%	74.9%	
Small pelagic fish	0.5%	0.9%	14.0%	55.5%
Medium benthic-pelagic fish	0.1%	0.1%	1.8%	7.2%
Large pelagic fish	0.0%	0.0%	0.4%	1.4%
Medium benthic-demersal fish	0.3%	0.4%	7.1%	28.4%
Large benthic-demersal fish	0.1%	0.1%	1.7%	6.9%
Sea birds	0.0%	0.0%	0.1%	0.3%
Dolphins	0.0%	0.0%	0.1%	0.3%
Detritus groups	43.4%			

Table 10. Percentages of the biomass consumed in the end-to-end North Aegean Sea 1990s model. The trophic groups of the model were aggregated to simplify the interpretation.



Mixed trophic impact

The Mixed Trophic Impact analysis (MTI) quantifies the trophic impact that a hypothetical change in the biomass of a group would have on each functional group including fisheries. Cumulative MTI of each FG, analyzed using the Mixed trophic impact routine of the EwE software, are shown in Figure 31. Detritus, phytoplankton, mesozooplankton and anchovy had the highest positive MTI, since they constitute the most important preys of the food-web. On the contrary, the FGs with the highest negative MTI were annelids, picophytoplankton (which were set to prey upon detritus groups), bacteria and benthopelagic cephalopods.

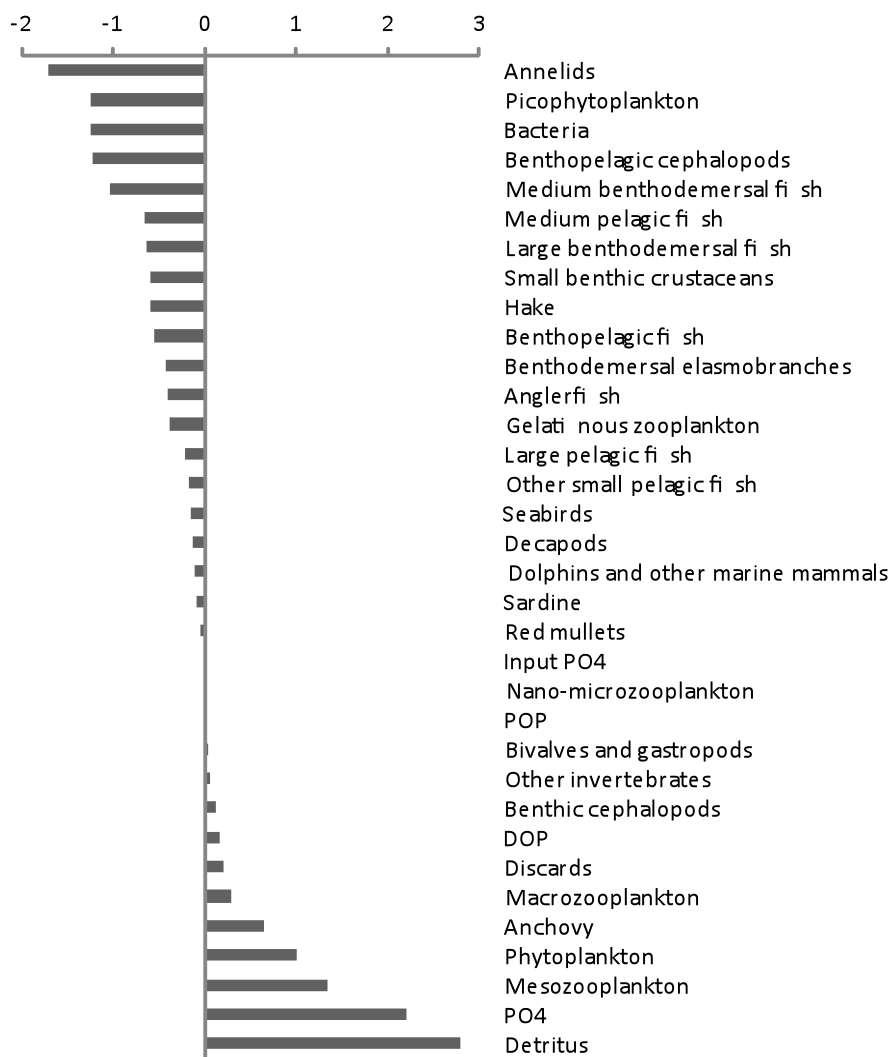


Figure 31. Cumulative mixed trophic impact of each functional group on all the other groups.

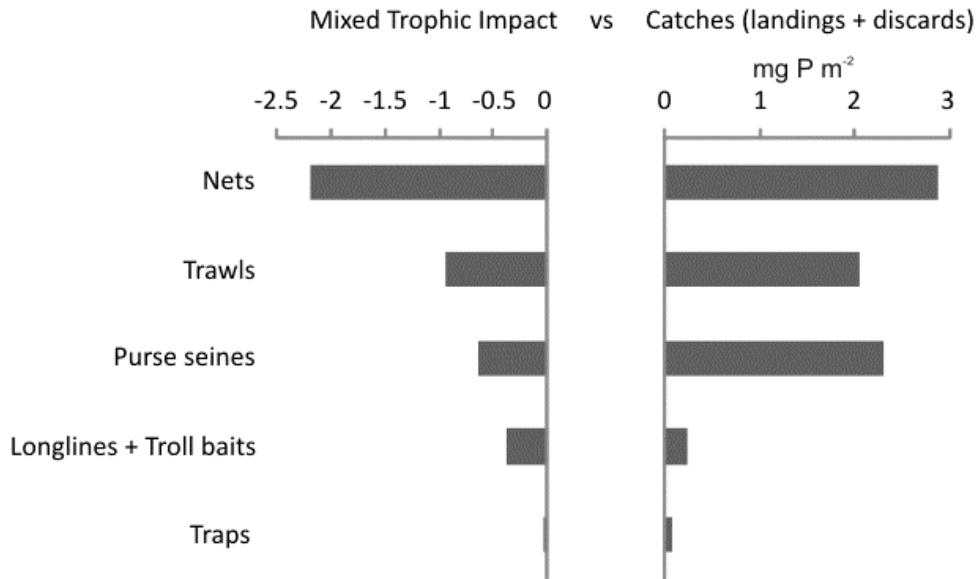


Figure 32. Graphic representation of (a) the cumulated mixed trophic impact of each gear on the other groups and (b) catches (where catches represent the sum of landings and discards) by gear.

Fisheries impact

Three of the fishing fleets are responsible for >95% of landings; static nets catch 38% of landings, followed by purse seines and bottom trawls with 30.5% and 27% respectively (Figure 5). However, trawls are ranking higher than trawls in the cumulative MTI (Figure 5). Probably, this is related to the multi-species nature of the trawl fishery, in contrast to the highly selective purse seine fisheries (Tsagarakis *et al.*, 2012), which creates cascade effects in the food web.

Summary statistics

Summary statistics (flows, biomasses, catches, related ratios and ecological indices) of the N. Aegean food web in the 1990s are presented in Table 11. Some of these are related to vigor, organization and resilience, i.e. attributes that can define ecosystem health (Costanza and Mageau, 1999). Indicatively, total system throughput is related to **vigor**, capacity is related to the **organization**, overhead is related to **resilience**, and ascendancy is related both to **vigor** and **organization**.

This is the first effort towards an end-to-end ecosystem modelling approach in the Aegean Sea. Data from LTL and HTL model were combined and first results aiming to assess the functioning of the model were presented. Overall, results are in line with previous works in the area, although not directly comparable due to differences in structure and, mainly in the units used. Results indicate the importance of planktonic ecosystem and detritus, as well as the impact of other key FGs (e.g. small pelagic fish, benthopelagic cephalopods), as also identified in earlier works (Tsagarakis *et al.*, 2010).



Table 11. Ecological indicators related to community energetic, structure, flows and information theory. Bold characters indicated results of the N. Aegean Sea Ecopath model related to vigor, organization and resilience.

Global indices	index	unit
Sum of all consumption	8641.398	mg P/m ² /year
Sum of all exports	10.561	mg P/m ² /year
Sum of all respiratory flows	0.002	mg P/m ² /year
Sum of all flows into detritus	7137.844	mg P/m ² /year
Total system throughput	15790	mg P/m²/year
Sum of all production	5717	mg P/m ² /year
Gross efficiency (catch/net p.p.)	0.015118	
Calculated total net primary production	500	mg P/m ² /year
Total primary production/total biomass	3.036	
Total biomass/total throughput	0.01	
Total biomass (excluding detritus)	164.712	mg P/m ²
Total catches	7.559	mg P/m ² /year
Connectance Index	0.315	
System Omnivory Index	0.261	
Ascendency	33122.7	(flowbits)
Ascendency	48.4	(%)
Overhead	35303.6	(flowbits)
Overhead	51.6	(%)
Capacity	68426.4	(flowbits)
Information	2.098	(bits)
Throughput cycled (excluding detritus)	0	mg P/m ² /year
Predatory cycling index	0	% of throughput w/o detritus
Throughput cycled (including detritus)	15061.05	mg P/m ² /year
Finn's cycling index	95.39	% of total throughput
Finn's mean path length	1,495	
Finn's straight-through path length	371	without detritus
Finn's straight-through path length	69	with detritus

The developed end-to-end model can be used to some extent as a useful tool to assess MSFD goals. Fitting with time series and performing dynamic simulations will be used to estimate indices related to vigor, organization and resilience through time. Trends of such indices can be used to provide an assessment of ecosystem health, compare among ecosystems and estimate the effect of managerial and environmental changes.

2.4.2.5 Black Sea global

E. Akoglu, B Salihoglu, G. Korotaev, V. Dorofeyev (IMS-METU, MHI)

The Black Sea, one of the major semi-enclosed seas of the world oceans, has



experienced striking ecological changes under concurrent impacts of climate change, intense eutrophication, and population explosion of invasive species, unsustainable fishery, and their density-dependent feedback processes. Nitrate loading increased nearly four-fold during the 1970s due to increased use of agricultural fertilizers. Rapidly intensifying eutrophication has caused comparable increases both in the subsurface nitrate concentrations and phytoplankton biomass, degradation of the classical mesozooplankton-dominated food web by flourishing of the opportunistic species *Noctiluca scintillans* and *Aurelia aurita* in the 1980s. The intense eutrophication phase was ended by a sequence of events; the collapse of anchovy stock (Oguz et al., 2012) and the simultaneous outburst of ctenophore *Mnemiopsis leidyi* population at 1989-1991 (Shiganova et al., 2001; Purcell et al., 2001) and the subsequent marked decline of anthropogenic nutrient loads from the River Danube and other northwestern rivers following the disintegration phase of the former Soviet Union during the early 1990s (Oguz and Velikova, 2010). The subsequent years are referred to as the post-eutrophication phase in which the nutrient reduction led to approximately a two-fold decrease in the phytoplankton and anchovy standing stocks and *Noctiluca* and *Mnemiopsis* populations (BSC, 2008), and 30-40% decline in the subsurface nitrate and phosphate peak concentrations. Invasion of the opportunistic gelatinous species *Beroe ovata* and their predation on the *Mnemiopsis* population has introduced further changes in the food web structure by the end of 1990s. These aspects of the structural changes observed in the Black Sea ecosystem have been studied quantitatively by modelling studies (e.g. Oguz et al., 2000, 2001a, b; Oguz and Merico, 2006; Lancelot et al., 2002; Daskalov, 2002; Gregoire and Friedrich, 2004; Gregoire and Soetaert, 2010; Staneva et al., 2010; He et al., 2012). They focused particularly on the impacts of eutrophication, fishery and invasion of alien gelatinous species.

The Black Sea, with a surface area of 423,000 km², is approximately one-fifth of the surface area of the Mediterranean. It has a total volume of 547,000 km³, and a maximum depth of around 2200 m. It contains narrow shelves and very strong topographic variations around its periphery. The northwestern shelf (NWS), occupying ~20% of the total area, is the only major shelf region with discharges from three of Europe's largest rivers: Danube, Dniepr and Dniestr. In the north, the sea is connected to the shallow Sea of Azov by the Kerch Strait. At its southwestern end, it communicates with the Aegean basin of the Mediterranean Sea through the Sea of Marmara and the Bosphorus and Dardanelles Straits. According to the data presented by Unluata et al. (1989), the sum of fluxes due to precipitation (~300 km³ yr⁻¹) and runoff (~350 km³ yr⁻¹) exceeds that of evaporation (~350 km³ yr⁻¹). The freshwater excess of 300 km³ yr⁻¹ is balanced by the net outflow through the Bosphorus defined as the difference between the transports of its two layers.

The upper layer waters of the Black Sea are characterized by a predominantly cyclonic, strongly time-dependent and spatially-structured basinwide circulation (Figure 33). Many details of the circulation system have been explored using recent hydrographic data (Oguz et al., 1993, 1994, 1998; Oguz and Besiktepe, 1999; Gawarkiewicz et al., 1999; Krivosheya et al., 2000), AVHRR data (Oguz et al., 1992; Sur et al., 1994, 1996; Sur and Ilyin, 1997), altimeter data (Korotaev et al., 2001 and 2003; Sokolova et al., 2001), and CZCS and SeaWIFS data (Ozsoy and Unluata, 1997; Oguz et al., 2002a; Ginsburg et al., 2002b). These analyses reveal a complex, eddy-dominated circulation with different types of structural organizations within the



interior cyclonic cell, the Rim Current flowing along the abruptly varying continental slope and margin topography around the basin, and a series of anticyclonic eddies in the onshore side of the Rim Current (Figure 33). The interior circulation comprises several sub-basin scale gyres, each of them involving a series of cyclonic eddies. They evolve continuously by interactions among each other, as well as with meanders, and filaments of the Rim Current. The Rim Current structure is accompanied by coastal-trapped waves with an embedded train of eddies and meanders propagating cyclonically around the basin (Sur et al., 1994; Sur et al; 1996; Oguz and Besiktepe, 1999; Krivosheya et al., 2000; Ginsburg et al., 2002a, b).

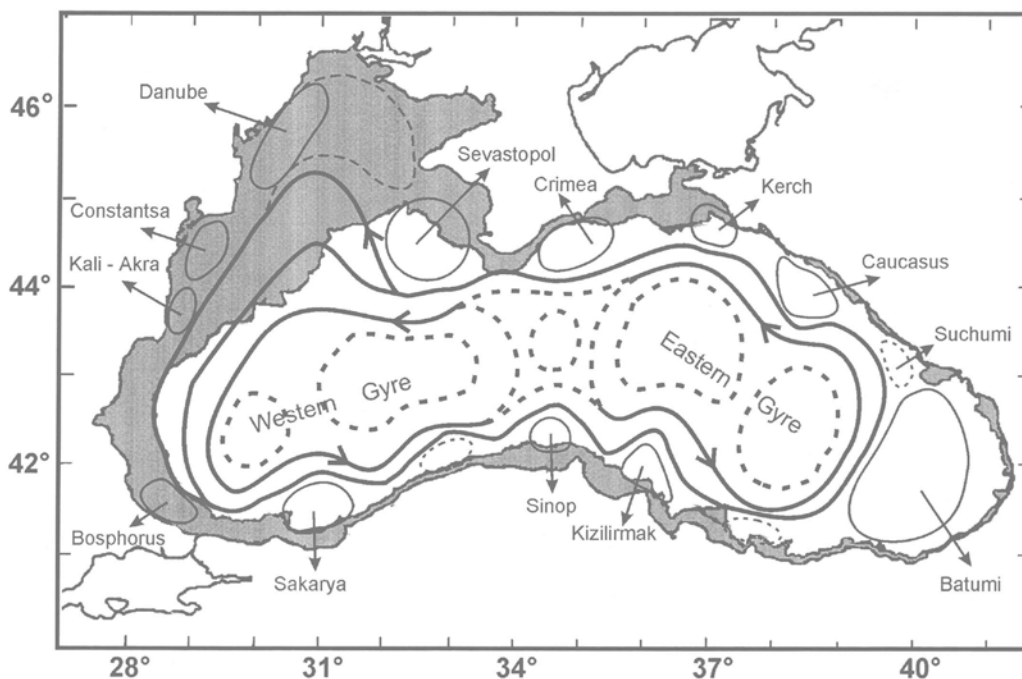


Figure 33. The schematic diagram showing major quasi-permanent/recurrent features of the upper layer circulation identified by synthesis of hydrographic studies and analysis of the Topex-Poseidon and ERS-I,II altimeter data.

The upper layer biogeochemical structure overlying the deep and lifeless anoxic pool (except anaerobic bacteria) involves four distinct layers. The uppermost part from the free surface to the depth of 1% light level is covered by a shallow euphotic zone with a maximum thickness of nearly 50 m. This is the layer of active planktonic processes (e.g uptake, grazing, mortality, microbial loop, etc.), and is characterized by high oxygen concentrations on the order of 300 μM as well as seasonally varying nutrient and organic material concentrations supplied laterally from rivers and vertically from sub-surface levels through vertical mixing. In the interior basin, the surface mixed layer waters are poor in nutrients for most of the year except for occasional incursions from coastal regions, and by wet precipitation. Below the seasonal thermocline and in the deeper part of the euphotic zone, nitrate concentrations increase due to their recycling as well as continuous supply from the nutricline. Nitrate accumulation in this light-shaded zone generally supports summer subsurface phytoplankton production (Oguz et al. 2000). In winter, nutrient stocks in the euphotic zone waters are renewed from the nutricline depths through upwelling, vertical diffusion and seasonal wind and buoyancy-induced entrainment



processes, and depleted by biological utilization. About 90% of the sinking particles are remineralized inside the euphotic zone and the subsequent 20–30 m part of the oxygenated, aphotic zone (the so-called “upper nitracline” zone) where nitrate concentrations increase up to $\sim 8 \mu\text{M}$ at $\sim 70\text{--}80$ m in cyclonic regions, and are re-supplied back to the surface waters to refuel the biological pump. Only a small fraction of particulate matter sinks to the deeper anoxic part of the sea (Lebedeva and Vostokov, 1984; Karl and Knauer, 1991), which occupies the water column below ~ 100 m depth within the interior parts and ~ 200 m in the onshore, anticyclonically-dominated side of the Rim Current. This loss is compensated by lateral nitrogen input mainly from the River Danube (Cociasu et al., 1996), by wet deposition and nitrogen fixation. The nutrient fluxes of anthropogenic origin are transported across the shelf and around the basin through the Rim Current system, and supplied ultimately to the interior basin, and some of it is lost in the form of Bosphorus surface flow in winter months (Polat and Tugrul, 1995).

Input data (LTL & HTL)

To run the Black Sea BIMS-ECO model and EwE for the 2000-2020 year time frame selected for PERSEUS the following input data is necessary: atmospheric forcing, river forcing, fishing mortality and biomass estimations for demersal and small pelagic fishes.

Atmospheric forcing is provided by CMCC and the chosen emission scenario is RCP4.5 (Meinshausen et al., 2011). RCPs (Representative Concentration Pathways) specify the expected radiative forcing over the 21st century. In particular, RCP4.5 is a stabilization scenario in which the total radiative forcing is stabilized at 4.5 W/m^2 at 2100. The spatial resolution of simulations is 14 km, in order to provide a detailed description of the climate variability on local scale.

Land based forcing functions (river runoff and nutrient load) are not yet ready. We are in the process of compiling these for the 2000-2010 period.

Fishing mortality (F) values and biomass estimations for some demersal and small pelagic fishes were derived from WG (STECF, 2011) and biomass estimations for the remaining species and catch statistics were complemented from BSC (2008) and SAUP database (Sea Around Us Project 2011), respectively. The parameterization of the higher trophic level groups of the coupled model was based on Akoglu (2013).

The ERA40 driven simulation covers the period 1971-2000, and is used to validate the model output over a past period. The CMCC-MED driven simulation, instead, covers the period 1971-2020.

As the river forcing for the simulations are not complete yet, instead two 20-year simulation from 1980-1999 (using ERA40 vs IPSL forcing) using river data available from the SESAME river data base (Ludwig et al. 2009, 2010) were completed instead. Surface forcing was prescribed using 6-hourly fields of wind stress, fresh water fluxes (evaporation, convective precipitation and large-scale precipitation), and radiation fields (surface shortwave radiation, surface long-wave radiation, evaporative heat flux, and convective heat flux). The two scenarios differed only in atmospheric forcing. The ERA40 hindcast was forced with atmospheric data extracted from European Centre for Medium-Range Weather Forecasts (ECMWF) 40-year Reanalysis Data Archive and IPSL hindcast scenario was forced with the data extracted from



Institut Pierre Simon Laplace (IPSL) Climate Model 4 (CM4) Ocean Atmosphere Global Circulation Model (OA-GCM) (Marti et al., 2006). Output of both the circulation and lower trophic level model were used to validate the model and do a skill assessment.

Work achieved

The pelagic ecosystem model used in this study is BIMS-ECO developed from the 1D model by Oguz et al. (2001b). The model domain extends to 150 m depth. It has 23 z-levels with a 2 m resolution near the surface and 20 m near the lower boundary. The model has 12 state variables (Figure 34) that include two phytoplankton groups, small and large phytoplankton (Ps, Pl; smaller and larger than 10 mm representing flagellate and diatoms), micro- and mesozooplankton (< 0.2 mm Zs and > 0.2-2 mm Zl), bacterioplankton (B), labile pelagic detritus (Pn), DON (Dn), nitrate (N), ammonium (A), as well as the opportunistic heterotrophic dinoflagellate *Noctiluca scintillans* (Zn) and the gelatinous carnivores *Aurelia aurita* (Za) and *Mnemiopsis leidyi* (Zm). *M. leidyi* has been introduced into the Black, Marmara, and northern Aegean Seas following the early 1980s (Vinogradov et al., 1989; Studenikina et al., 1991; Shiganova, 1998; Shiganova et al., 2001) and was considered widespread in the Black Sea by 1988 (Vinogradov, 1989). In 1990 *Beroe ovata*, another alien species, was identified in the Black Sea (Konsulov and Kamburska, 1998) and was established there by 1998 whence it became a key predator of *M. leidyi* (Vinogradov et al., 2000). The model formulation applied in this study was similar to that described by Oguz et al. (2001a) with *M. leidyi* introduced into the model at the start of 1988. The model applied in this study differs in the introduction during 1998 of *B. ovata* as a grazing term on *M. leidyi*.

A LTL-HTL coupled model scheme (Figure 35) has been developed and is now functional and ready to use. It has been tested using output from the above-described two 20-year simulations and provides good results. Input data for BIMS-ECO LTL model is still being prepared to produce coupled model run results for the time frame 2000-2020. As soon as the input data is achieved, final results will be provided. During this period, EwE with the standardized functional groups were setup and evaluated. The methodology followed to couple the EwE and BIMS-ECO models is based on Libralato and Solidoro (2009).

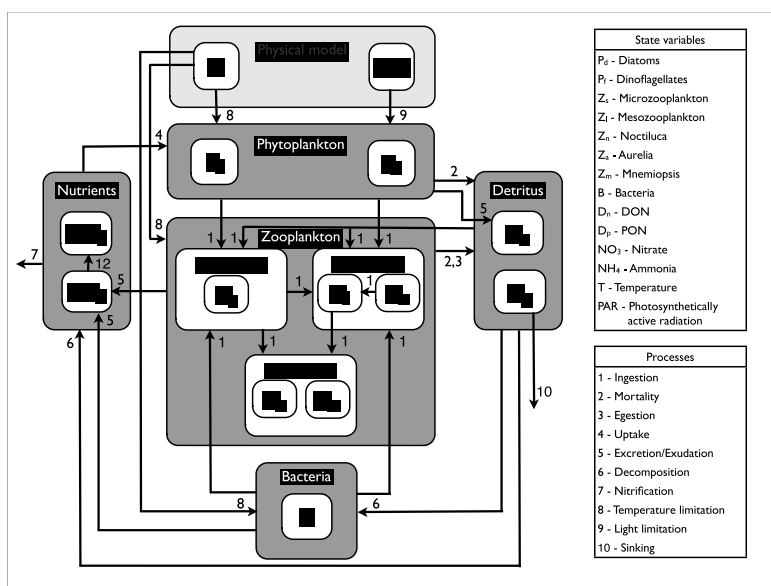


Figure 34. Schematic of BIMS_Eco model setup and trophic interactions

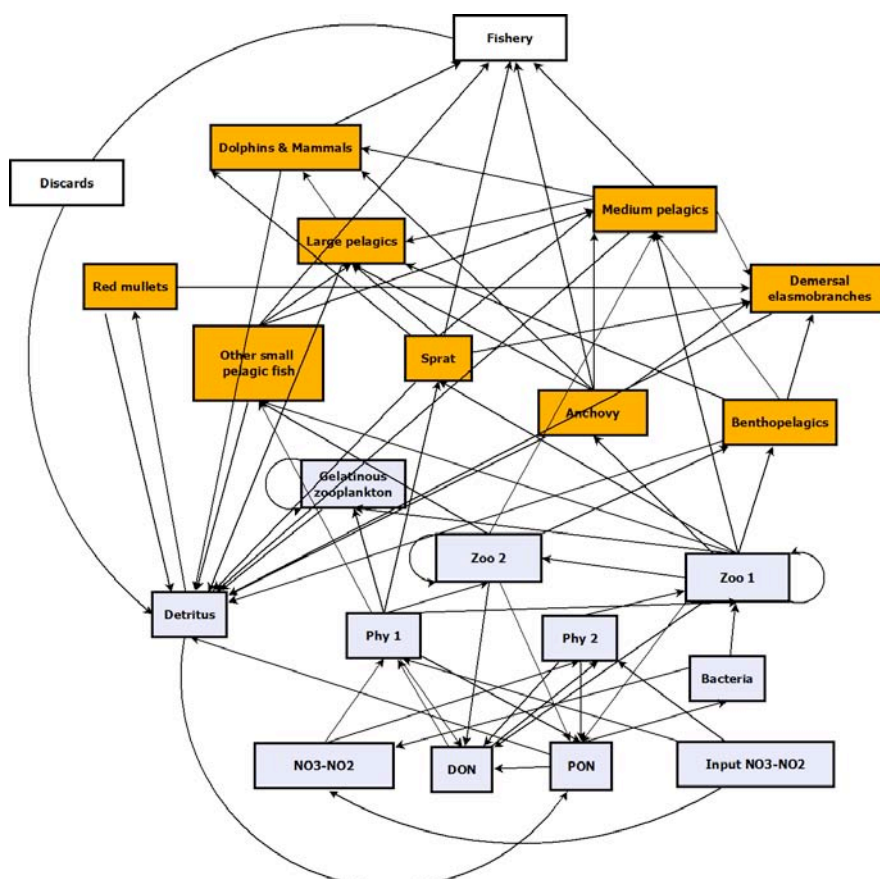


Figure 35. Flow diagram of the coupled BIMS-ECO&EwE model scheme (Grey boxes refer LTL (BIMS-ECO), orange boxes are for HTL model (EwE))

Skill assessment (comparison and first test with data)

Because of above-mentioned difficulties to acquire riverforcing data, the skill



assessment of the LTL model was carried out using ERA40 and IPSL model output during 1998-1999. The simulated chlorophyll distribution for this test runs was evaluated against SeaWiFS chlorophyll available during the time period 1998-1999 (Figure 36). Mean errors in the ERA40 and IPSL surface chlorophyll concentrations averaged over these two years were -0.01 mg m^{-3} and -0.13 mg m^{-3} respectively. Model errors were positive (indicating model overestimation of surface chlorophyll concentrations) during the spring and autumn bloom periods but negative (model underestimation of surface chlorophyll concentrations) at other times of the year, suggesting much of the error in the model representation of phytoplankton blooms resulted from a temporal rather than a spatial mismatch in bloom dynamics in both model simulations.

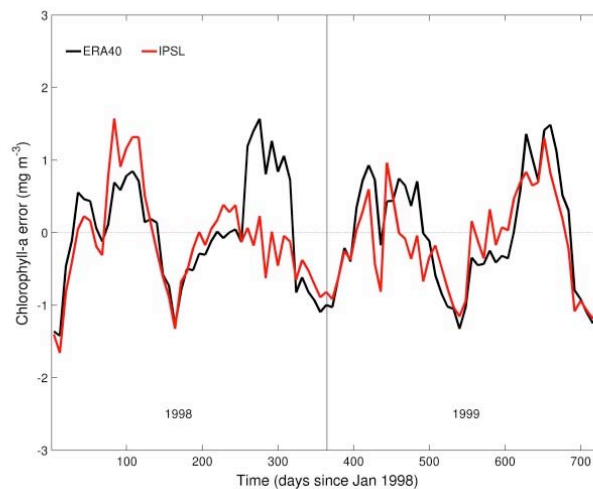


Figure 36. Mean differences in modelled surface chlorophyll distributions relative to SeaWiFS chlorophyll during 1998 and 1999. ERA40 simulation errors are shown in black and IPSL simulation errors are shown in red.

The coupled model validation was carried out by comparing simulated biomass and catch values to time series of catch statistics and Virtual Population Analysis (VPA) estimates of fish group biomasses derived from the catch data. For biomass and catch estimates simulated by the EwE model, the goodness of fit measure was the weighted sum of squared deviations (SS, Mood et al., 1974) of log biomasses/catches from log predicted biomasses and/or catches and Akaike Information Criterion (AIC; Akaike, 1974). There were 30 time-series of catch and biomass from field and statistical catch data which were used to fit the model.

The Sum of Squared Deviations (SS) for 33 time series and AIC for 72 data points were calculated as 76.46 and 440.2, respectively. Considering that the time series had gaps for most demersal species; and some fish species; i.e. large pelagic fish and medium pelagics, did not have stock estimates but only catch statistics, the SS and AIC values can be evaluated as the model has reasonable fit and medium uncertainty (Figures 37 and 38), however, further tuning is required.

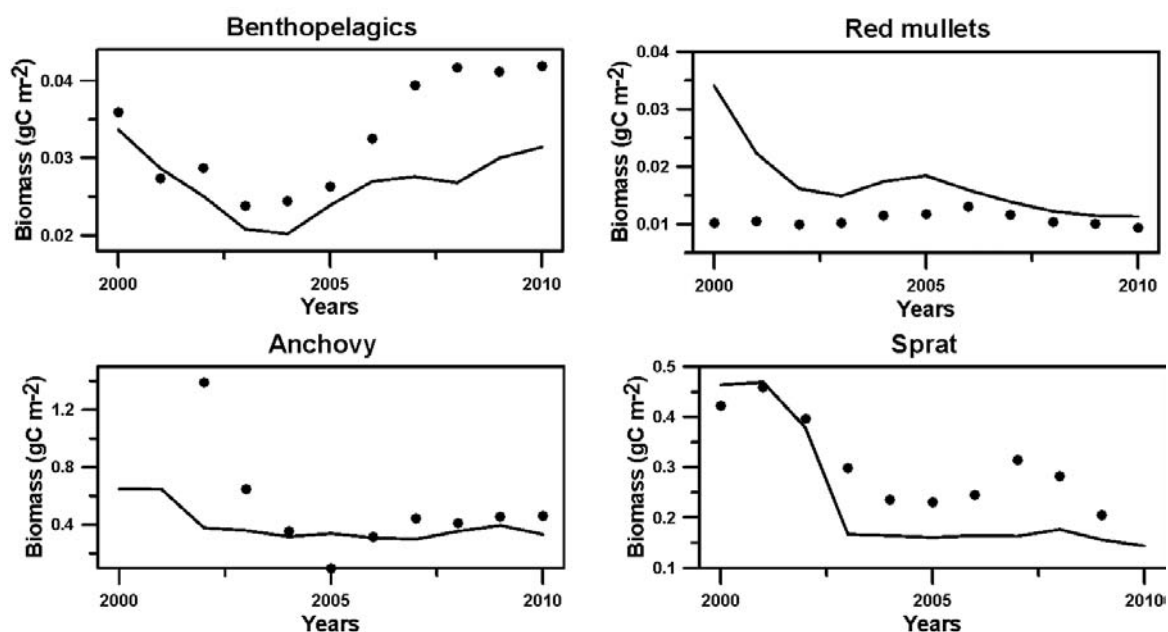


Figure 37. Simulated biomass changes (solid lines) of the model compartments and their degree of agreement with Virtual Population Analysis (VPA) estimates (dots) in the Black Sea.

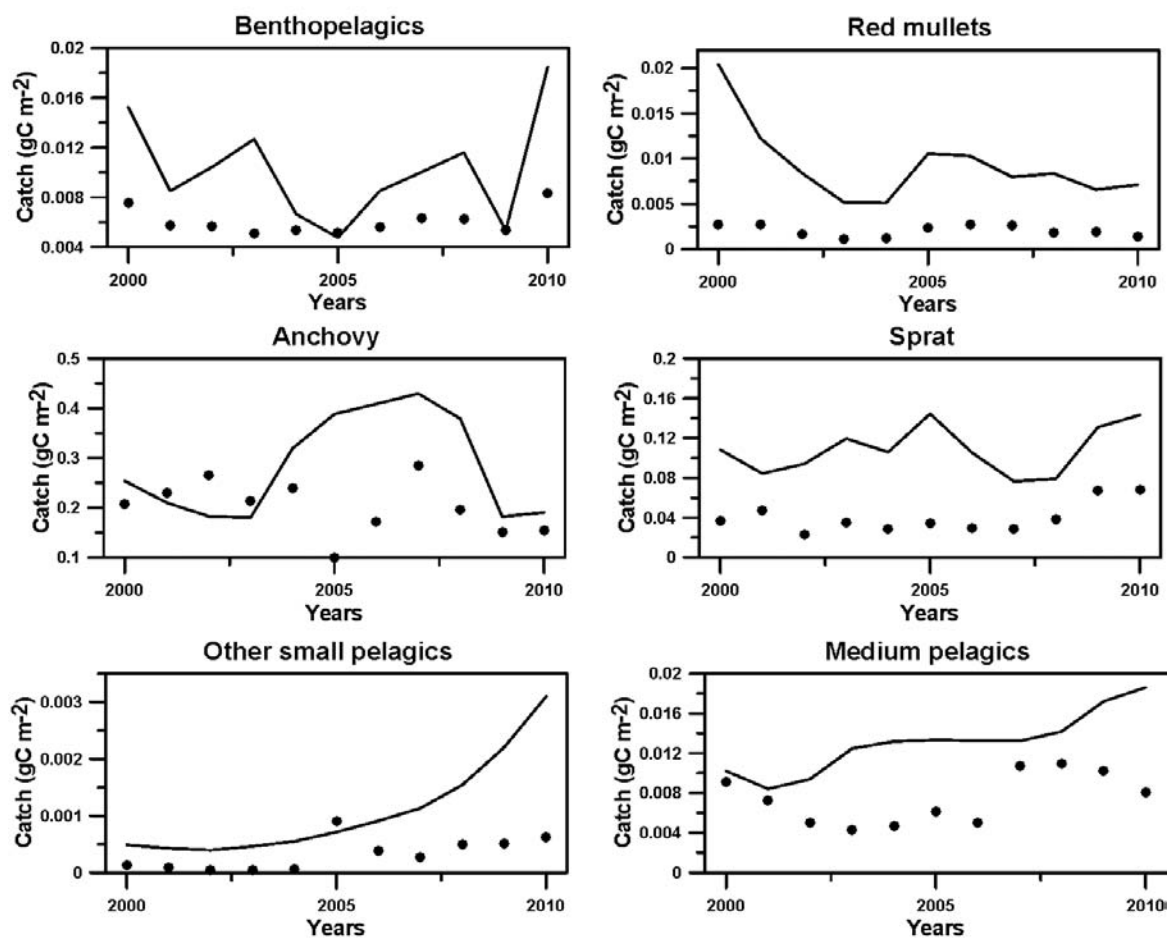


Figure 38. Simulated catch (solid lines) of the model compartments and their degree of agreement with Virtual Population Analysis (VPA) estimates (dots) in the Black Sea



Advantage and limitations of the method

The coupled scheme of LTL and HTL models provide a useful tool to assess the impact of climate and nutrient load on the whole ecosystem. However, the numbers of functional groups in the model were standardized to make comparative analysis possible with the results from all of the case studies. Therefore, this situation increased the uncertainty of the Black Sea model due to introduction of numerous additional functional groups which should be neglected in the Black Sea case study either because they have no functional importance for/in the ecosystem or the data to parameterize and validate against were absent. This could be regarded as a pitfall of the methodology. Advantage and limitations of this method will be more elaborate after the coupled model work is completed in the following periods and sensitivity studies are carried out.

2.4.2.6 Black Sea regional

IBER-BAS, ULg, DMG-SU

Western Black Sea LTL model (ULg)

A 3D coupled hydrodynamical-biogeochemical model is used to reproduce the bottom-up processes affecting of the Black Sea food webs, i.e. the climate- and river-driven influence on planktons growth.

For the western Black Sea the physical model is the GeoHydrodynamic and Environmental Research (GHER) 3D hydrodynamical model described in, e.g., Beckers 1991, Delhez, 1996, and used in the particular case of the Black sea in Gregoire et al, 1998 , Grégoire et al., 2004 ; Stanev, 1999 and Beckers et al . 2002. The implementation used in the frame of these simulations is described in Capet et al., 2012. This model resolves the currents and the physical state of the sea, which are temperature, salinity, internal mixing and surface elevation.

The biogeochemical model (Figure 39) simulates oxygen, nitrogen, phosphorus, silicate and carbon cycling and explicitly represents processes in anoxic and suboxic conditions. It is described in detail in Grégoire et al., 2008 . Compared to Grégoire et al., 2008 , the model has been coupled (online) in 3D with the GHER 3D hydrodynamic model and extended with a dynamic representation of the benthic compartment based on the comparative analysis performed by Soetart et al ., 2000 (in Grégoire et al, 2008 , a reflective boundary condition was used for describing benthic degradation). The benthic compartment is described by a semi-empirical model whose state variables are 2D variables (vertically integrated C and N content with two degrees of lability). From these 2D stock variables, the fluxes of solutes are estimated using bulk parameters (i.e. fraction of organic matter degraded by denitrification and anaerobic oxidation, oxygen consumption in nitrification Soetart et al ., 2000). The organic matter accumulated in the sediments stocks is subjected to resuspension from the action of wave and current induced bottom stress, which is modelled using the setting presented in Stanev and Kandilarov, 2012.

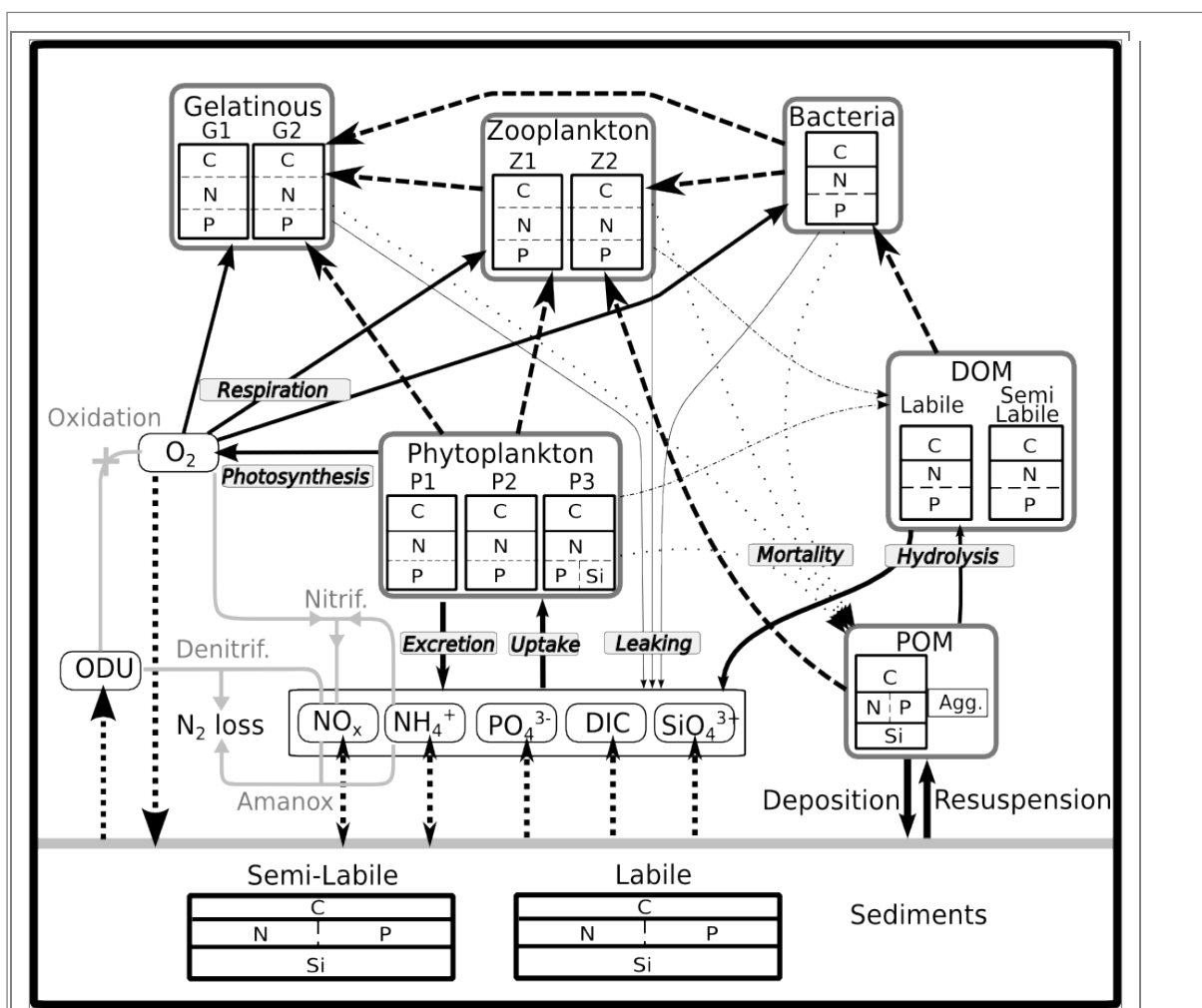


Figure 39: Main processes of the biogeochemical model. Dotted separation amongs the different elements (C,N, P, Si) of each group indicates fixed molar ratios. Dashed arrows among the groups represents trophic interactions.

The coupling between the three components of the model (hydrodynamic, biogeochemical, benthic) is fully online. For instance, the transport of biogeochemical variables is determined at each time step from the advection and diffusion fields computed by hydrodynamical model. Additionally, the rate of each biogeochemical process depends on the temperature field and the oxygen solubility is also dependent on the salinity. On the other hand, the penetration of solar radiation which governs the heating of the upper layer, is influenced by the vertical distribution of phytoplankton and organic matter computed by the biogeochemical model. Similarly the benthic component receives from the overlaying waters the export of detritus and diatoms and provides the flux of solutes issued from sediment degradation. The dynamics of benthic detritus depends on environmental conditions of bottom waters (temperature, currents including waves, oxygen, nitrate and ammonium).

The model domain covers the whole Black Sea, on a 15 km Arakawa-C grid, with 31 vertical levels using double sigma coordinates. The total Black Sea riverine discharge is delivered through the 6 main rivers : Danube, Dniestr, Dniepr, Rioni, Kizilmark and Sakarya (the first three flowing directly on the NWS).



Averaged and constant atmospheric deposits of nitrate and phosphate are imposed all over the basin (NO_x : $0.78 \text{ g m}^{-2} \text{ yr}^{-1}$, PO_4 : $0.7 \text{ g m}^{-2} \text{ yr}^{-1}$ which represents 3 Gmol N yr^{-1} for the NWS. Average concentrations of nitrogen organic forms are estimated for the three shelf rivers (Cauwet, 2002; Reschke, 2002, Walling and Fang, 2003). When multiplied by the considered discharges, this leads to a total load of $10.1 \text{ Gmol N yr}^{-1}$ (7, 0.8 and 2.3 for Danube, Dniepr and Dniestr, respectively). Atmospheric forcings are issued from the ERA-interim reanalysis provided by the ECMWF data centre¹ with a 6-hour and 0.75° horizontal resolution. The new forcing data provided within PERSEUS will be implemented together with the new rivers forcings, due to some delay in the delivering of these data.

Skill assessment

The model ability of resolving the Black Sea hydrodynamical structure is evaluated by computing in-situ data to their model equivalents (same location, same time). The quantitative outcomes of this comparison is represented in a Taylor Diagram (Figure 40). In order to stress the validation on the resolution of the vertical structure, the saline and thermal component of potential energy anomaly (Holt et al., 2005) were also derived from the vertical profiles and compared with model results.

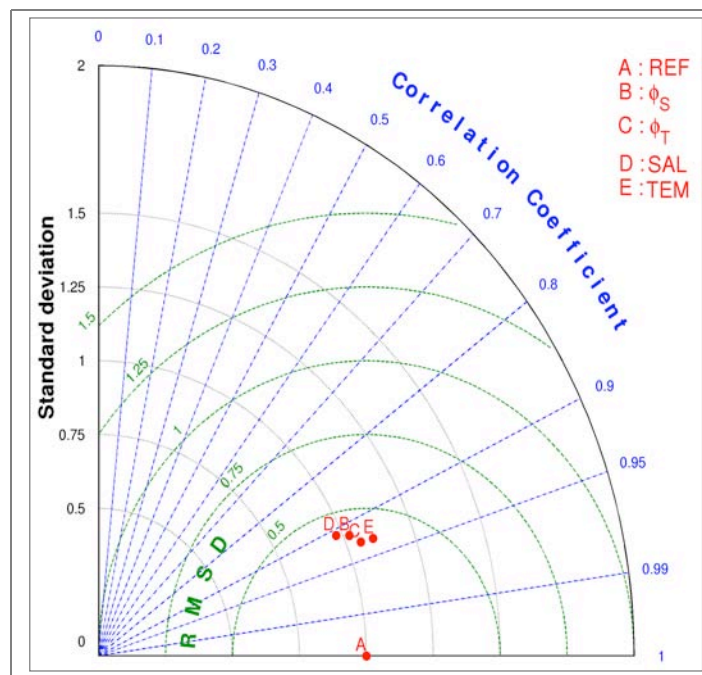


Figure 40: Taylor diagram representing the model skill for temperature, salinity and the saline and thermal component of the potential energy anomaly.

The ability of the physical model to reproduce the driving mode of the interannual variability (Empirical Orthogonal Functions) of the surface temperature and sea

¹ European Center for Medium-Range Weather Forecasts (<http://www.ecmwf.int/>)



surface elevation, hence the main hydrodynamic features, has been demonstrated by comparing the model results to satellite imagery, as detailed in Capet et al; 2012 and illustrated in Figure 41 for the sea surface temperature.

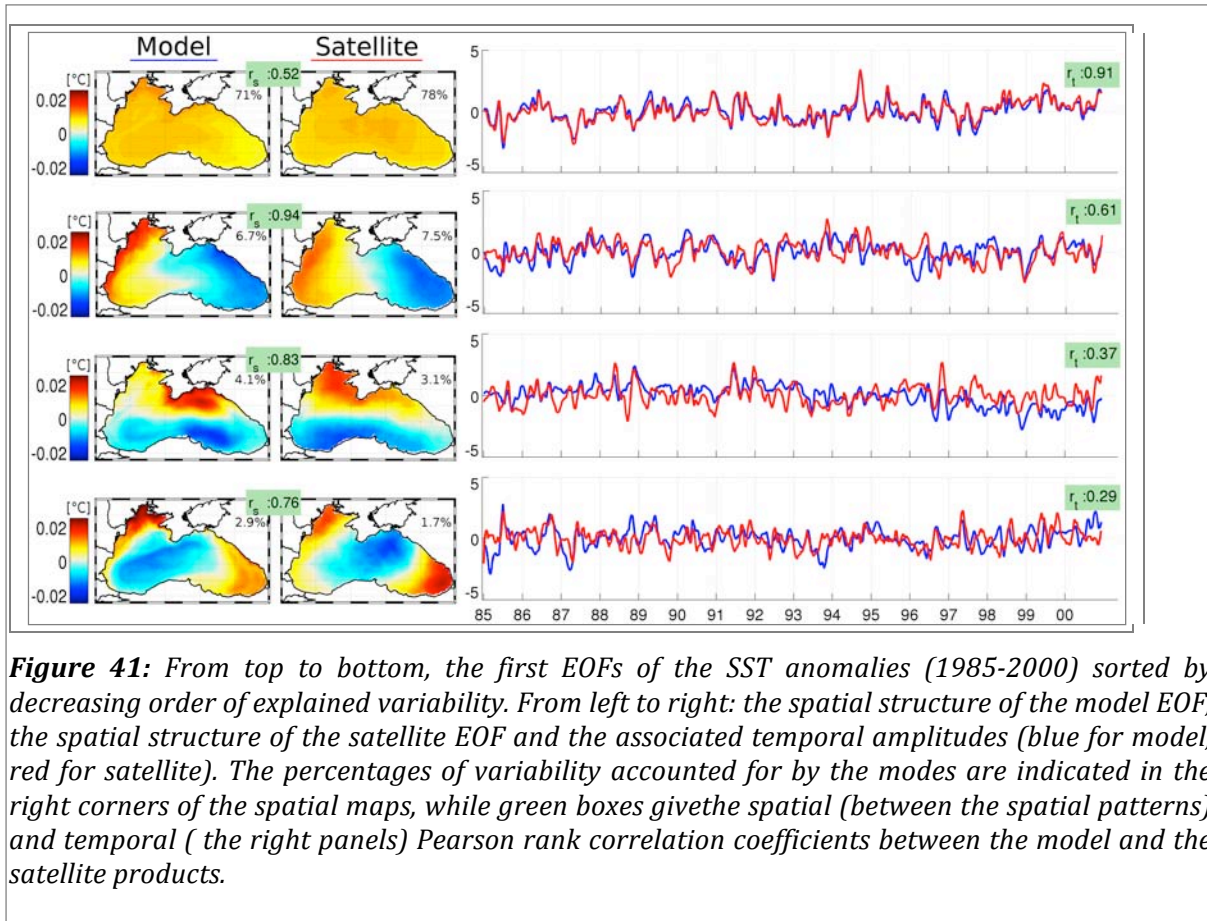


Figure 41: From top to bottom, the first EOFs of the SST anomalies (1985-2000) sorted by decreasing order of explained variability. From left to right: the spatial structure of the model EOF, the spatial structure of the satellite EOF and the associated temporal amplitudes (blue for model, red for satellite). The percentages of variability accounted for by the modes are indicated in the right corners of the spatial maps, while green boxes give the spatial (between the spatial patterns) and temporal (the right panels) Pearson rank correlation coefficients between the model and the satellite products.

The dynamic of the biogeochemical component of the model has been extensively explored in the shelf waters in relation with the dynamic of oxygen, since this area is strongly affected by the occurrence of seasonal hypoxia. In-depth quantitative validation procedure asserted the model ability to represent specifically the seasonal, interannual and spatial variability of oxygen (Capet et al., 2013). We only reproduce here the Figure concerning the spatial repartitions of oxygen (Figure 42) and refer to the publication for further details about the seasonal and interannual component. Since benthic fluxes in the north-western shelf were also validated against in-situ estimates (Figure 43) , this implies a correct representation of the balance between primary production and respiration in the Black Sea north Western Shelf waters.

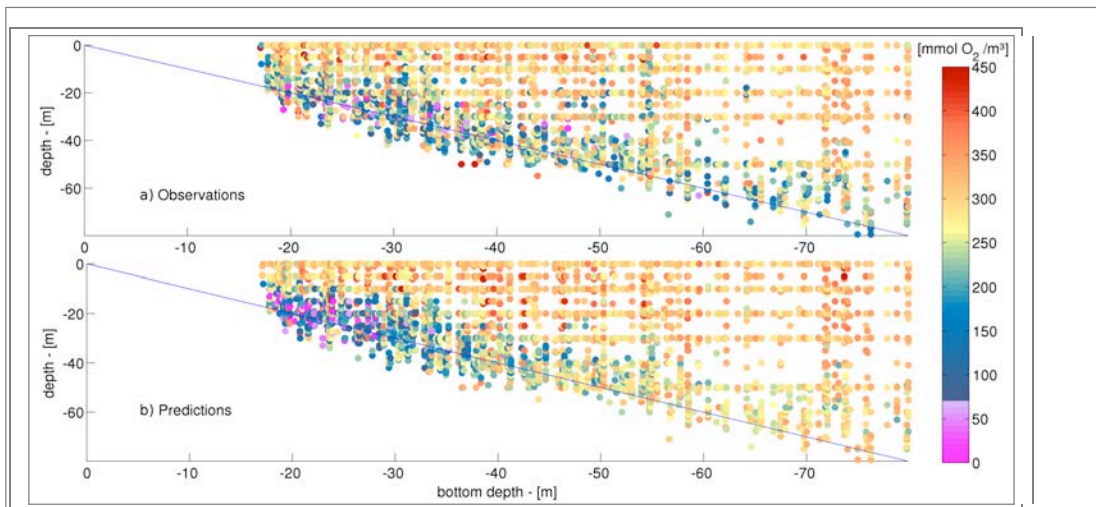


Figure 42: Visual comparison of the oxygen distribution along the bathymetric gradient.

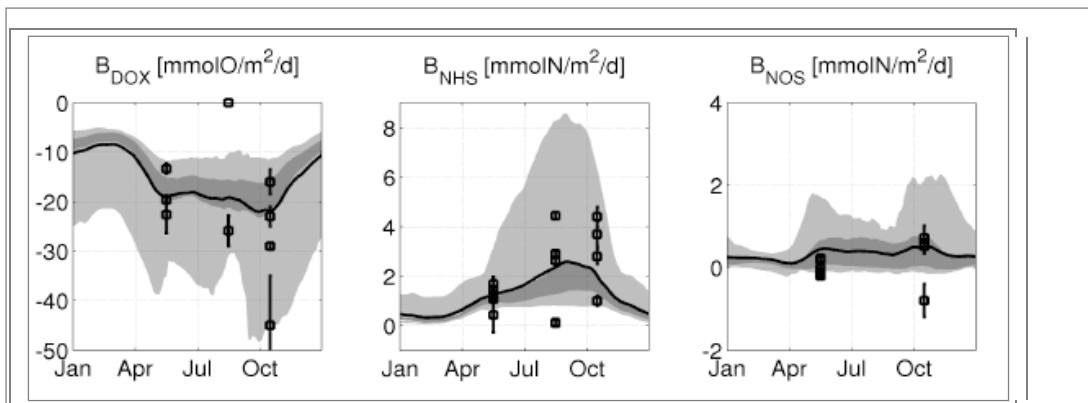
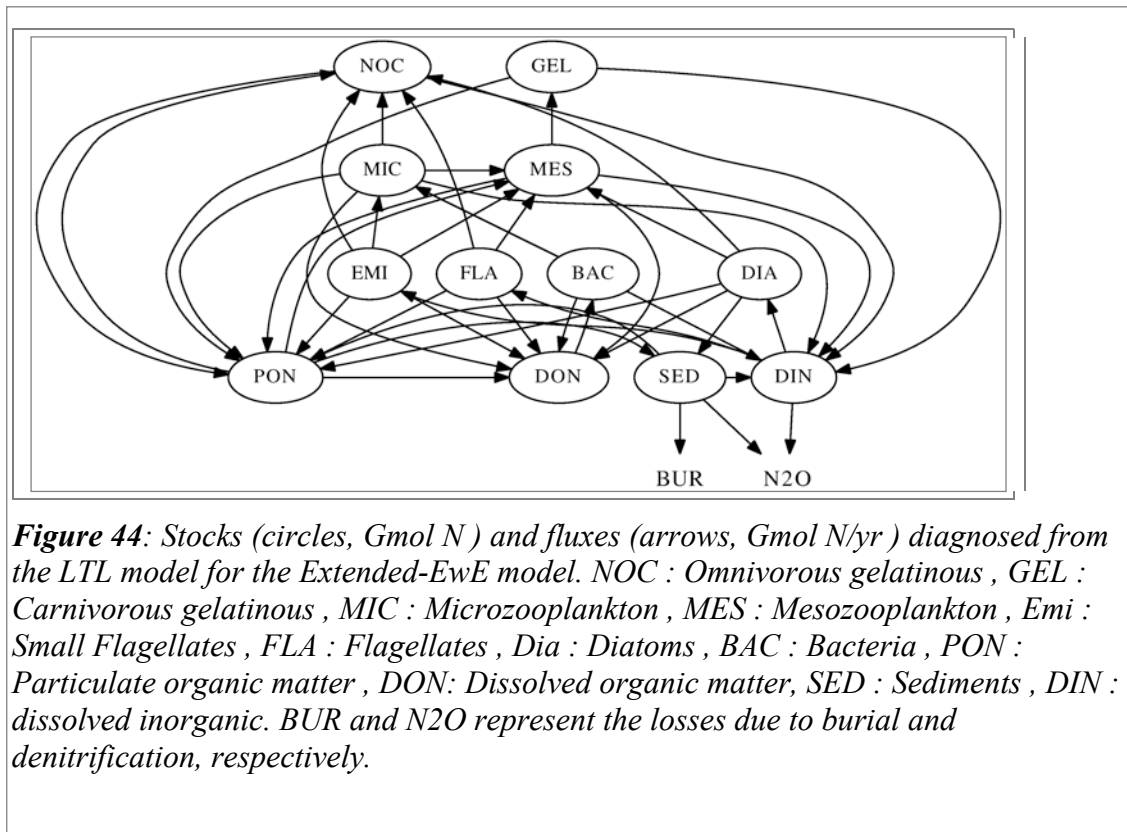


Figure 43: Benthic fluxes of Oxygen (DOX) , Ammonium (NHS) and Nitrogen (NOS) in the Black Sea northwestern shelf. Model results : light and dark gray area represent the 2.5 - 97.5 % and 25 - 75 % interquartile of the spatial variability, respectively. In-Situ measurements are indicated by the squares with their error bars.

Extraction of data for HTL model

A specific diagnosis framework has been set to match the HTL coupling requirements. Time series issued from the LTL model for every nitrogen form consist in integrated stocks over the shelf domain (Figure . 44) at a monthly time step (the currency agreed for the coupled model is nitrogen). Estimates of the Ecopath flows parameters are derived from the flows among these stocks, integrated during the model run and expressed in G mol N /yr. In order to match the unit system of Ecopath these are translated in terms of mg N /m² and mg N /m²/yr using the surface of the shelf area.



The following Ecopath conceptual approach was used to derive the consumption (Q) and Production (P) from the LTL stocks and flows diagnosis.

- ⤴ Production = predation mortality + natural mortality + export
- ⤴ Consumption = production + unassimilated + respiration

Given the nitrogen currency framework of the Extended-EwE model, and the fact that dissolved inorganic nitrogen is explicitly represented, there is no respiration losses in the sense of the Ecopath context. Finally the consumption for each stocks is thus given by the sum of the fluxes entering that stock, while additional diagnosis (e.g. natural mortalities) were computed in order to estimate the productions terms.

Forcing Functions

In order to introduce in the Extended-EwE framework the influence of river forcings and atmospheric conditions, time series are extracted from the LTL model to conditions the growth of the phytoplankton groups. EwE allows different types of mediating functions, depending whether on the time, or allowing some stock to influence the growth of another stock.

According to the agreement with the other users of the Extended-EwE approach the temporal production rate for the phytoplankton groups should match the following equation :

$$(P/B) = (P/B)_0 \cdot F(t) \cdot f(N)$$

, in which $(P/B)_0$ is the time average (P/B) used in Ecopath, $F(t)$ a temporal function reproducing the impact of the physical factors, and $f(N)$, a function of the DIN stock limiting the phytoplankton growth. Ecosim forcing function must always have an average of 1. $F(t)$ is mainly imposing the seasonal cycle and is computed as a



multilinear combination of physical factors : sea surface temperature (SST), mixed layer depth (MLD), and available light in the upper meters (PAR) .

Assuming this seasonal variability is more important than interannual variability we identify $F(t)$ by deriving the coefficients a_1, a_2, a_3 which fit the function $F(t) = a_1 \cdot \text{SST} + a_2 \cdot \text{PAR} + a_3 \cdot \text{MLD}$ to the signal $(P/B)/(P/B)_0$.

The next step is to identify $f(N)$ which form is imposed as $f(N) = b_1 \cdot (N/N+K)$, where b_1 is introduced to allow $\langle f(N(t)) \rangle = 1$, as required by Ecosim. Again we compute the coefficients b_1 and K to fit $f(N)$ to the signal $(P/B)/(P/B)_0 / F(t)$, but as it is mainly the interannual signal that import here the time series N and $(P/B)/(P/B)_0 / F(t)$ are smoothed with a 3 years moving average (Figure 45).

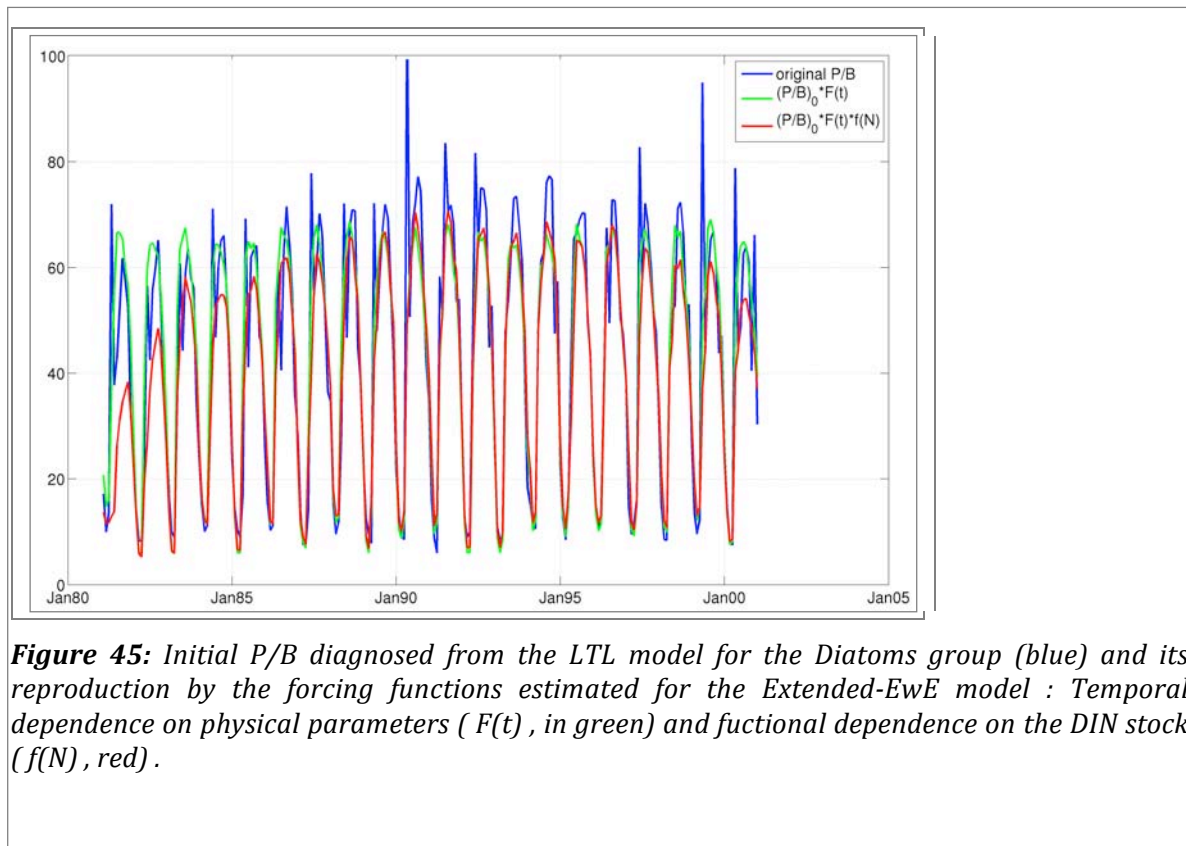


Figure 45: Initial P/B diagnosed from the LTL model for the Diatoms group (blue) and its reproduction by the forcing functions estimated for the Extended-EwE model : Temporal dependence on physical parameters ($F(t)$, in green) and fuctional dependence on the DIN stock ($f(N)$, red) .

Eastern Black Sea LTL model

(DMG-SU, USOF)

The physical model

The hydrodynamical model is based the three-dimensional GFDL MOM. Solid boundaries are non-slip and insulating for temperature and salinity. Convection is parameterized by convective adjustment that is often used to remove static instabilities. The model has 24 vertical levels, with model depths at 2.5, 7.5, 12.5, 17.5, 25, 35, 45, 55, 65, 75, 85, 105, 140, 185, 240, 310, 400, 515, 665, 870, 1145, 1470, 1820, and 2125 m. Mixing and diffusion in the horizontal are parameterized with biharmonic operators. The coefficients for momentum and tracers are:



$A_h=K_h=0.1 \times 10^{19} \text{ cm}^4 \text{ s}^{-1}$. The vertical mixing coefficient is $A_v=1.5 \text{ cm}^2 \text{ s}^{-1}$. The vertical diffusion in the model is parameterized as stability dependent: $K_v=aN^{-1}$, where N is the Vaaisaala frequency, $a=0.004 \text{ cm}^2 \text{ s}^{-2}$. The bottom is insulating:

Additionally we will set-up and use NEMO for the eastern Black Sea with the same horizontal resolution as GFDL-MOM.

The biogeochemical model

The structure of the BIOGEN model (state variables and processes linking them) is schematically illustrated in the Figure 46. The model describes the cycling of carbon, nitrogen, phosphorus and silicon through aggregated chemical and biological compartments of the planktonic and benthic systems. Each biological component represents a set of different organisms grouped together according to their trophic level and functional ecological behaviour. BIOGEN thus includes 34 state variables assembled in five models. These describe: (1) the growth physiology (photosynthesis, growth, exudation, respiration) of phototrophic flagellates (NF), diatoms (DA) and opportunistic non-siliceous microphytoplankton (OP); (2) the dynamics (grazing, growth, nutrient regeneration, egestion) of the dominant micro- (MCZ) and meso- (COP) zooplankton populations; (3) the feeding and growth activity of the omnivorous giant dinoflagellate *Noctiluca* (NOC) and the carnivorous *Aurelia* (AUR) and *Mnemiopsis* (MNE) gelatinous organisms; (4) the dynamics of organic matter (particulate, POM and dissolved, DOM; each with two classes of biodegradability) degradation by bacteria (BAC) and its coupling with nutrient regeneration; and (5) the benthic diagenesis and nutrient release by local sediments. The model is closed by gelatinous organism mortality and by fish pressure. The latter is indirectly included in the model through the mortality of mesozooplankton (COP) and is described as first-order kinetics.

All forms of major inorganic nutrients are considered. All phytoplankton groups assimilate NO_3 , NH_4 and PO_4 . Silicic acid (SiO) is taken up only by DA and released into the surrounding medium after diatom lysis and zooplankton feces dissolution. PO_4 and NH_4 , the latter only when the chemical composition of the bacterial substrate (BS) is N-depleted, are directly used by bacteria (BAC). Both NH_4 and PO_4 are regenerated through BAC, MCZ, COP, NOC, AUR and MNE catabolic activity. All organisms undergo autolytic processes, which release dissolved (DOM) and particulate (POM) polymeric organic matter, each with two classes of biodegradability, into the water column. Large phytoplankton (DA and OP), detrital particulate organic matter (POM) and zooplankton (COP, NOC, AUR, MNE) fecal pellets undergo sedimentation. Sedimented biogenic material is pooled as benthic particulate organic matter (BPOM) with two classes of biodegradability. Benthic nutrient exchanges are calculated from organic matter degradation, oxygen consumption and nutrient release and transformation (nitrification/ denitrification), taking into account PO_4 and NH_4 adsorption on particles and mixing processes in the interstitial and solid phases of the sediment.). BIOGEN innovation is the representation of the feeding mode of the gelatinous organisms NOC, AUR and MNE. The omnivorous *Noctiluca* (NOC) feed on all auto- and heterotrophic microorganisms and detrital POM. The gelatinous carnivores AUR and MNE eat mesozooplankton (COP). All gelatinous organisms are 'top-predators' and no trophic link exists between them. Thus, lysis is the only mortality process affecting them.

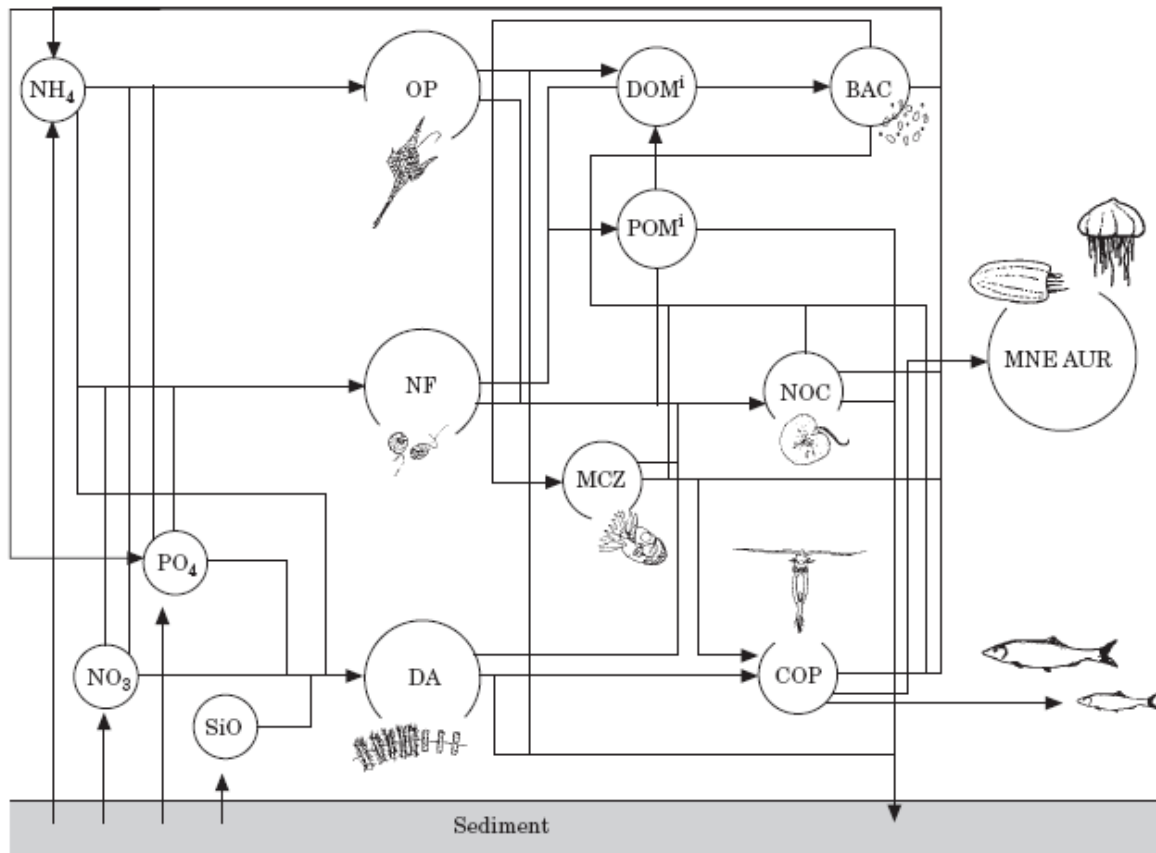


Figure 46: Diagrammatic representation of the structure of the BIOGEN model. Inorganic nutrients include ammonium (NH_4), nitrate (NO_3), phosphate (PO_4) and silicic acid (SiO). Organic matter is composed of dissolved ($\text{DOM}_{1,2}$) and particulate ($\text{POM}_{1,2}$) matter each with two different biodegradability classes. Phytoplankton is composed of three groups: diatoms (DA), autotrophic nanoflagellates (NF) and opportunists (OP). Bacterioplankton is represented by BAC . Zooplankton includes microzooplankton (MCZ) and copepods (COP). The gelatinous food-chain is composed of Noctiluca (NOC), Aurelia (AUR) and Mnemiopsis (MNE).

Numerical Implementation

A fully on-line coupling is performed between the hydrodynamical and biogeochemical models. For the eastern Black Sea the coupled hydrodynamical-biogeochemical model is implemented with a resolution of 9 km. The model is forced with ERA-40 data provided by the ECMWF. The data provided by PERSEUS project will be later also use to the run the coupled model.

State of advancement

The impact of vertical stratification and forcing with different time scales on the functioning of biological system (described by five compartment, NPZD, Fasham-Ducklow, pelagic ecosystem model) has been studied by Staneva et al. (1998). The analyses revealed that the high frequency oscillation of the external forcing are very important for the temporal variability of both, the physical and biological system. The results of coupling between different physical models (mixed layer model, box-like



model and 3-D basin-wide general circulation model) and ecosystem model (Lancelot et al., 2002) demonstrate that simulated phytoplankton evolution compares well with the SeaWiFS and CSCZ satellite data. These works quantify the capability of a strongly polluted system to recover after changing agricultural activities in the former socialist countries in South-eastern Europe. The mechanisms of matter transfer from the land (Danube Delta) to the sea and across the Western Black Sea continental margin revealed from simulations with suitable physical and biogeochemical models based on off line coupling between coupled BFM and POM . The impact of natural and anthropogenic matter from the land to the coastal environment and identifying limitations on the nutrient capacity of the coastal waters by studying extreme events for the north-western Black Sea have been studied (see Staneva et al., 2007 and Kourafalou et al, 2005). In PERSEUS we implement the nested grid model for the eastern and central Black Sea . The newly available atmospheric and river data from PERSEUS partners will be used to forced the coupled physical-biogeochemical model. The models will be validated with up to date satellite data . Additionally the newly available ARGO floats will also be used for model comparisons. As described below, new model diagnostics are performed to make the coupling with the HTL possible.

Skill assessment

Below Figures 47-49 show some comparisons between model simulations and observational data for the Eastern Black Sea. Using most of the available data observational data we performed monthly averages. The data from the numerical simulations have been extracted for the same locations and time as the observational ones. It is clearly seen that there is a good agreement between model and observations giving the confidence to proceed with the next step, namely further coupled the model with the HTL

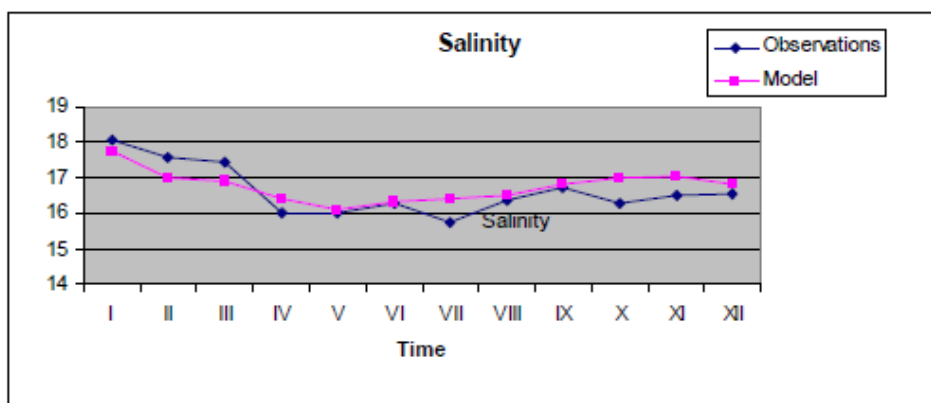


Figure 47: Monthly mean salinity derived from the model simulations (pink line) and the observations (blue line)

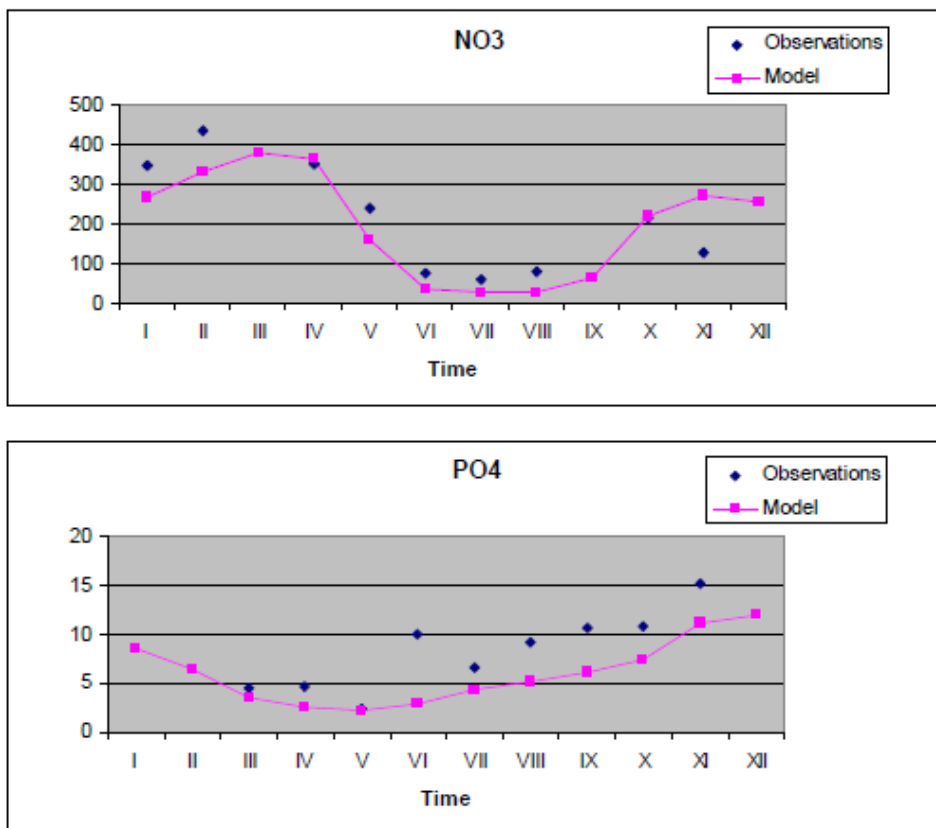


Figure 48: Monthly mean NO3 and PO4 derived from the model simulations (pink line) and the observations (blue line).

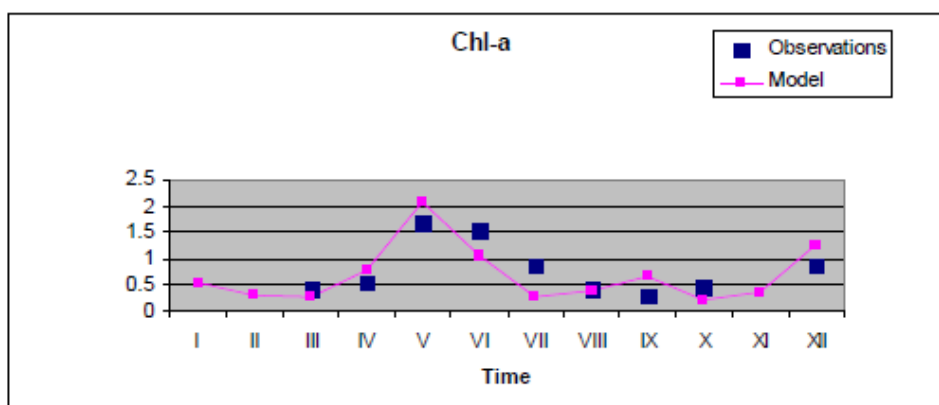


Figure 49: Monthly mean concentration of Chlorophyll derived from the model simulations (pink line) and the observations (blue line)

Numerical Modelling of Biogeochemical Regime Response to Decadal Atmospheric Variability During 1960–2000

Based on an analysis of observations and coupled hydrophysical biogeochemical model, long-term variability of the physical and biogeochemical structure of oxic and



suboxic layers in the Black Sea is shown. The performance of the model is illustrated in Figure 50 by validating the simulations against observations from the Knorr Black Sea Cruise in the centre of the Black Sea Western Gyre in 2003. Because the processes in the Black Sea align to isopycnals, we present simulated profiles against depth and density separately. Figure bellow reveals the typical vertical distribution of temperature, salinity, oxygen and hydrogen sulphide. Overall, the comparison is quite good; however, some differences are to be mentioned: the cold intermediate layer (CIL) in the model is a little more diffuse than in the observations, and the oxygenated water penetrates slightly deeper in the upper layer. As a success of the simulation, one could mention the approximate agreement of the isopycnic depth of the suboxic layer (a layer characterized by the absence of dissolved oxygen and hydrogen sulphide; Murray et al. (2005) in the observations and simulations.

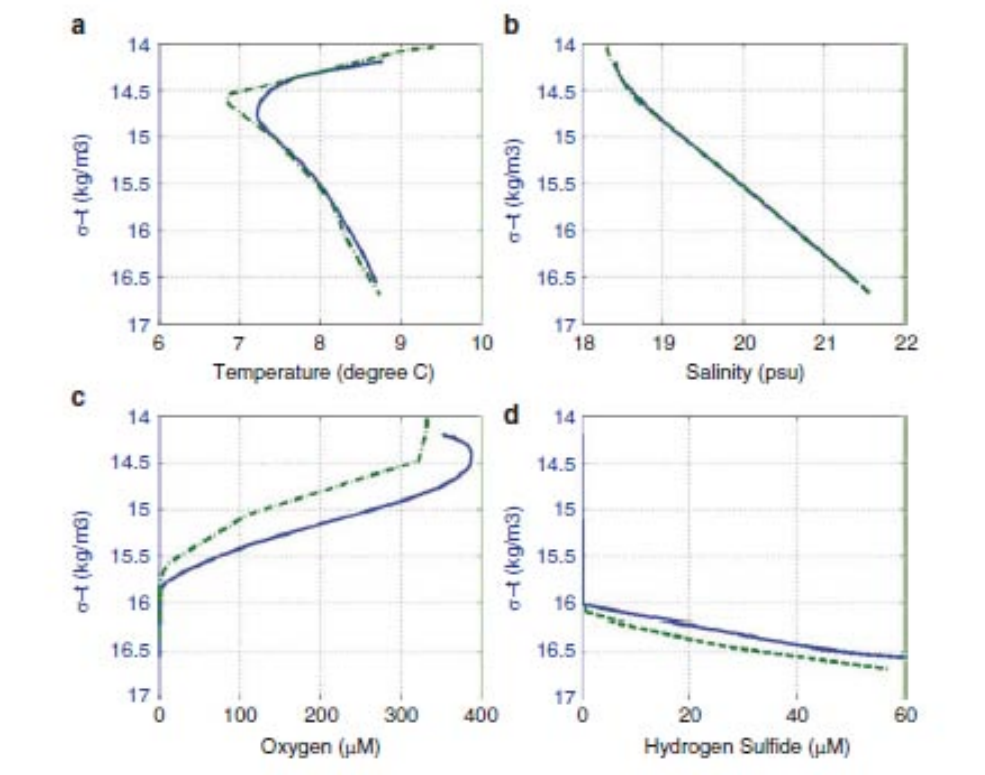


Figure 50: Comparisons of vertical distribution of temperature, salinity, oxygen and hydrogen sulphide between simulation and observation versus depth and density. Observations used for intercomparisons are taken from Knorr Cruise in 2003.

Interannual Variability of Simulated Biogeochemistry Responses

Decadal and interannual variability in atmospheric state, in particular in the European region, is well pronounced when analysing data for winter months. Interannual variability in the physical system has been analysed by Stanev et al. (2004) and Tsimplis et al. 2004. One important result from the above studies is that the deep layers of the Black Sea do not show pronounced sensitivity to interannual variations in forcing. This is due to the strong stratification decoupling surface and deep layers. However, as it has been demonstrated by Staneva et al. (2001), responses in the upper layers and down to the depth of CIL are very clear. Recently,



the response of a number of biogeochemical parameters to long-term atmospheric variability has been addressed by Oguz (2007).

According to the model simulations (see the Figure 51), the NAO index in winter influences the anomalies of oxygen, phytoplankton and nitrate concentrations at both surface and CIL. The oxygen concentration at the surface had same trend of increasing with NAO in 1962–2000 that is opposite to temperature. Before 1990, the oxygen anomaly kept negative and became positive in the most time of 1990s, when it might be caused by high solubility of oxygen due to the colder SST. From the middle 1970s to middle 1980s, oxygen maintained relatively stable, while phytoplankton and nitrate appeared maximum. Furthermore, the correlation of general trend between winter NAO and phytoplankton and nitrate in surface layers was clearly negative. Noteworthy is that the correlation between above phytoplankton and nitrate in the surface layer is much stronger than oxygen, which may reflect that at surface phytoplankton concentration depends on nitrate, while the surface layer oxygen can be affected by other factors, i.e. temperature-forced changes in the air–water exchange.

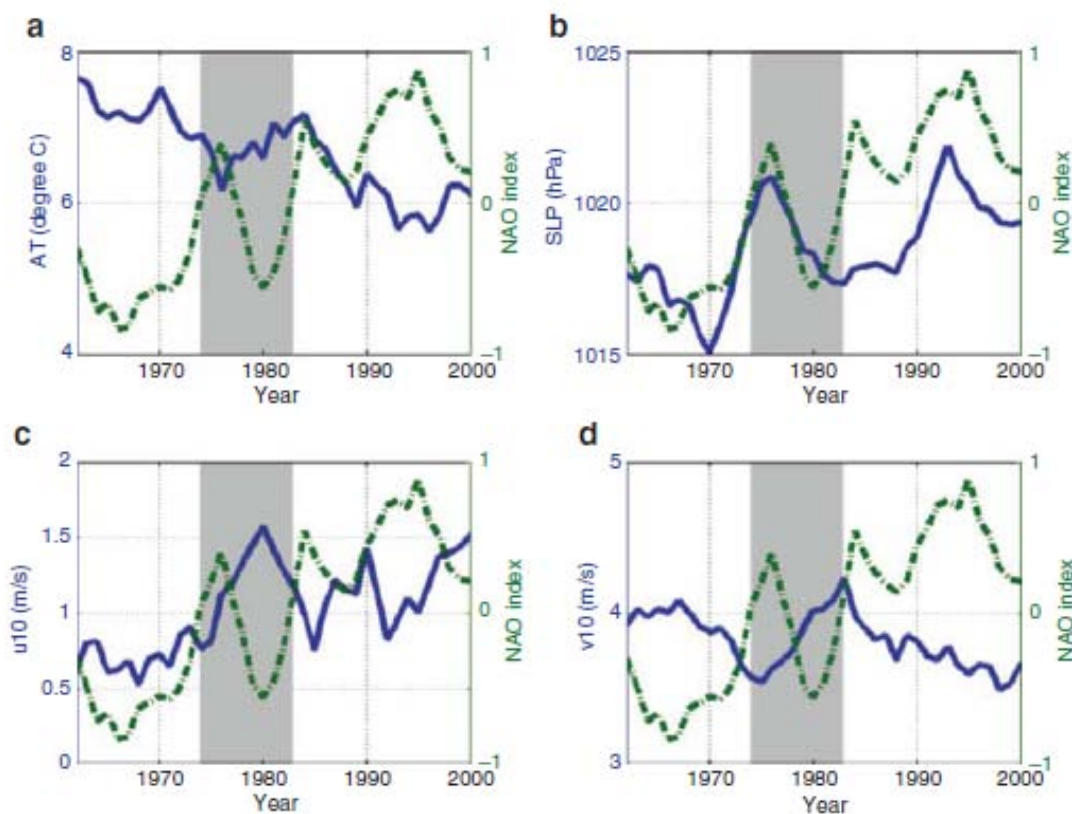


Figure 51: Interannual variability of air temperature (a), SLP (b) and wind components u_{10} (c) and v_{10} (d) in winter (December–February) compared with the winter NAO index. Data were 5-year moving averaged.

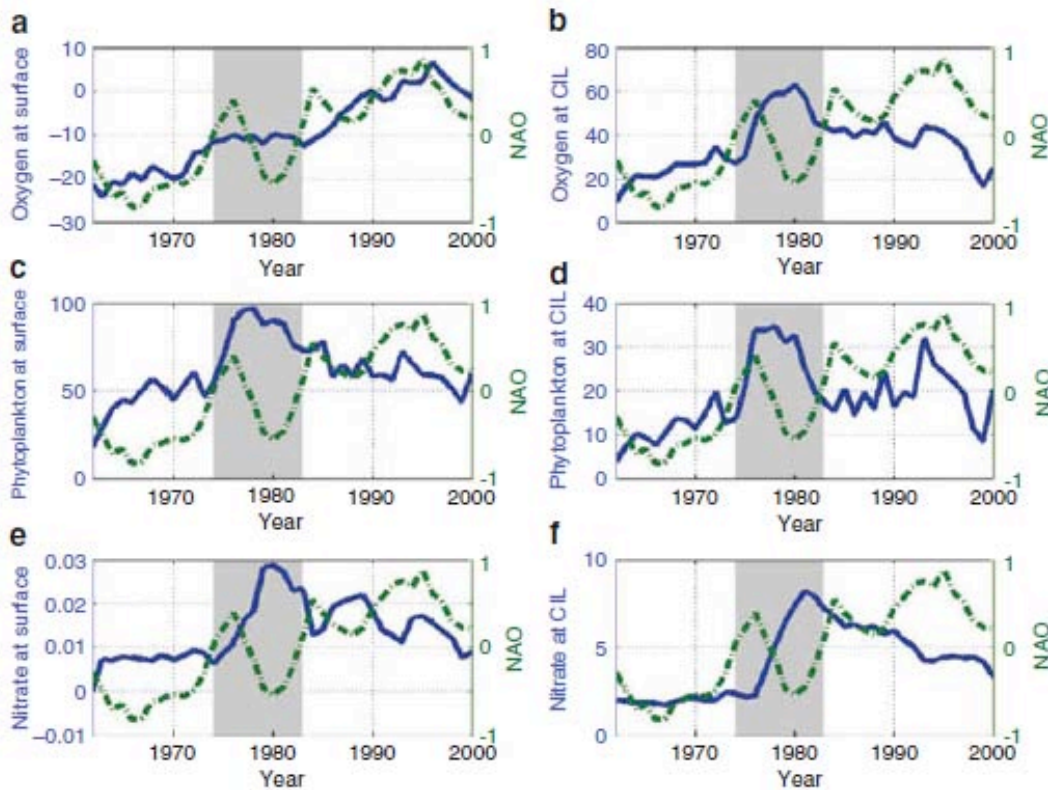


Figure 52: Interannual variability in anomalies of oxygen, phytoplankton and nitrate concentrations in winter time simulated at sea surface (0–5 m) (left) and CIL (60–90 m) (right) versus winter NAO index (December–February). (a) Oxygen at surface versus winter NAO index; (b) oxygen at CIL versus winter NAO index; (c) phytoplankton at surface versus winter NAO index; (d) phytoplankton at CIL versus winter NAO index; (e) nitrate at surface versus winter NAO index; (f) nitrate at CIL versus winter NAO index

Model diagnostics for coupling with the HTL model

As for the North Western Black Sea shelf model of GHER, a number of new model diagnostics has been performed by BIOGEN for the requirements of the HTL models. In order to facilitate the coupling between HTL and LTL but also to make the results comparable, the diagnostics from the LTL model BIOGEN were done using similar analyses as well as adjusting variables and processes to those for the north western Black Sea. Time series for the eastern and open Black Sea has been transformed in Ecopath unit requirements to mg N / m^2 and $\text{mg N / m}^2/\text{y}$. They have been first given as monthly mean values from which average rates and flow matrixes can be easily calculated (see Figure 53). In order to take into consideration the response of the system to the atmospheric variability and the river run-off forcing functions have been extracted using the same procedure as described for the Eastern Black Sea.

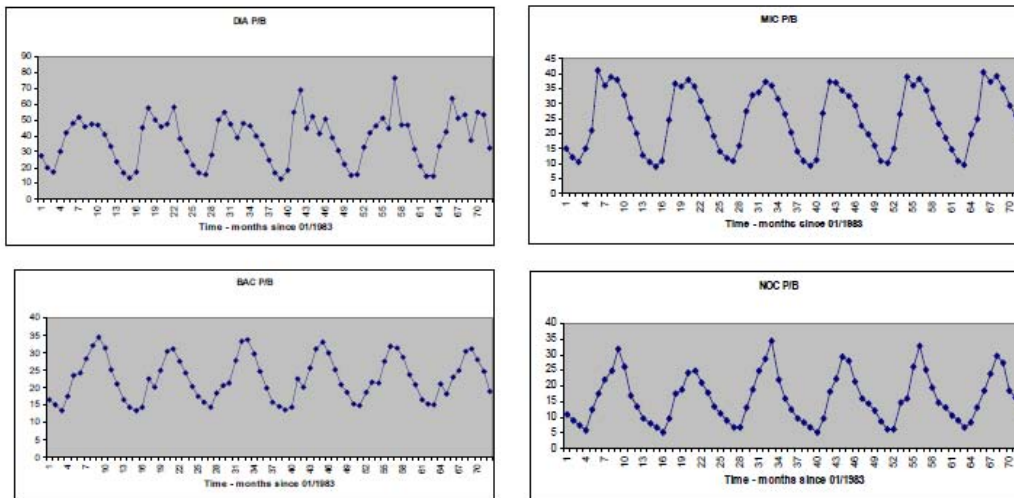


Figure 53: The P/B diagnosed from the BIOGEN Model for some of the state variables.

Ecopath (EwE) coupled with LTL

(IBER-BAS)

An almost entirely new EwE model has been constructed in order to couple with the LTL models and to respond to the need for regionalisation.

The original EwE model (Daskalov 2002) encompasses only 15 functional groups, where fish stocks are pulled into 3 aggregated groups: small pelagic planktivorous fish (mainly sprat, anchovy and horse mackerel), pelagic predatory fish (bonito, bluefish, mackerel), and demersal fish (whiting, dogfish, and other demersal fish). In unpublished update (Daskalov et al. 2012) the model has been updated by adding information about zoobenthos consisting of 6 more functional groups.

The present model contains separated fish groups in accordance to general model structure agreed between all partners to allow for inter-regional comparison. In order to encompass broad regions of the Black Sea the model distinguishes between the Western Shelf and the Open sea areas. As it can be seen from the input parameters (Table 12) the Shelf and the Open sea subsystems have clear differences in terms of external forcing and biomass flows. However they also present broad interactions between them. Namely, it is well known (e.g. Ivanov and Beverton 1976, Zaitsev and Mamaev 1997) that fish stocks migrate around the Black Sea. In this way some major stocks e.g. anchovy, horse mackerel, can be found in different areas according to their annual life cycle e.g. feeding mainly in the Northwest and wintering (when most of the fisheries catch is taken) in the south and southeast of the sea. For that reason only the LTL components of the model have been separated between Shelf and the Open sea areas, and the HTL components were kept generic (Table 12).

After revising the available data, information, and present knowledge of the Black Seasystem, the project expert group decided that to perform initially a natural regionalization for developing and implementing of the coupling between the different LTL regional models (GHER and USOF) with the HTL(IBER-BAS) one. The implementation of the coupling will be initially performed first for the Shelf and Open sea



regions of the Black Sea. It was also agreed by the Black Sea WP4 partners, that the two regions should be interacting inside of one E2E model with the HTL components kept generic as presented in Table 12.

Such a model structure is obviously a compromise driven by the constraints of the present availability of data and knowledge. A better option would be to construct a full spatio-temporal model of the Black Sea containing regional (spatial) information of abundance, distribution, diets, and migration of the most (if not all) the model's functional groups, which is not available at present. The EwE tool is not yet developed to simulate spatio-temporal dynamics considering simultaneous spatial and temporal forcings.

The Regional Black Sea (RBS) model structure was set to 39 functional groups including inorganic nitrogen (DIN) as nutrient (2 groups), bacteria (2 groups), primary producers (phytoplankton, 4 groups), protozoans (Noctiluca, 2 groups), invertebrates (zooplankton and zoobenthos, 14 groups), fish (9 groups), dolphins (1), and detritus groups (5, Table 12) and 8 fishing fleets (Table 14).

The model is relative to the Black Sea divided into Western Shelf region (88824 km²) and Open Sea region (348560 km²) for LTL components (DIN, bacteria, phyto-, and zooplankton, and Noctiluca). Biomass flows are expressed in nitrogen weight (mgN*m⁻²*year⁻¹). The model refers to the 1980s as parameters are estimated as averages over 1975-1989. The relative production (P/B) in fishes is assumed to be equivalent to the total mortality (Z, Allen 1971), which is the sum of the fishing and natural mortality: Z=F+M. The model is parameterised using estimates of biomass, production and consumption rates and diet composition compiled from stock assessments, literature sources, and previous models (e.g. Daskalov 2002, Daskalov et al 2012). Recent stock assessments (Daskalov et al. 2011) are used to set biomass and P/B = Z of the fish compartments. The previous model structure (Daskalov 2002) has been updated with fish stocks as separate functional groups for those stock for which there are analytical stock assessments: anchovy, sprat, horse mackerel, shad (*Alosa pontica*), whiting, turbot and spiny dogfish (*Squalus acantias*). Two aggregate groups contains stocks which are not currently assessed analytically: bonito, bluefish and mackerel are merged into the Pelagic predatory fish group and gobies, mullets, rays and other fall into the Other demersal fish group (Table 12).

Zoobenthos functional groups have been recently added such as: Black mussels, *Chamelea gallina*, *Rapana venosa*, Other mollusca, Benthic crustacean, and Worms (Table 12, Daskalov et al 2012). The first 3 groups are of utmost ecological importance as dominant or key-stone species. They are also important objects for respective fisheries (see also Table 14). The group Other molluscs is also very abundant and include such important species as *Mya arenaria*, *Anadara cornea*, and others molluscs (mainly bivalves). Data on zoobenthos is very limited and fragmentary, especially in recent years. Our main sources of data are the reviews of Kiseleva (1979) and Grese (1979), though the information published there apply to the 1960s and 1970s. Data on later years were updated where possible using recent reviews such as these of Chikina and Kucheruk (2005) and Revkov et al. (2008).



Table 12. Input values and results (in bold) from the mass-balance Regional Black Sea model in the 1980s. Flows are in $\text{mgN} \cdot \text{m}^{-2} \cdot \text{year}^{-1}$ and rates are on annual basis. In the last two columns initial values of biomass and P/B (called Biomass^0 , P/B^0 respectively) are shown.

Trophic group	Trophic level	Biomass	P/B	Q/B	EE	PQ	Biomass ⁰	P/B ⁰
DIN open	1	1077.51	22.27	-	0.70	-	620.51	
Din shelf	1	6735.71	11.10	-	0.70	-		7.90
Bacteria open	2	72.36	22.79	107.16	0.63	0.21		
Phytopl small open	2	106.62	72.13	72.13	0.85	-	79.49	
Phytopl large open	2	286.91	31.75	31.75	0.75	-		
Zoopl small open	3	32.66	26.92	126.74	0.78	0.21		
Zoopl large open	2.7	36.66	83.46	162.13	0.31	0.52		
Noctiluca open	2.77	79.11	17.60	110.86	0.00	0.16		
Bacteria shelf	2	178.74	32.77	152.61	0.91	0.22		
Phytopl small shelf	2	266.76	92.48	92.48	0.64	1.00		
Phytopl large shelf	2	1211.38	22.82	22.82	0.79	1.00		
Zoopl small shelf	3	57.23	34.75	90.78	0.85	0.38	34.04	
Zoopl large shelf	2.67	115.06	50.53	101.10	0.23	0.50		
Noctiluca shelf	2.75	271.45	17.48	116.72	0.00	0.15		
Pleurobrachia	3.84	7.93	10.95	29.20	0.00	0.38		
Aurelia	3.84	42.81	10.95	29.20	0.00	0.38		
Mnemiopsis	3.84	39.47	10.95	29.20	0.00	0.38		
Sagitta	3.81	5.84	36.50	73.00	0.17	0.50		
Sprat	3.74	18.58	1.30	8.47	0.95	0.15		
Anchovy	3.74	43.45	1.30	11.73	0.77	0.11		
Horse Mackerel	4.11	8.10	1.00	7.28	0.57	0.14		
Alosa	4.43	0.27	0.80	5.33	0.43	0.15		
Pelagic predatory fish	4.83	0.88	0.80	5.33	0.75	0.15		
Whiting	4.55	10.87	1.00	2.50	0.80	0.40	8.40	
Turbot	4.31	0.60	0.80	5.33	0.21	0.15		
Dogfish	5.18	3.15	0.30	3.00	0.25	0.10		
Other demersal fish	3.92	9.56	1.00	3.00	0.95	0.33		
Dolphins	4.85	0.18	0.35	19.00	0.02	0.02		
Mussels	2.7	73.86	3.00	74.07	0.24	0.04		
Chamelea	2.6	22.46	4.00	98.77	0.15	0.04		
Rapana	3.69	0.34	0.50	3.33	0.01	0.15		
Other molluscs	2.7	44.74	3.00	74.07	0.20	0.04		
Benthic crustations	2.74	3.27	9.70	64.67	0.95	0.15	2.25	
Worms	2.08	20.35	6.30	60.00	0.76	0.11		
POM open	1	5040.69	-	-	0.52	-		
DOM open	1	4591.14	-	-	0.39	-		
POM shelf	1	28265.60	-	-	0.40	-		



DOM shelf	1	16200.19	-	-	0.41	-
Detritus shelf	1	13794.27	-	-	0.05	-

Table 13. Flow to various detrital groups in %

Trophic group	POM open	POM shelf	DOM open	DOM shelf	Detritus shelf	Export	Sum
DIN open						100%	100%
Din shelf						100%	100%
Bacteria open			100%				100%
Phytopl small open				100%			100%
Phytopl large open	58%		42%				100%
Zoopl small open		54%		46%			100%
Zoopl large open	62%		37%			1%	100%
Noctiluca open		43%		29%	28%		100%
Bacteria shelf	68%		32%				100%
Phytopl small shelf		63%		37%			100%
Phytopl large shelf	69%		31%				100%
Zoopl small shelf		64%	0%	36%			100%
Zoopl large shelf			100%				100%
Noctiluca shelf				100%			100%
Pleurobrachia		65%		20%	15%		100%
Aurelia		65%		15%	20%		100%
Mnemiopsis		65%		15%	20%		100%
Sagitta		65%		20%	15%		100%
Sprat		5%		5%	90%		100%
Anchovy		5%		5%	90%		100%
Horse Mackerel		5%		5%	90%		100%
Alosa		5%		5%	90%		100%
Pelagic predatory fish		5%		5%	90%		100%
Whiting		5%		5%	90%		100%
Turbot		5%		5%	90%		100%
Dogfish		5%		5%	90%		100%
Other demersal fish		5%		5%	90%		100%
Dolphins		5%		5%	80%	10%	100%
Mussels		5%			95%		100%
Chamelea		5%			95%		100%
Rapana		5%			95%		100%
Other molluscs		5%			95%		100%
Benthic crustations		5%			95%		100%
Worms		5%			95%		100%
POM open			90%			10%	100%



DOM open		37%	63%	100%
POM shelf	100%			100%
DOM shelf		100%		100%
Detritus shelf	4%		96%	100%

Table 14. Fisheries catches (in mgN*m⁻²*year⁻¹) used in the model

Trophic group	Sprat fleets	Anchovy fleets	Coastal nets	Predat. fish fleets	Demersal fleets	Mussel fleets	Chamelea fleets	Total
Sprat	2.36							2.36
Anchovy		13.33						13.33
Horse Mackerel		2.71						2.71
Alosa			0.09					0.09
Pelagic predatory fish				0.53				0.53
Whiting					0.93			0.93
Turbot					0.10			0.10
Dogfish					0.23			0.23
Other demersal fish					0.41			0.41
Mussels						0.11		0.11
Chamelea							0.02	0.02
Total	2.36	16.04	0.09	0.53	1.67	0.11	0.02	20.82

Preliminary skill-assessment - Fitting to biomass time series 1965-2000

A previously constructed Ecosim model has been fitted to time-series data of biomass of the main functional groups (Daskalov et al. 2012). As biomass data are empirically obtained, the procedure of fitting (adjustment) Ecosim to time-series data essentially represents a validation procedure. As data for the HTL groups of this model are the same as those used to parameterise the coupled Regional Black Sea model described in this report, the time series fitting of the HTL model can be regarded as preliminary "skill assessment" of the HTL components.

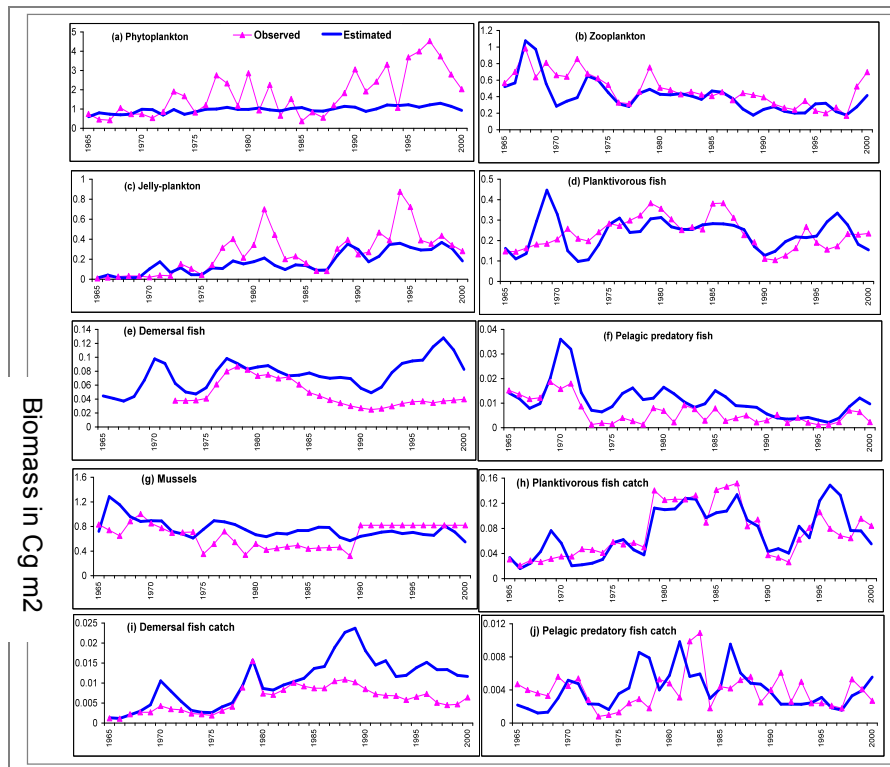


Figure 54. Time dynamic model estimates (blue lines) of the main trophic groups in the Ecosim model 1965-2000, fitted to empirical data (purple lines and diamonds)

The fitted model over 1965-2000 shows very good resemblance to empirical time-series data (Figure 54). In almost all groups the long-term patterns are well imitated in both amplitude and frequency. The trend in planktivorous fish depicts well the rise and fall in the stocks during the 1980s and 1990s respectively (Figure 54d). The step-wise increase in jelly-plankton is also well imitated by means of both suitable choice of vulnerability settings and "fine tuning" by the jelly-plankton anomaly (Figure 54c). As a result the hindcasted large zooplankton biomass fits very well the empirical data (Figure 54b). Some more unrealistic feature is the simulated increase in demersal fish biomass at the end of the 1990s which is not supported by the empirical data (Figure 54e). This also results in unrealistically high demersal catches over the late 1990s. Low trophic levels (e.g. Large phytoplankton, Figure 54a) are also less satisfactorily represented but this is a well known deficiency of the EwE modelling approach.

The fitting procedure will be repeated and further developed with the coupled Regional Black Sea model where time-series from the LTL will be used to additionally force and adjust the model.

Balancing the coupled Regional Black Sea model

A preliminary "skill assessment" of the coupled Regional Black Sea model can be performed by the procedure of obtaining a 'mass balance' of the Ecopath model.

Ecopath requires that, for each group, the modeller specifies three out of four of the following input parameters: B, P/B, Q/B, EE (Christensen et al. 2005). The fourth unknown parameter (usually EE, which cannot be measured on-field) can be unknown and will be estimated by Ecopath (or, if known, it can be used to "calibrate" the



model) by solving the system of linear equations behind Ecopath. It is possible that, when Ecopath estimates the unknown parameters through the solution of the linear system, an un-balanced network is found, e.g. calculated respiration for a group is negative, or EE is higher than 1. This means that the resulting network is not balanced and hence is unrealistic. In this case, the modeller must change the inputs within known uncertainty ranges, by hand or using automatic algorithms (Kavanagh et al. 2004), and paying attention to other “tricks” (e.g. using physiologically feasible P/Q and R/B ratios for each group), until a combination of input parameters yielding a balanced, realistic network is found. The resulting network of biomass flows, namely the trophic exchanges among groups, respiration, flows to detritus, migrations, fishery catches and other exports, is a final 'mass balance' Ecopath model.

Adjustments made in parameter values in order to achieve mass balance are shown on Table 12. Initial values of biomass and P/B (called Biomass⁰, P/B⁰ respectively) are shown in the last two columns of the table. It can be seen that mass-balance is obtained with relatively few changes of the initial values that can serve as a validation of the model internal consistency. The model is validated by estimating realistic EE and P/Q values (in bold on Table 12).

Preliminary results and indicators

Food web structure and biomass flows

After balancing, the model biomass estimates are presented in Table 12. Total fish biomass in the Black Sea over 1975-1989 is about 2 millions of tons and the catches are about half of million of tons on average. This is the period of the highest fish abundance and respectively highest catches (Prodanov et al. 1997, Daskalov et al. 2007). Dominant shares in the biomass have small pelagic fishes: sprat and anchovy, horse mackerel, whiting and small demersal fishes (Table 12, Figure 55). Most of the catch as a quantity is taken from sprat, anchovy and horse mackerel (Table 14, Figure 55). The relative importance of different groups in consumption is shown on Figure 55. About 90% of the consumption goes to sprat, anchovy and horse mackerel (Figure 55, column 3) while biggest shares of fish as prey are from sprat and anchovy, whiting and small demersal fishes (Figure 55, column 4).

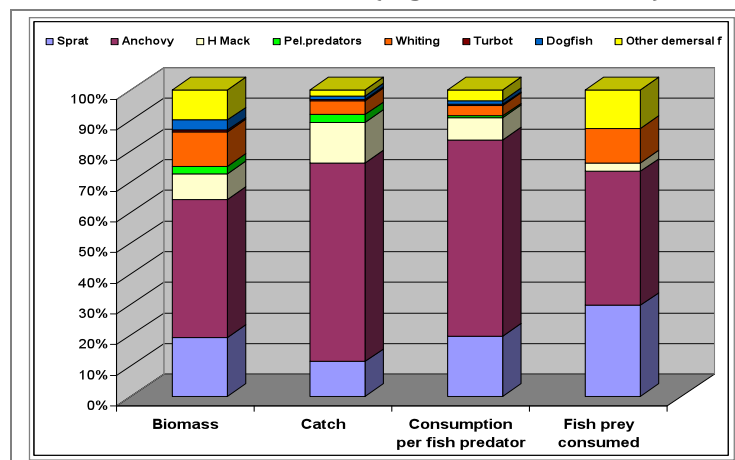


Figure 55. Structure of fish biomass, catch and consumption from the HTL model: 1st column is the % of each fish group in the total biomass, 2nd column is % quantity of each fish group in the catch, 3rd column is the % consumption of fish per predator groups; 4th column is the % quantity of each fish group consumed by all predators



Structure of consumption and mortality

Acknowledging ecological interactions, such as predation and competition, is a key to the Ecosystem Approach to Fisheries Management (EAFM). Trophic interactions raise two concerns for the fisheries management. The first is the decline in the food resource of commercially and functionally important stocks causing their damage. The second is the indirect effect of decreasing fish biomass on ecosystem functioning (e.g. trophic cascade, Daskalov 2002). We used various ecosystem indicators (e.g. as reviewed in Cury et al. 2006) to evaluate the interactions between the different components, and of structural ecosystem changes resulting from exploitation.

On Figure 56 are presented the quantities of fish and invertebrates consumed by the fishes and dolphins. The dominant fish predators are the pelagic predatory fishes, dolphins, dogfish, whiting and turbot. Horse mackerel and shad (*Alosa*) consume also a great deal of invertebrates (both zooplankton and zoobenthos) and sprat and anchovy are zooplanktivorous. The highest predation on fish is caused by whiting, horse mackerel, pelagic predatory fish and dogfish (Figure 57). Sprat is the dominant prey of whiting and dolphins, while anchovy dominate the diets of the horse mackerel and pelagic predatory fish (Figure 57B).

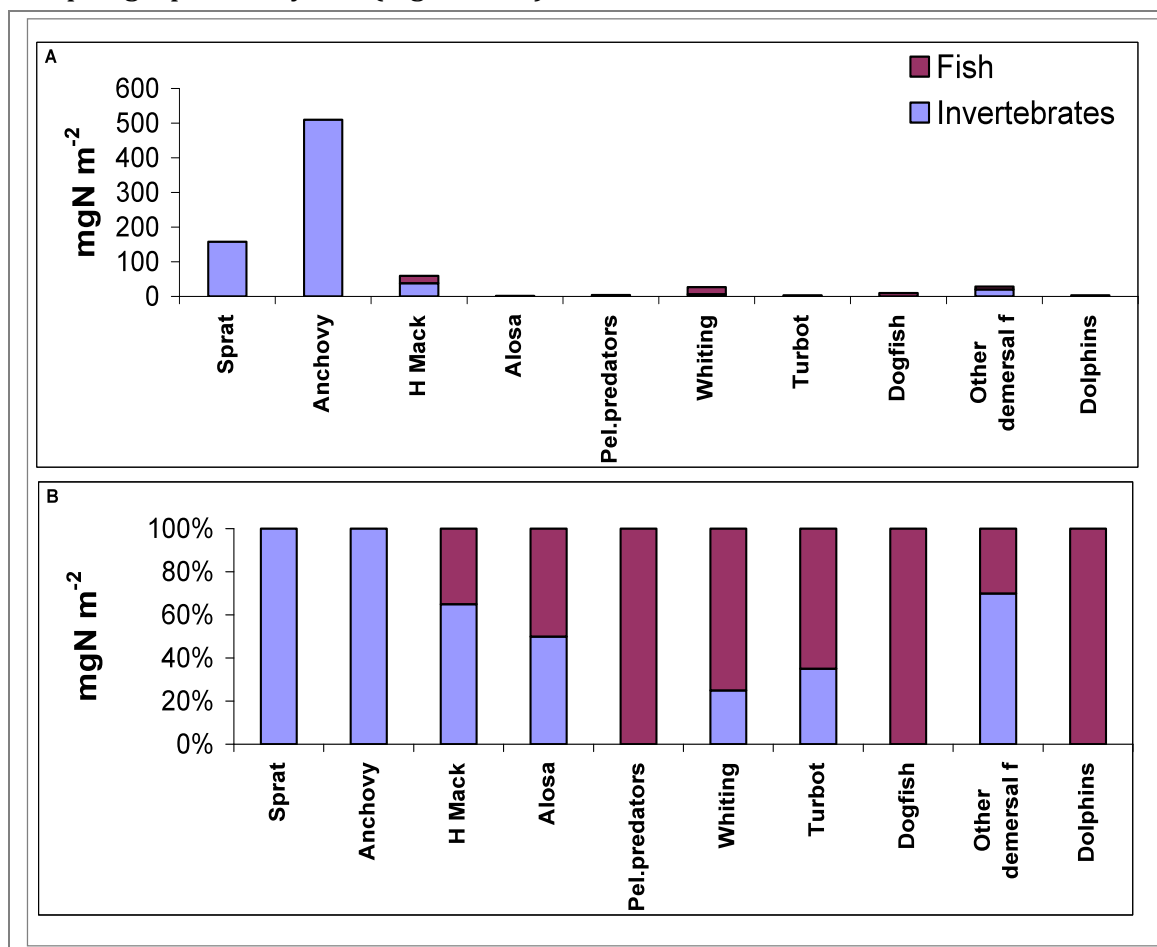


Figure 56. Biomass of fish and invertebrates consumption by fish: A. in biomass; B in %

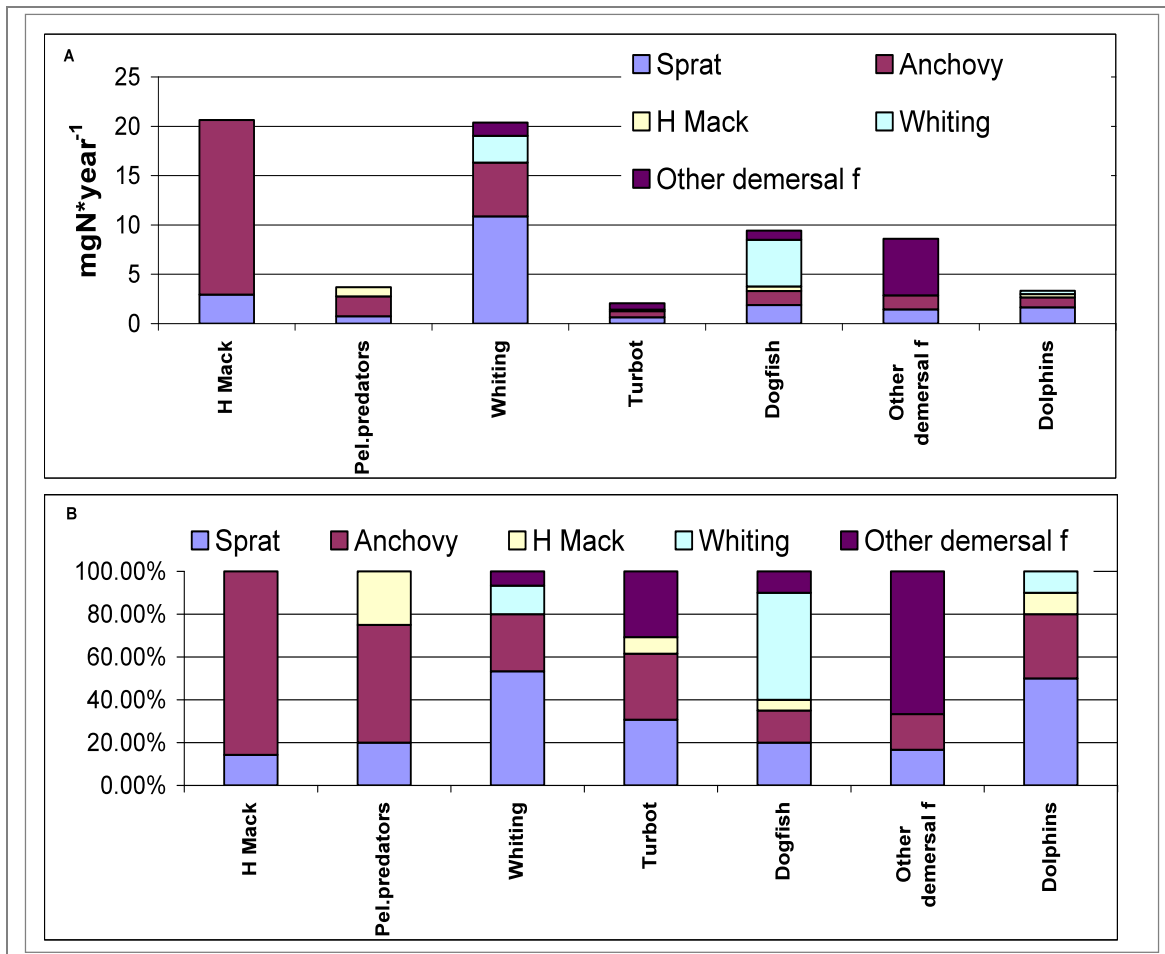


Figure 57. Biomass of fish consumed by fish: A. in biomass; B in %

Among all sources of mortality, predation mortality (M2) is highest in prey fish, such as sprat, anchovy, and small demersal fishes (Figures 58). Predation is high also on whiting including cannibalism. The representation of the partial predation mortality on Figure 59 demonstrates how different predators contribute to the total M2 of the main fish prey groups in the system: sprat, anchovy, whiting and small demersal fishes. In the case of sprat, whiting is the dominant predator followed by the horse mackerel, dogfish and dolphins (Figure 59A), horse mackerel and whiting exert the strongest effect on anchovy (Figure 59B), and dogfish and cannibalism on whiting (Figure 59C). Small demersal fishes are affected by other demersal predators (Figure 59D). The highest fishing mortality is applied on pelagic predatory fish shad and horse mackerel (Figure 58). Fishing mortality of turbot and dogfish might be underestimated due to underreporting and illegal fishing.

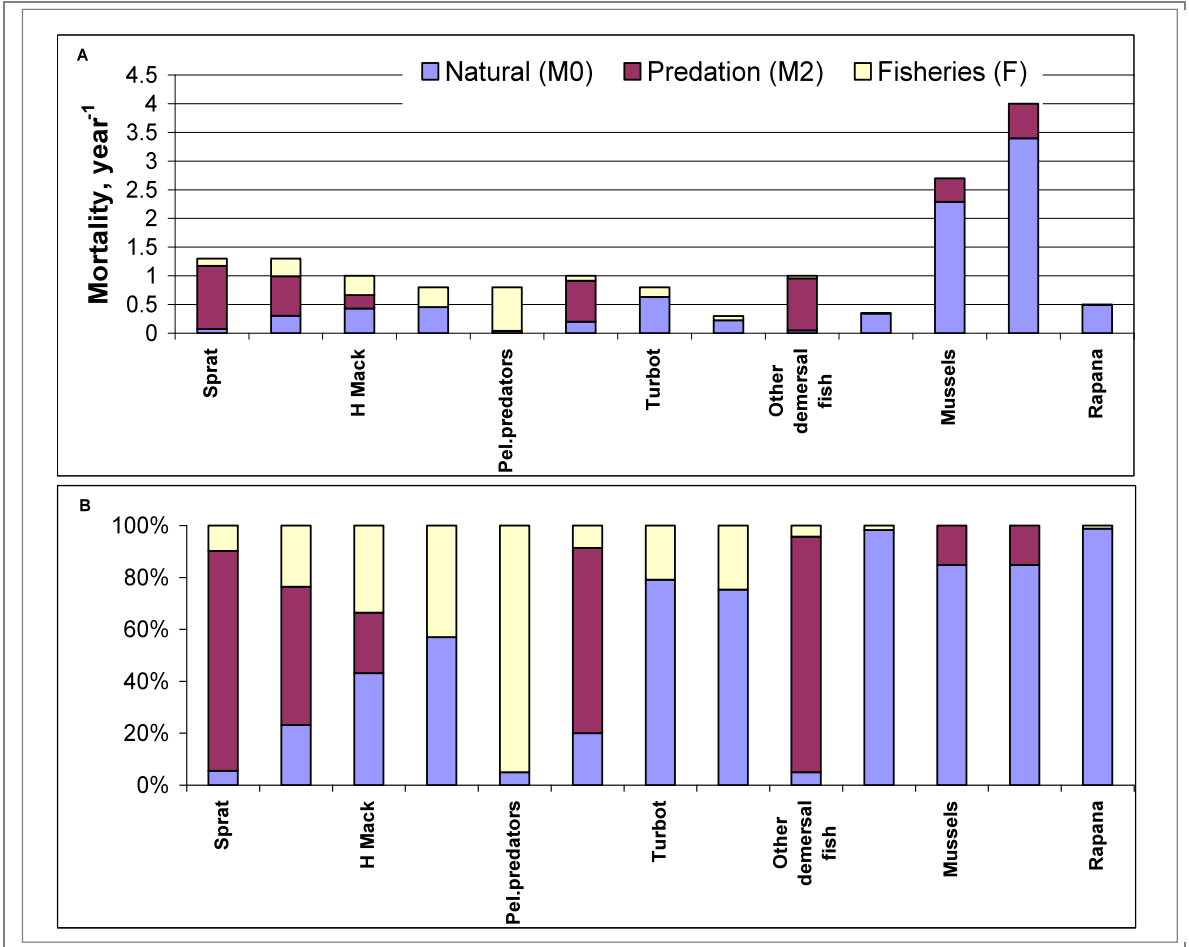


Figure 58. Structure of mortality: A. natural mortality (M0), predation mortality (M2) and fisheries mortality (F); B. percentage of the total mortality.

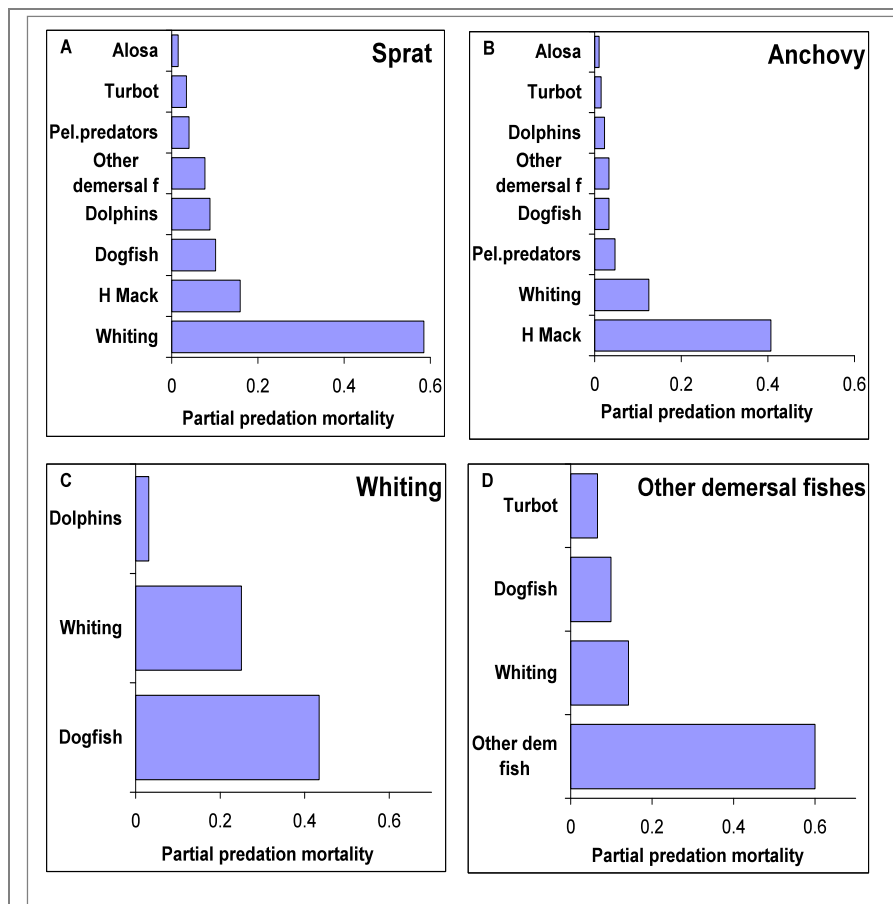


Figure 59. Partial predation mortality (M_2) of some important prey fish by various predators (sorted on the ordinate): A. Sprat; B. Anchovy; C. Whiting, D. Other demersal fishes

Mixed Trophic Impacts

The mixed trophic impacts (MTI) are indicators of the relative impact of change in the biomass of one component on other components of the ecosystem (Ulanowicz and Puccia, 1990). They are calculated by multiplication of the matrix of the direct impacts which is compiled using the diet (positive direct impact) and consumption (negative direct impact) matrices (Ulanowicz and Puccia, 1990). The mixed impact is a sum of the direct and indirect impacts. The indirect impacts can be associated with inter-group competition and trophic cascades. MTIs of some groups are shown on Figure 60.

The estimation of the impacts shows that the large zooplankton on the shelf affects negatively large zooplankton in the open sea as a competitor and large phytoplankton on the shelf as a top-down (grazing) impact (Figure 60A). It has a positive effect on its consumers, as well as on the anchovy fishery. Anchovy (Figure 60B) has a negative effect on competitors, such as sprat and horse mackerel a positive effect on predators and fisheries. It also demonstrate some trophic cascade effect by affecting negatively large zooplankton and positively (indirect effect) large phytoplankton on the shelf. Whiting affects negatively its preys and competitors and positively the demersal fishery (Figure 60C). Benthic crustacean affect negatively mussels and worms as preys and competitors (Figure 60D). POM on the shelf has a small positive impact on most of the HTL groups that demonstrate the effects of the detritus feedback loop.



MTIs can also be used as indicator of direct and indirect effects of fishing (Figure 60E). For instance, we can see the dominant impact of the demersal fleets on turbot and dogfish. Fishing practices can exert some indirect positive effects, due to increased growth of populations that are preys or competitors with those, which are targeted by the fisheries: for instance even if the demersal fleet is targeting also whiting (actually it has a largest share of the catch Table 14) it has a stronger positive indirect impact, because whiting is a prey of turbot and dogfish that are affected negatively by the demersal fleet (Figure 60E).

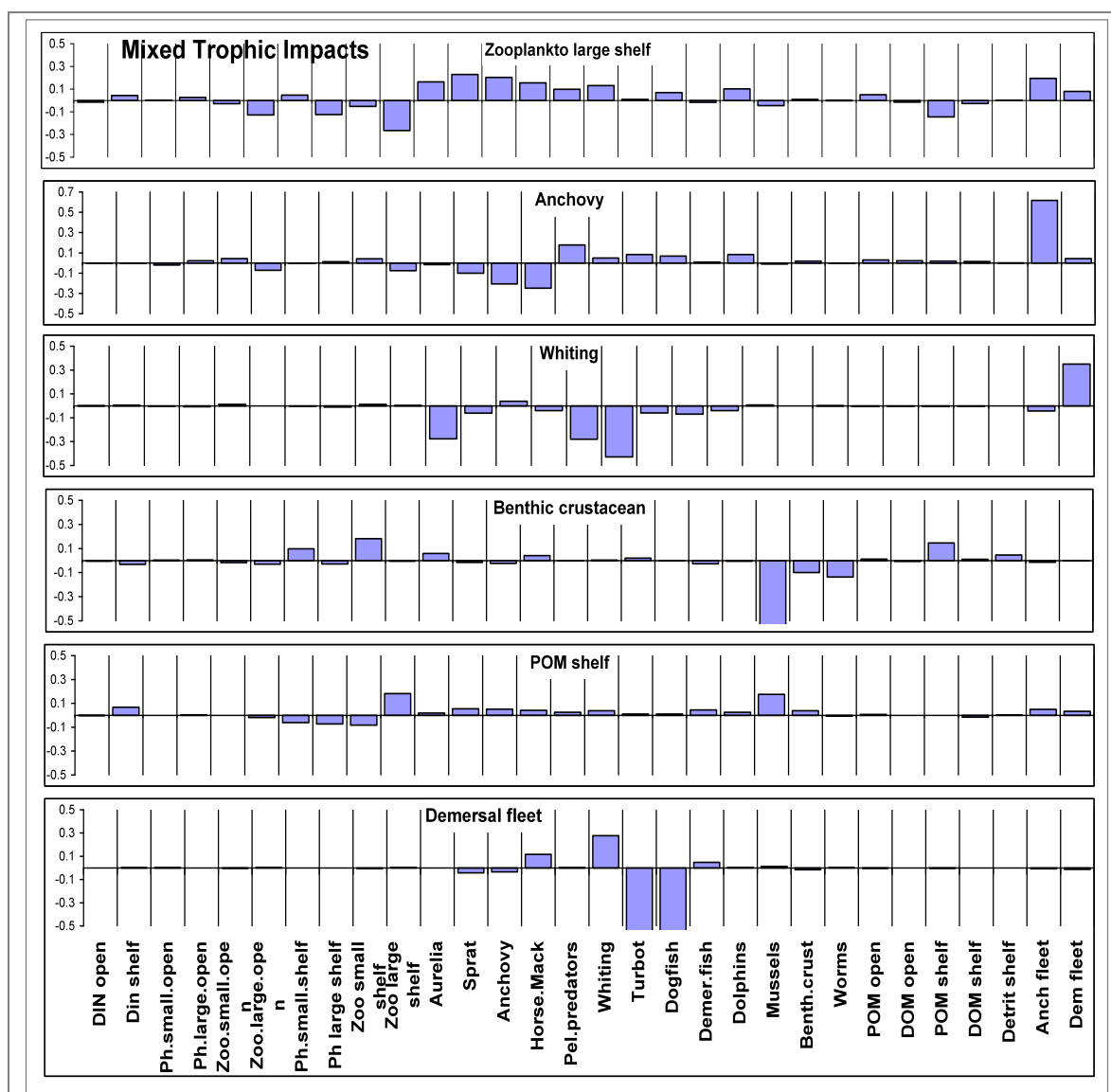


Figure 60. Mixed trophic impacts (MTIs) of selected fish groups: A. Zooplankton large shelf; B. Anchovy; C. Whiting; D. Benthic crustaceans; E. POM shelf; F. Demersal fleet



2.4.3 A preliminary comparison of “health” indices for Mediterranean areas

Solidoro C.¹ Libralato S.¹, Akoglu E.², Ballerini T.³, Banaru D.³, Capet A.⁴, Daskalov G.⁵, Gregoire M.⁴, Kandilarov R.⁶, P. Lazzari¹, Salihoglu B.², Staneva J.⁶, Tsagarakis K.⁷

1) OGS; 2) METU-IMS; 3) UNIVMED; 4) Ulg; 5) IBER-BAS; 6) DMG-SU; 7) HCMR

The European Marine Strategy Framework Directive (**MSFD**) (EU, June 2008) requires that by 2020 a good environmental status (“health”) will be reached in all of the European seas. Two of the 11 qualitative descriptors requested by MSFD to assess the health of marine ecosystems are: marine foodwebs (D4) and exploited species (D3). Moreover, according to the Food and Agriculture Organization (FAO, 1995, 2002) “the achievement of real marine ecosystem-based management of fisheries implies the regulation of the use of the living resources based on the understanding of the structure and dynamics of the ecosystem of which the resource is a part”. This requires an improvement in our understanding of the structure and functioning of marine ecosystems and of the alterations induced in them by human and environmental factors. Ecosystem modeling has been proposed as a tool to inform management decision for marine fisheries (Plagányi, 2007) and also in Mediterranean Sea (Cochrane and de Young, 2008).

Ecopath with Ecosim (EwE) is a software for ecosystem modeling that has been largely used worldwide to provide quantitative descriptions of the structure of aquatic food webs and to assess fishing impacts on exploited marine ecosystems (Christensen and Walters, 2004; Pauly et al., 2000). Costanza and Mageau (1999) proposed to use some outputs from EwE to characterize the status of marine ecosystems. In particular, indicators such as **vigor** (i.e. total system throughput and calculated total net primary production), **organization** (i.e. ascendancy and capacity) and **resilience** (i.e. overhead) can be used alone or in combination to characterize the “health” of the marine ecosystem Costanza and Mageau (1999): see Figure 61.

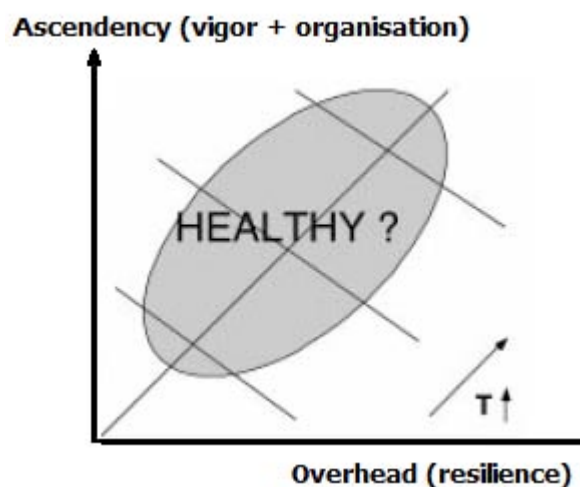


Figure 61. A conceptual diagram of the network analysis-based on quantitative indexes of ecosystem health. The ‘healthy’ region is indicated by the shaded area, and represents a balance between system vigor, organization, and resilience. Modified from Costanza and Mageau (1999).



These three indicators were selected in the **WP4 “Integrated tools for environmental assessment in the Western Mediterranean”** in the frame of PERSEUS FP7 project, to describe and compare the “health” of the food webs of three Mediterranean systems: Gulf of Lions, Adriatic Sea and Aegean Sea.

Since - prior to the actual comparison - an extensive work needed to be done, in order to define how to standardize models and model output across different mediterranean subregion, results must be considered very preliminary. And still provisional .

However, indexes could be computed, and a comparison among area (table 15 and Figures 53 and 54) indicate highest vigor and organization and resilience for the Gulf of Lions and lowest for Northern Aegean Sea. Intermediate values are identified for Adriatic model.

On this regard, it should be stressed, however, that additional thought on interpretation normalization of these indexes is required. As an example, even if a normalization over area seems to be prescribed for a comparison of measures, it appears clear that normalized data cannot be used, by themselves, as representative of the ecological function of a region. As an example a larger area might be more resilient of a smaller one just because of size, even if space-normalized indicators would indicate the opposite. Similar consideration holds true also for productivity.

Therefore more elaboration will be required to identify new and more comprehensive indicators

	ADR	GOL	NAE	Ecosystem health
TST	20980.77	34222	15790mgP m ⁻² year ⁻¹	vigor
sum Productions	6604.889	12801	5717mgP m ⁻² year ⁻¹	vigor
Sum of all consumption	11237.99	18995.8	8641.398mgP m ⁻² year ⁻¹	
Sum of all exports	7.524261	662.307	10.561mgP m ⁻² year ⁻¹	
Total catch	7.659231	7.062	7.559mgP m ⁻² year ⁻¹	
total biomass	424.1732	1831.201	164.712mgP m ⁻²	
TST cycled	20779.72	25867.75	15061.05mgP m ⁻² year ⁻¹	organization & vigor
TST cycled/TST	99.0%	75.6%	95.4%%	organization?
SOI	0.246504	0.237	0.261	organization?
Overhead	52266.8	87981.2	35303.6flowbits	resilience
Ascendency	45262.5	77544.1	33122.7flowbits	vigor & organization
Capacity	97529.4	165525.3	68426.4flowbits	vigor
AMI	0.464	0.468	0.484	organization

Table 15. Main synthetic indices of the Mediterranean E2E standardized models (34 functional groups): ADR (Adriatic), GOL (Gulf of Lyon), NAE (Northern Aegean Sea).

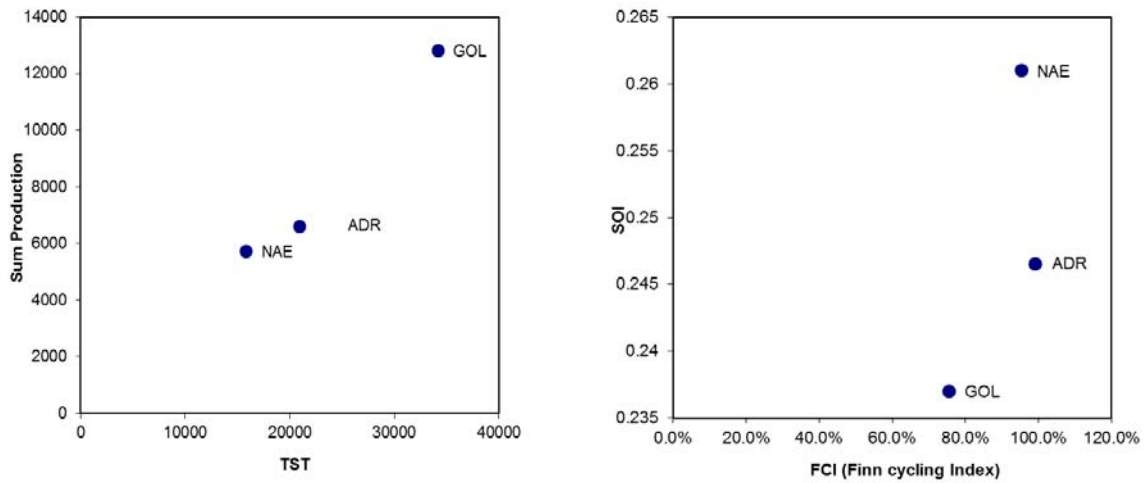


Figure 54: Indices for the three areas of the Mediterranean Sea. (Left panel) indices related to VIGOR; (right panel) indices related (positively or negatively) with ORGANIZATION

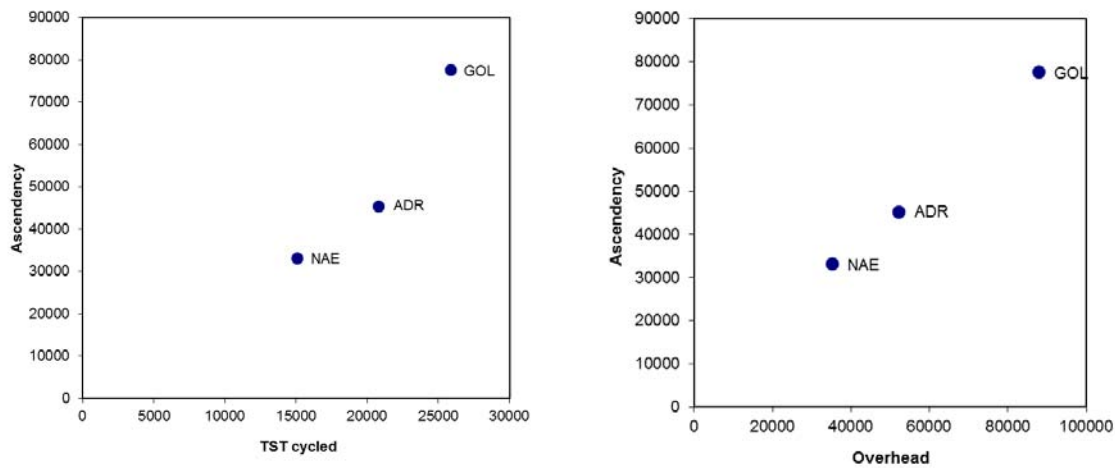


Figure 55: Indices for the three areas of the Mediterranean Sea. (left panel) indices related with VIGOR & ORGANIZATION ; (right panel) indices of VIGOR & ORGANIZATION (y axis) vs indices of RESILIENCE (x-axis)

References

- Agostini, V.N., Bakun, A., 2002. "Ocean triads" in the Mediterranean Sea: Physical mechanisms potentially structuring reproductive habitat suitability (with example application to European anchovy). *Fisheries Oceanography*, 11(3):129-142.
- Akaike, H., 1974. A new look at the statistical model identification. *IEEE Transactions on Automatic Control* 19 (6): 716-723.
- Akoglu, E. (2013). Nonlinear Dynamics of the Black Sea Ecosystem and Its Response to Anthropogenic and Climate Variations. PhD Thesis, Middle East Technical University, Institute of Marine Sciences, Erdemli, Turkey.
- Aldebert, Y., Recasens, L., 1996. Comparison of methods for stock assessment of European hake *Merluccius merluccius* in the gulf of Lion (Northwestern Mediterranean). *Aquatic Living Resources*, 9: 13-22.



- Allen, R. R. 1971. Relation between production and biomass. *J. Fish. Res. Board Can.*, 28:1573-1581.
- Angelini, R., Agostinho, A.A., 2005. Food web model of the upper Paraná River foodplain: description and aggregation effects. *Ecological Modelling* 181, 109– 121.
- Anon (2008) National Program for the Collection of Fisheries Data (2007-2008). Technical Report (EC 1543/2000). Athens, Greece, Fisheries Research Institute and Hellenic Center for Marine Research. 331pp.
- Arneri, E., 1996: Fisheries resources assessment and management in the Adriatic and Ionian Seas. FAO Fisheries Report, 533 (Suppl.),7–20.
- Aubry, F.B., Cossarini G., Acri F., Bastianini M., Bianchi F., Camatti E., De Lazzari A., Pugnetti A., Solidoro C., Socal G., 2012. Plankton communities in the northern Adriatic Sea: Patterns and changes over the last 30 years. *Estuarine, Coastal and Shelf Science* doi:10.1016/j.ecss.2012.03.011
- Azzali, M. 2002. Valutazione acustica della biomassa, distribuzione e struttura delle popolazioni pelagiche in Adriatico, in relazione con i dati ambientali ricavati da satellite. Echo-survey IRPEM-CNR. 4-A-42. Informe final.
- Baklouti, M., Faure, V., Pawlowski, L., Sciandra A., 2006. Investigation and sensitivity analysis of a mechanistic phytoplankton model implemented in a new modular numerical tool (Eco3M) dedicated to biogeochemical modelling. *Progress in Oceanography*, 71: 34-58.
- Bănaru, D., Mellon-Duval, C., Roos, D., Bigot, J. L., Souplet, A., Jadaud, A., Fromentin, J. M., 2012. Trophic structure in the Gulf of Lions marine ecosystem (north-western Mediterranean Sea) and fishing impacts. *Journal of Marine Systems*.
- Bas, C., Maynou, F., Sardà, F., Lleonart, J., 2003. Variacions demogràfiques a les poblacions d'espècies demersals explotades: els darrers quaranta anys a Blanes i Barcelona. *Institut d'Estudis Catalans. Secció de Ciències Biologia*, 135: 1-202.
- Bearzi, G., D. Holcer and G. Notarbartolo Di Sciara. 2004. The role of historical dolphin takes and habitat degradation in shaping the present status of northern Adriatic cetaceans. *Aquatic Conservation of Marine and Freshwater Ecosystems*, 14: 363–379.
- Beaubrun, P.C., 1995. Atlas préliminaire de distribution de cétacés en Méditerranée. CIESM, Musée Océanographique de Monaco. 87 pp.
- Beckers, Jean-Marie: Application of the GHER 3D general circulation model to the Western Mediterranean, *JMS* 1(4), 315–332, 1991
- Béranger, K., Drillet, Y., Houssais, M.-N., Testor, P., Bourdalle-Badie, R., Alhammoud, B., Bozec, A., Mortier, L., Bouruet-Aubertot, P., and Crepon, M.: Impact of the spatial distribution of the atmospheric forcing on water mass formation in the Mediterranean Sea, *J. Geophys. Res.*, 115,C12041, doi:10.1029/2009JC005648, 2010.
- Bernardi Aubry F., Acri F., Bastianini M., Bianchi F., Cassin D., Pugnetti A., Socal G. (2006a) Seasonal and interannual variations of phytoplankton in the Gulf of Venice (Northern Adriatic Sea). *Chemistry and Ecology*, 22 (Suppl.1), S71–S91.
- Bertrand, J.A., De Sola, L.G., Papaconstantinou, C., Relini, G. and Souplet, A. (2002) The general specifications of the MEDITS surveys. *Scientia Marina*, 66, 9-17.
- Bosc, E., Bricaud, A. and Antoine, D. (2004) Seasonal and interannual variability in algal biomass and primary production in the Mediterranean Sea, as derived from 4 years of SeaWiFS observations. *Global Biogeochem. Cycles*, 18, GB1005.1001-GB1005.1017
- Brambati, A., M. Ciabatti, G. P. Fanzutti, F. Marabini and R. Marocco. 1983. A new sedimentological textural map of the northern and central Adriatic Sea. *Bolletino di Oceanologia Teorica ed Applicata*, Vol. I: 4.
- BSC (2008). State of the Environment of the Black Sea (2001-2006/7). The Commission on the Protection of the Black Sea against Pollution publication, 448 pp.
- Cabrini M , Fornasaro D., Cossarini G., Lipizer M., Virgilio D. Phytoplankton temporal changes in a coastal northern Adriatic site during the last 25 years *Estuarine, Coastal and Shelf Science* doi:10.1016/j.ecss.2012.03.011 <http://dx.doi.org/10.1016/j.ecss.2012.07.007>
- Camatti E., Com'aschi A., Acri F. (2002). Variazioni di popolazioni mesozooplanctoniche in Adriatico settentrionale (luglio 1999–ottobre 2000). *Biologia Marina Mediterranea*, 9 (1), 441–444.
- Capet, A., Beckers, J.-M., and Grégoire, M.: Drivers, mechanisms and long-term variability of seasonal



- hypoxia on the Black Sea northwestern shelf – is there any recovery after eutrophication?, *Biogeosciences*, 10, 3943-3962, 2013.
- Capet, Arthur, Barth, Alexander, Beckers, Jean-Marie, and Grégoire, Marilaure: Interannual variability of Black Sea's hydrodynamics and connection to atmospheric patterns, *DSRII 77-80(0)*, 128-142, 2012.
- Cataletto, B., Feoli, E., Fonda Umani, S. and Cheng-Yong, S., 1995. Eleven years of time-series analysis on the net-zooplankton community in the Gulf of Trieste. *Journal of Marine Science*, 52:669-678.
- Cataudella S., Spagnolo M., 2012. Lo stato della pesca e dell'acquacultura nei mari italiani. Ministero delle Politiche Agricole, Alimentari e Forestali. 876 ppg.
- Cauwet, G., Déliat, G., Krastev, A., Shtereva, G., Becquevort, S., Lancelot, C., Momzikoff, A., Saliot, A., Cociasu, A., and Popa, L.: Seasonal DOC accumulation in the Black Sea: a regional explanation for a general mechanism, *MC 79(3)*, Elsevier, 193-205, 2002
- Chikina, M. V. and Kucheruk, N. V. (2005) Long-term changes in the structure of coastal benthic communities in the Northeastern part of the Black Sea: influence of alien species. *Oceanology* 45(Suppl. 1), S176-S182.
- Christensen V, Pauly D (1992) *ECOPATH II - a software for balancing steady-state ecosystem models and calculating network characteristics*. *Ecological Modelling* 61: 169-185.
- Christensen, V., C. Walters and D. Pauly. 2005. *Ecopath with Ecosim: a User's guide*. Fisheries Centre of University of British Columbia, Vancouver, Canada. 154 pp.
- Christensen, V., Guenette, S., Heymans, J.J., Walters, C., Zeller, D., Pauly, D., 2003. Hundred-year decline of North-Atlantic predatory fishes. *Fish and Fisheries*, 4: 1-24.
- Christensen, V., Walters, C., 2004. *Ecopath with Ecosim: methods, capabilities and limitations*. *Ecological Modelling*, 172(2-4): 109-139.
- Cingolani, N., G. G Giannetti and E. Arneri. 1996. Anchovy fisheries in the Adriatic Sea. *Scientia Marina*, 60(Suppl. 2): 269-277.
- Cochrane, K., de Young, C., 2008. Ecosystem approach to fisheries management in the Mediterranean. *Options Méditerranéennes, Series B*, 62: 71-85
- Cociasu, A., L. Dorogan, C. Humborg and L. Popa, 1996. Long-term ecological changes in the Romanian coastal waters of the Black Sea. *Marine Pollution Bulletin*, 32, 32-38.
- Coll, M. and Libralato, S. (2012) Contributions of food web modelling to the ecosystem approach to marine resource management in the Mediterranean Sea. *Fish and Fisheries*, 13, 60-88.
- Coll, M., A. Santojanni, E. Arneri, I. Palomera and S. Tudela. 2007. An ecosystem model of the Northern and Central Adriatic Sea: analysis of ecosystem structure and fishing impacts. *Journal of Marine Systems*, 67: 119-154
- Coll, M., A. Santojanni, I. Palomera, E. Arneri. 2009. Food-web dynamics in the North-Central Adriatic marine ecosystem (Mediterranean Sea) over the last three decades. *Marine Ecology Progress Series*, 381: 17-37.
- Cossarini G. and Solidoro C., 2008 Global sensitivity analysis of a trophodynamic model of the gulf of Trieste. *Ecological modelling*, 212: 16-27. doi:10.1016/j.ecolmodel.2007.10.009.
- Cossarini G., Solidoro C., Fonda Umani S., 2012. Dynamics of biogeochemical properties in temperate coastal areas of freshwater influence: Lessons from the Northern Adriatic Sea (Gulf of Trieste). *Estuarine, Coastal and Shelf Science* doi:10.1016/j.ecss.2012.02.006
- Costanza, R., Mageau, M., 1999. What is a healthy ecosystem? *Aquatic Ecology*, 33: 105-115.
- Cury, P. M., Shannon, L. J., Roux, J-P, Daskalov, G. M., Jarre, A., Moloney, C. L., and Pauly, D. 2005. Trophodynamic indicators for an ecosystem approach to fisheries. *ICES Journal of Marine Science*, 62: 430-442
- Daskalov GM, Friedrich J, Todorova V, 2012. D8.2 Report on environmental status of the Black Sea (regional scale), including issues such as water quality, quality of marine habitats, ecosystem structure and functioning. EC FWP 7, KnowSeas: Knowledge-based Sustainable Management for Europe's Seas
- Daskalov, G. M. 2002. Overfishing drives a trophic cascade in the Black Sea. *Marine Ecology Progress Series* 225: 53-63
- Daskalov, G. M., Grishin, A., Rodionov, S. and Mihneva, V. 2007 Trophic cascades triggered by



overfishing reveal possible mechanisms of ecosystem regime shifts. *Proceedings of the National Academy of Sciences* 104, 10518-10523, doi 10.1073/pnas.0701100104.

Daskalov, G., Cardinale, M., Gümüş A, Zengin, M., Panayotova, M., Duzgunes, E., Shlyakhov, V., Genç, Y., Radu, G., Yankova, M., Maximov, V., Mikhaylyuk, A., Raykov, V. and Rätz, H.-J. 2011. Assessment of Black Sea Stocks (STECF-OWP-11-04) Scientific, Technical and Economic Committee for Fisheries, Joint Research Centre – Institute for the Protection and Security of the Citizen, EUR 25020 EN, 213 pp Luxembourg: Publications Office of the European Union, 2011 – 212 pp. EUR – Scientific and Technical Research series – SSN 1831-9424 (online), ISSN 1018-5593 (print) ISBN 978-92-79-21872-9 doi:10.2788/94711 <http://stecf.jrc.ec.europa.eu>

Delhez, Eric: Reconnaissance of the general circulation of the North-Western European Continental Shelf by means of a three-dimensional turbulent closure model, *ESR* 41(1-2), 3–29, 1996

Eisenhauer, L., Carlotti, F., Baklouti, M., Diaz, F., 2009. Zooplankton population model coupled to a biogeochemical model of the North Western Mediterranean Sea ecosystem. *Ecological Modelling*, 220: 2865-2876.

El.Stat. (2011) Quantity of fish landed by fishing area and fishing tools. Hellenic Statistical Authority, <http://www.statistics.gr>.

European Marine Strategy Framework Directive (MSFD) (EU, June 2008)

FAO, 2009. Rapport de la trente-troisième session de la Commission générale des pêches pour la Méditerranée (CGPM). Tunis, 23-27 mars 2009. 132 pp.

Farrugio, H., Alvarez Prado, F., Lleonart, J., De Ranieri, S., 1991. Etude pour l'aménagement et la gestion des pêches en Méditerranée occidentale. Rapport final Commission des Communautés Européennes, Contrat no. MA-1-232, 454 pp.

Fonda Umani, S. 1996. Pelagic production and biomass in the Adriatic Sea. *Sci. Mar.*, 60(Supl. 2): 65-77.

Fonda Umani, S. and Beran, A., 2003. Seasonal variations in the dynamics of microbial plankton communities: first estimates from experiments in the Gulf of Trieste, Northern Adriatic Sea. *Marine Ecology Progress Series*, 247: 1-16

Fonda Umani, S., Franco, P., Ghirardelli, E. and Malej, A., 1992. Outline of oceanography and the plankton of the Adriatic Sea. In: G. Colombo, I. Ferrari, V.U. Seccherelli, and R. Rossi (Editors), *Marine Eutrophication and population dynamics*, Proc 25th Eur Mar Biol Symp. Olsen & Olsen, Fredensborg, pp. 347-365.

Fortibuoni T., S. Libralato, S. Raicevich, O. Giovanardi and C. Solidoro, 2010. Coding early naturalists' accounts into long-term fish community changes in the Adriatic Sea (1800-2000). *PlosOne*, 5(11): e15502. doi:10.1371/journal.pone.0015502

Froese, R.J. and Pauly, D. (2012) Fishbase. World wide web electronic publication. Available from <http://www.fishbase.org>.

Gaudy, R., Youssara, F., Diaz, F., Raimbault, P., 2003. Biomass, metabolism and nutrition of zooplankton in the Gulf of Lions (NW Mediterranean). *Oceanologica Acta*, 26(4): 357-372.

Gawarkiewicz, G., G. Korotaev, S. Stanichny, L. Repetin, and D. Soloviev, 1999. Synoptic upwelling and cross-shelf transport processes along the Crimean coast of the Black Sea. *Cont. Shelf Res.*, 19, 977–1005.

Giani M. Djakovac T., Degobbis D., Cozzi S., Solidoro C., Fonda Umani S. Recent changes in the marine ecosystems of the northern Adriatic Sea *Estuarine, Coastal and Shelf Science* <http://dx.doi.org/10.1016/j.ecss.2012.08.023>

Giannoulaki, M., Iglesias, M., Tugores, P., Bonanno, A., Patti, B., De Felice, A., Leonori, I., Bigot, J.L., Ticina, V., Pyrounaki, M., Tsagarakis, K., Machias, A., Somarakis, S., Schismenou, E., Quinci, E., Basilone, G., Cuttitta, A., Campanella, F., Miquel, J., Onate, D., Roos, D. and Valavanis, V. (2013) Characterising the potential habitat of European anchovy *Engraulis encrasicolus* in the Mediterranean Sea, at different life stages. *Fisheries Oceanography*, 22, 69-89.

Giannoulaki, M., Pyrounaki, M.M., Liorzou, B., Leonori, I., Valavanis, D.V., Tsagarakis, K., Machias, A., Bigot, J.L., Roos, D., De Felice, A. and Arneri, E. (2011) Habitat suitability modelling for sardine (*Sardina pilchardus*) juveniles in the Mediterranean Sea. *Fisheries Oceanography*, 20, 367-382.

Ginsburg, A.I., A.G., Kostianoy, N.P., Nezlin, D.M., Soloviev, S.V., Stanichny, 2002a. Anticyclonic eddies in the northwestern Black Sea. *J. Mar. Syst.*, 32, 91–106.



- Grégoire, M. and K. Soetaert, 2010. Carbon, nitrogen, oxygen and sulfide budgets in the Black Sea: A biogeochemical model of the whole water column coupling the oxic and anoxic parts. *Ecological Modelling*, 221, 2287–2301.
- Grégoire, M., Friedrich, J., 2004. Nitrogen budget of the north-western black sea shelf as inferred from modeling studies and in-situ benthic measurements. *Marine Ecology Progress Series* 270, 15–39.
- Grégoire, Marilaure, Beckers, Jean-Marie, Nihoul, Jacques C., and Stanev, Emil: Reconnaissance of the main Black Sea's ecohydrodynamics by means of a 3D interdisciplinary model, *JMS* 16(1–2), 85–105, 1998
- Grégoire, Marilaure, Raick, C., and Soetaert, Karline: Numerical modeling of the central Black Sea ecosystem functioning during the eutrophication phase, *PO* 76(3), Pergamon-Elsevier Science, 286–333, 2008
- Grégoire, Marilaure, Soetaert, Karline, Nezhin, N., and Kostianoy, Andrey G.: Modeling the nitrogen cycling and plankton productivity in the Black Sea using a three-dimensional interdisciplinary model, *Journal of Geophysical Research (Oceans)* 109(C18), C05007, 2004
- Greze VN 1979. Production of benthos. p 239-341. In: Greze VN (ed) *Productivity of the Black Sea*. Naukova Dumka, Kiev. pp 392. In Russian
- Groombridge, B. 1990. Marine turtles in the Mediterranean: distribution, population status, conservation. European Council, Nature and environment series, n° 48. Strasbourg, France.
- Hall, S.J., 1999. *The Effects of Fishing on Marine Ecosystems and Communities*. Fish Biology and Aquatic Resources. Series Blackwell Science. 274 pp.
- Harmelin-Vivien, M., Loizeau V., Mellon, C., Beker, B., Arlhac, D., Bodiguel, X., Ferraton, F., Hermand, R., Philippon, X., Salen-Picard, C., 2008. Comparison of C and N stable isotope ratios between surface particulate organic matter and microphytoplankton in the Gulf of Lions (NW Mediterranean). *Continental Shelf Research*, 28(15): 1911-1919.
- He, Y., E. V. Stanev, E. Yakushev, J. Staneva (2012) Black Sea biogeochemistry: Response to decadal atmospheric variability during 1960-2000 inferred from numerical modeling. *Marine Environmental Research*, 77, 90-102.
- Hermand, R., Salen-Picard, C., Alliot, E., Degiovanni, C., 2008. Macrofaunal density, biomass and composition of estuarine sediments and their relationship to the river plume of the Rhone River (NW Mediterranean). *Estuarine Coastal and Shelf Science*, 79(3): 367-376.
- Heymans J.J. & Baird D., 2000. Network analysis of the northern Benguela ecosystem by means of NETWRK and ECOPATH. *Ecological Modelling*, 131: 97-119.
- Hjerne, O., Hansson, S., 2002. The role of fish and fisheries in Baltic Sea nutrient dynamics. *Limnology and Oceanography*, 47: 1023–1032.
- Holt, Jason T., Allen, J. Icarus, Proctor, Roger, and Gilbert, Francis: Error quantification of a high-resolution coupled hydrodynamic-ecosystem coastal-ocean model: Part 1 model overview and assessment of the hydrodynamics, *JMS* 57(1-2), 167–188, 2005,
- Hu, Z.Y., Doglioli, A.M., Petrenko, A.A., Marsaleix, P., Dekeyser, I., 2009. Numerical simulations of eddies in the Gulf of Lion. *Ocean Modelling*, 28(4): 203-208.
- Ivanov, L. and Beverton, R.J.H., 1985. The fisheries resources of the Mediterranean, part two: Black Sea. *FAO Studies and reviews*, 60. 135pp.
- Jackson, J.B.C., Kirby, M.X., Berger, W.H., Bjorndal, K.A., Botsford, L.W., Bourque, B.J., Bradbury, R.H., Cooke, R., Erlandson, J., Estes, J.A., Hughes, T.P., Kidwell, S., Lange, C.B., Lenihan, H.S., Pandolfi, J.M., Peterson, C.H., Steneck, R.S., Tegner, M.J., Warner, R.R., 2001. Historical overfishing and the recent collapse of coastal ecosystems. *Science*, 293: 629-638.
- Jennings, S., Kaiser, M.J., 1998. The effects of fishing on marine ecosystems. *Advances in Marine Biology*, 34: 201-351.
- Jukic-Peladic, S., N. Vrgoc, S. Krstulovic-Sifner, C. Piccinetti, G. Piccinetti-Manfrin, Marano, G. and N. Ungaro. 2001. Long-term changes in demersal resources of the Adriatic Sea: comparison between trawl surveys carried out in 1948 and 1998. *Fisheries Research*, 53(1): 95-104.
- Karageorgis, A.P., Kaberi, H.G., Tengberg, A., Zervakis, V., Hall, P.O.J. and Anagnostou, C.L. (2003) Comparison of particulate matter distribution, in relation to hydrography, in the mesotrophic Skagerrak and the oligotrophic northeastern Aegean Sea. *Continental Shelf Research*, 23, 1787-1809.



- Karageorgis, A.P., Perissoratis, C. and Anagnostou, C.L. (2005) Characteristics of surface sediments. In: State of the Hellenic marine environment. E. Papathanassiou and A. Zenetos (eds) Athens: HCMR Publ. pp. 34-42.
- Karl, D.M., and G.A. Knauer, 1991. Microbial production and particle flux in the upper 350 m of the Black Sea. *Deep Sea Res.*, 38, Supp. 2A, S655-S661.
- Katsanevakis, S., Maravelias, C.D., Damalas, D., Karageorgis, A.P., Tsitsika, E.V., Anagnostou, C. and Papaconstantinou, C. (2009) Spatiotemporal distribution and habitat use of commercial demersal species in the eastern Mediterranean Sea. *Fisheries Oceanography*, 18, 439-457.
- Kavanagh, P., Newlands, N., Christensen, V., Pauly, D., 2004. Automated parameter optimization for Ecopath ecosystem models. *Ecological Modelling*, 172: 141-150.
- Korotaev, G.K., T. Oguz, A. Nikiforov, C. J. Koblinsky, 2003. Seasonal, interannual and mesoscale variability of the Black Sea upper layer circulation derived from altimeter data. *J. Geophys. Res.*, 108(C4), 3122, doi:10.1029/2002JC001508.
- Kourafalou, V., K. Tsiaras and J. Staneva (2004), Numerical studies on the dynamics of the Northwestern Black Sea shelf, *Med. Mar. Sci.*, Vol.5/1, 133-142.
- Krivosheya, V.G., V. B. Titov, I.M. Ovchinnikov, R.D. Kosyan, A.Yu. Skirta, 2000. The influence of circulation and eddies on the depth of the upper boundary of the hydrogen sulfide zone and ventilation of aerobic waters in the Black Sea. *Oceanology (Eng. Transl.)*, 40, 767-776.
- Labropoulou, M. and Papaconstantinou, C. (2004) Community structure and diversity of demersal fish assemblages: the role of fishery. *Scientia Marina*, 68, 215-226.
- Labrune, C., Gremare, A., Guizien, K., Amouroux, J.M., 2007. Long-term comparison of soft bottom macrobenthos in the Bay of Banyuls-sur-Mer (north-western Mediterranean Sea): A reappraisal. *Journal of Sea Research*, 58(2): 125-143.
- Lancelot C, Staneva J, Van Eeckhout D, Beckers JM, Stanev E (2002) Modeling the impact of the human forcing on the ecological functioning of the northwestern Black Sea. *Estuarine, Coastal and Shelf Science* 54: 473-500.
- Lancelot, C. L., J. V. Staneva, D. Van Eeckhout, J.-M. Beckers, and E. V. Stanev (2002), Modelling the Danube-influenced North-western continental shelf of the Black Sea. Ecosystem response to changes in nutrient delivery by the Danube River after its damming in 1972. *Estua. Coast and Shelf Sci.*, 54, 473-499.
- Lazzari, P., Solidoro, C., Ibello, V., Salon, S., Teruzzi, A., Béranger, K., Crise, A., 2012. Seasonal and inter-annual variability of plankton chlorophyll and primary production in the Mediterranean Sea: a modelling approach. *Biogeosciences*, 9(1), 217-233.
- Lazzari, P., Teruzzi, A., Salon, S., Campagna, S., Calonaci, C., Colella, S., Tonani, M. and Crise, A. (2010) Pre-operational short-term forecasts for Mediterranean Sea biogeochemistry. *Ocean Science*, 6, 25-39.
- Lebedeva, L.P. and S. V. Vostokov, 1984. Studies of detritus formation processes in the Black Sea. *Oceanology (Engl. Transl.)*, 24(2), 258-263.
- Lefevre, D., Minas, H.J., Minas, M., Robinson, C., Williams, P.J.LeB., Woodward, E.M.S., 1997. Review of gross community production, primary production, net community production and dark community respiration in the Gulf of Lions. *Deep Sea Research Part II: Topical Studies in Oceanography*, 44(3-4): 801-819.
- Libralato S, Coll M, Santojanni A, Solidoro C, Arneri E, Palomera I., 2005. Comparison between trophic models of protected and fishing areas for an ecosystem approach to fisheries in Adriatic Sea. *ICES CM* 2005/BB:11.
- Libralato S., Coll. M., Tempesta M., Santojanni A., Spoto M., Palomera I., Arneri E., Solidoro C., 2010. Food-web traits of protected and exploited areas of the Adriatic Sea. *Biological Conservation* 143: 2182-2194.
- Libralato, S. and Solidoro, C. 2009. Bridging biogeochemical and food web models for an End-to-End representation of marine ecosystem dynamics: The Venice lagoon case study. *Ecological Modelling*, 220: 2960-2971.
- Ludwig, W., Bouwmann, A.F., Dumont, E., Lespinas F., 2010. Water and nutrients fluxes from major Mediterranean and Black Sea rivers: Past and future trends and their implications for basin scale budgets. *Global Biogeochem. Cy.* 24, GB0A13, doi 10.129/2009GB003594.



- Ludwig, W., Dumont, E., Meybeck, M., Heussner S. 2009. River discharges of water and nutrients to the Mediterranean and Black Sea: Major drivers for ecosystem changes during past and future decades? *Prog. Oceanogr.* 80(40271), 199-217.
- Lykousis, V., Chronis, G., Tselepidis, A., Price, N.B., Theocharis, A., Siokou-Frangou, I., Van Wambeke, F., Danovaro, R., Stavrakakis, S., Duineveld, G., Gergopoulos, D., Ignatiades, L., Souvermezoglou, A. and Voutsinou-Taliadouri, F. (2002) Major outputs of the recent multidisciplinary biogeochemical researches undertaken in the Aegean Sea. *Journal of Marine Systems*, 33– 34, 313- 334.
- Malej, A., Mozetic, P., Malacic, V. and Turk, V., 1997. Response of Summer Phytoplankton to Episodic Meteorological Events (Gulf of Trieste, Adriatic Sea). *Marine Ecology*, 18(3):273-288.
- Mannini, P. and F. Massa. 2000. Brief Overview of Adriatic fisheries landings trends (1972-97). In: Massa F. and P. Mannini (eds). Report of the First Meeting of Adriamed Coordination Comité. FAO-MiPAF Scientific Cooperation to Support Responsible Fisheries in the Adriatic Sea. GCP/RER/010/ITA/TD-01: 31-49.
- Marti, O., P.Braconnot, J.R.B. Bellier, S. Bony, P. Brockmann, P. Cadule, A. Caubel, S. Denvil, J.L. Dufresne, L. Fairhead, M.A. Filiberti, M.A. Foujols, T. Fichefet, P. Friedlingstein, H. Gosse, J.Y. Grandpeix, F. Hourdin, G. Krinner, C. Levy, G. Madec, I. Musat, N.D. Noblet, J. Polcher, and C. Talandier (2006) The new IPSL climate system model: IPSL-CM4, Note du Pole de Modelisation, 26.
- Mellon-Duval, C., de Pontual, H., Metral, L., Quemener, L., 2009. Growth of European hake (*Merluccius merluccius*) in the Gulf of Lions based on conventional tagging. *ICES Journal of Marine Science*, 67(1): 62-70.
- Millot, C., 1999. Circulation in the Western Mediterranean Sea. *Journal of Marine Systems* 20(1-4), 423-442.
- Mood, A. M., Graybill, F. A., Boes, D. C., 1974. *Introduction to the Theory of Statistics* (3rd Edition). McGraw-Hill, 480 pp.
- Morello E.B., Arneri E. 2009., Anchovy and Sardine in the Adriatic Sea - An Ecological Review. *Oceanography and Marine Biology: An Annual Review*, 47: 209-256.
- Mozetič P., C. Solidoro, G. Cossarini, G. Socal, R. Precali, J. Francé, F. Bianchi, C. De Vittor, N. Smodlaka, S. Fonda Umani, 2009. Recent Trends Towards Oligotrophication of the Northern Adriatic: Evidence from Chlorophyll a Time Series Estuaries and Coasts DOI 10.1007/s12237-009-9191-7
- Murray JW, Codispoti LA, Friederich GE (1995) Oxidation-reduction environments: the suboxic zone in the Black Sea. *Aquatic chemistry: interfacial and interspecies processes. Am Chem Soc Adv Chem Ser* 244:157-176
- Nikolioudakis, N., Isari, S., Pitta, P. and Somarakis, S. (2012) Diet of sardine *Sardina pilchardus*: an 'end-to-end' field study. *Marine Ecology Progress Series*, 453, 173-188.
- Oguz T and Velikova V. 2010, Abrupt transition of the northwestern Black Sea shelf ecosystem from a eutrophic to an alternative pristine state. *Mar. Ecol. Prog. Ser.*, 405: 231– 242.
- Oguz T, Gilbert D (2007) Abrupt transitions of the top-down controlled Black Sea pelagic ecosystem during 1960-2000: evidence for regime-shifts under strong fishery and nutrient enrichment modulated by climate-induced variations. *Deep Sea Res I*. doi:10.1016/j.dsr. 2006.09.010
- Oguz, T., and A. Merico (2006) Factors controlling the summer *Emiliania huxleyi* bloom in the Black Sea: a modeling study. *J. Marine Systems*, 59, 173-188.
- Oguz, T., A. G. Deshpande, and P. Malanotte-Rizzoli, 2002. On the Role of Mesoscale Processes Controlling Biological Variability in the Black Sea: Inferences From SeaWIFS- derived Surface Chlorophyll Field. *Continental Shelf Research*, 22, 1477–1492.
- Oguz, T., D.G., Aubrey, V.S., Latun, E., Demirov, L., Koveshnikov, H.I., Sur, V., Diacanu, S., Besik- tepe, M., Duman, R., Limeburner, V.V., Eremeev, 1994. Mesoscale circulation and thermohaline structure of the Black sea observed during HydroBlack'91. *Deep Sea Research I*, 41, 603–628.
- Oguz, T., H. W. Ducklow, and P. Malanotte-Rizzoli, 2000. Modeling distinct vertical biogeochemical structure of the Black Sea: Dynamical coupling of the Oxic, Suboxic and Anoxic layers. *Global Biogeochem. Cycles.*, 14, 1331–1352.
- Oguz, T., J. W. Murray, and A. E. Callahan, 2001a. Modeling redox cycling across the suboxic- anoxic interface zone in the Black Sea. *Deep-Sea Res. I.*, 48, 761–787.
- Oguz, T., P., La Violette, U., Unluata, 1992. Upper layer circulation of the southern Black Sea: Its



- variability as inferred from hydrographic and satellite observations. *J. Geophys. Res.*, 97, 12569–12584.
- Oguz, T., S., Besiktepe, 1999. Observations on the Rim Current structure, CIW formation and transport in the western Black Sea. *Deep Sea Res.*I, 46, 1733-1753.
- Oguz, T., V.S., Latun, M.A., Latif, V.V., Vladimirov, H.I., Sur, A.A., Makarov, E., Ozsoy, B.B., Kotovshchikov, V.V., Eremeev, U., Unluata, 1993. Circulation in the surface and intermediate layers of the Black Sea. *Deep Sea Res.* I, 40, 1597–1612.
- Oguz, T, L.I. Ivanov, S. Besiktepe, 1998. Circulation and hydrographic characteristics of the Black Sea during July 1992. In: *Ecosystem Modeling as a Management Tool for the Black Sea*, L. Ivanov and T. Oguz (eds). NATO ASI Series, Environmental Security-Vol.47, Kluwer Academic Publishers, Vol. 2, pp. 69–92.
- Orfanidis, S., Panayotidid, P. and Siakavara, A. (2005) Benthic macrophytes: main trends in diversity and distribution. In: *State of the Hellenic Marine environment*. E. Papathanassiou and A. Zenetos (eds) Athens: HCMR Publ. . pp. 226-235.
- Papaconstantinou, C., Farrugio, H., 2000. Fisheries in the Mediterranean. *Mediterranean Marine Science*, 1(1): 5-18.
- Pauly, D. 1980. On the interrelationships between natural mortality, growth parameters, and mean environmental temperature in 175 fish stocks. *Journal du Conseil, Conseil International pour l'Exploration de la Mer*, 39: 175-192.
- Pauly, D., Christensen, V. and Sambilay, V. (1990) Some features of fish food consumption estimates used by ecosystem modellers. *ICES CM/G:17*. 8pp.
- Pauly, D., Christensen, V., Walters, C., 2000. Ecopath, ecosim and ecospace as tools for evaluating ecosystem impact of fisheries. *ICES Journal of Marine Science*, 57: 697-706.
- Petrenko, A.A., Leredde, Y., Marsaleix, P., 2005. Circulation in a stratified and windforced Gulf of Lions, NW Mediterranean Sea: in situ and modelling data. *Continental Shelf Research*, 25: 7–27.
- Pinardi, N., E. Arneri, A. Crise, M. Ravaioli and M. Zavatarelli, in press. The physical, sedimentary and ecological structure and variability of shelf areas in the Mediterranean sea (27,s). *The Sea* ,Volume 14, edited by Allan R Robinson and Kenneth H.Brink. Harvard University Press
- Plagányi, É., 2007. Models for an Ecosystem Approach to Fisheries, FAO Food and Agriculture Organization, Fisheries Technical Paper, Rome, Italy, no. 477, 108 pp.
- Polat, S.Ç. and S., Tugrul, 1995. Nutrient and organic carbon exchanges between the Black and Marmara Seas through the Bosphorus Strait. *Continental Shelf Research*, 15, 1115– 1132.
- Politou, C.-Y. (2007) Current state of demersal fisheries resources. In: *State of Hellenic fisheries*. C. Papaconstantinou, A. Zenetos, V. Vassilopoulou and G. Tserpes (eds) Athens: HCMR Publ. pp. 183-191.
- Pranovi, F., S. Raicevich, G. Franceschini, M. G. Farrace and O. Giovanardi. 2000. Rapido trawling in the northern Adriatic Sea: effects on benthic communities in an experimental area. *ICES Journal of Marine Science*, 57: 517-524.
- Pranovi, F., S. Raicevich, G. Franceschini, P. Torricelli and O. Giovanardi. 2001. Discard analysis and damage to non-target species in the rapido trawl fishery. *Marine Biology*, 139: 863-875.
- Prodanov, K., K., Mikhaylov, G., Daskalov, K., Maxim, E., Ozdamar, V., Shlyakhov, A., Chashchin, and A. Arkhipov. 1997. Environmental management of fish resources in the Black Sea and their rational exploitation. *Studies and Reviews. GFCM*. 68, FAO, Rome. <http://www.fao.org/DOCREP/006/W5020E/W5020E00.HTM>
- Pugnetti A., Buzzoni A.M., Beran A., Bernardi Aubry F., Camatti E., Celassi M., Coppola J., Crevatin E., Del Negro P., Paoli A., 2008. Changes in biomass structure and trophic status of the plankton communities in a highly dynamic ecosystem (Gulf of Venice, Northern Adriatic Sea) *Marine Ecology* 29, pp.367–374
- Purcell, J.E., Shiganova, T.A., Decker, M.B. and Houde, E.D. (2001) The ctenophore *Mnemiopsis* in native and exotic habitats: U.S. estuaries versus the Black Sea basin. *Hydrobiologia*, 451, 145-176.
- Reschke, S., Ittekkot, V., and Panin, N.: The nature of organic matter in the Danube River particles and north-western Black Sea sediments, *ECSS* 54(3), Elsevier, 563–574, 2002
- Revkov N, Abaza V, Dumitrache C, Todorova V, Konsulova T, Mickashvidze E, Varshanidze M, Sezgin M, Ozturk B, Chikina MV, Kucheruk, NV 2008. Ch. 8 The state of zoobenthos. pp 273-290. In *BSC*, 2008. *State of the Environment of the Black Sea (2001-2006/7)*. Black Sea Commission Publications 2008-3,



Istanbul, Turkey, 419 pp

Rose, K.A., Allen, J.I., Artioli, Y., Barange, M., Blackford, J., Carlotti, F., Cropp, R., Daewel, U., Edwards, K., Flynn, K., Hill, S.L., HilleRisLambers, R., Huse, G., Mackinson, S., Megrey, B., Moll, A., Rivkin, R., Salihoglu, B., Schrum, C., Shannon, L., Shin, Y.-J., Smith, S.L., Smith, C., Solidoro, C., St. John, M. and Zhou, M. (2010) End-To-End Models for the Analysis of Marine Ecosystems: Challenges, Issues, and Next Steps. *Marine and Coastal Fisheries*, 2, 115-130.

Sacchi, J., 2008. Impact des techniques de pêche sur l'environnement en Méditerranée. *Études et revues*, General Fisheries Commission for the Mediterranean, 84: 1-82.

Santojanni, A., Arneri, E., Barry, C., Belardinelli, A., Cingolani, N., Giannetti, G. and Kirkwood, G. 2003. Trends of anchovy (*Engraulis encrasicolus*, L.) biomass in the northern and central Adriatic Sea. *Scientia Marina*, 67(3): 327-340.

Santojanni, A., N. Cingolani, E. Arneri, G. Kirkwood, A. Belardinelli, G. Giannetti, S. Colella, F. Donato and C. Barry. 2005. Stock assessment of sardine (*Sardina pilchardus*, Walb.) in the Adriatic Sea, with an estimate of discards. *Scientia Marina*, 69 (4): 603-617.

Sardà, F., 1998. Symptoms of overexploitation in the stock of the Norway lobster (*Nephrops norvegicus*) on the "Serola Bank" (Western Mediterranean Sea off Barcelona). *Scientia Marina*, 62 (3): 295-299.

Sardà, F., 1998. Symptoms of overexploitation in the stock of the Norway lobster (*Nephrops norvegicus*) on the "Serola Bank" (Western Mediterranean Sea off Barcelona). *Scientia Marina*, 62 (3): 295-299.

Shiganova, T.A., Mirzoyan, Z.A., Studenikina, E.A., Volovik, S.P., Siokou-Frangou, I., Zervoudaki, S., Christou, E.D., Skirta, A.Y. and Dumont, H.J. (2001) Population development of the invader ctenophore *Mnemiopsis leidyi* in the Black Sea and other seas of the Mediterranean basin. *Marine Biology*, 139, 431-445.

Soetaert, Karline, Middelburg, Jack J., Herman, Peter M., and Buis, Kerst: On the coupling of benthic and pelagic biogeochemical models, *ESR* 51(1-4), 173-201, 2000

Sokolova, E., E.V. Stanev, V. Yakubenko, I. Ovchinnikov, R. Kosyan, 2001. Synoptic variability in the Black Sea. Analysis of hydrographic survey and altimeter data. *J. Mar. Syst.*, 31, 45-63.

Solidoro C., Bandelj, V., Barbieri P., Cossarini G., Fonda Umani S., 2007. Understanding dynamics of biogeochemical properties in the northern Adriatic Sea by using Self-Organizing Maps and k-means clustering *Journal Geophysical Research*, 112, C07S90, doi:10.1029/2006JC003553.

Solidoro C., Cossarini G., Libralato S., Salon S., 2010b. Remarks on the redefinition of system boundaries and model parameterization for downscaling experiments. *Progress in Oceanography*, 84: 134-137

Solidoro C., Del Negro P., Libralato S., Melaku Canu D. (Eds), 2010a. *Sostenibilità della miticoltura Triestina*. Istituto Nazionale di Oceanografia e di Geofisica Sperimentale OGS, p. 88.

Stanev E., J. Staneva, J. L. Bullister, J.W. Murray, 2004, Ventilation of the Black Sea Pycnocline Inferred from Observed and Model Simulated Chlorofluorocarbon Data. Submitted, *Deep Sea Research*, *Deep-Sea Res.*, 51(12), 2137-2169

Stanev E., M. Bowman, E. Peneva, and J. Staneva, 2003. Control of Black Sea intermediate water mass formation by dynamics and topography: comparisons of numerical simulations, survey and satellite data. *Journal of Marine Research*, 26, 69-99.

Stanev, Emil, and Kandilarov, Rostislav: *Sediment dynamics in the Black Sea: numerical modelling and remote sensing observations*, OD 62, Springer Berlin / Heidelberg, 533-553, 2012.

Staneva J.V., E.V. Stanev and T. Oguz (1998) The Impact of Atmospheric Forcing and Water Column Stratification on the Yearly Plankton Cycle, NATO- in: T. Oguz and L. Ivanov (eds.) NATO-ASI Kluwer academic publisher, 301-323.

Staneva, J., V. Kourafalou, and K. Tsiaras (2010) Seasonal and Interannual Variability of the North-Western Black Sea Ecosystem. *Terr. Atmos. Ocean. Sci.*, 21, 163-180.

Staneva, J., V.H. Kourafalou and E.V. Stanev, 2003. The response of the Black Sea ecosystem to changes of nutrient discharge from the Danube River. In: "Oceanography of the Eastern Mediterranean and Black Sea," A. Yilmaz (ed.), Tubitak publ., Ankara, Turkey, pp. 307-313.

Staneva, J.V., V.H. Kourafalou and K. Tsiaras, 2007, Modeling the seasonal cycle of the Northwestern black Sea ecosystem. *Mediterranean Marine Systems*.



- STECF (2011) EU Report STECF-OWP-11-06 Assessment of Black Sea Stocks, Ed. by Daskalov G. & Rätz H.-J.
- Stergiou, K.I., Christou, E.D., Georgopoulos, D., Zenetos, A. and Souvermesoglou, C. (1997) Hellenic Seas: physics, chemistry, biology and fisheries. *Oceanography and Marine Biology an Annual Review*, 35, 415-538.
- Stergiou, K.I., Machias, A., Somarakis, S. and Kapantagakis, A. (2003) Can we define target species in Mediterranean trawl fisheries? *Fisheries Research*, 59, 431-435.
- Sterner, R.W., George, N.B., 2000. Carbon, nitrogen, and phosphorus stoichiometry of cyprinid fishes. *Ecology*, 81: 127–140.
- Sur, H.I. and Y.P. Ilyin, 1997. Evolution of satellite derived mesoscale thermal patterns in the Black Sea. *Prog. Oceanogr.*, 39, 109–151.
- Sur, H.I., E., Ozsoy, U., Unluata, 1994. Boundary current instabilities, upwelling, shelf mixing and eutrophication processes in the Black Sea. *Progr. Oceanogr.*, 33, 249–302.
- Sur, H.I., E., Ozsoy, Y.P., Ilyin, U., Unluata, 1996. Coastal/deep ocean interactions in the Black Sea and their ecological/environmental impacts. *J. Marine Systems*, 7, 293–320, 1996.
- Townsend, C.R., Begon, M., Harper, J.L., 2003. *Essentials of Ecology - 2nd edition*, Blackwell Publishing, Oxford, UK.
- Tsagarakis, K., Coll, M., Giannoulaki, M., Somarakis, S., Papaconstantinou, C. and Machias, A. (2010) Food-web traits of the North Aegean Sea ecosystem (Eastern Mediterranean) and comparison with other Mediterranean ecosystems. *Estuarine, Coastal and Shelf Science*, 88, 233-248.
- Tsagarakis, K., Vassilopoulou, V., Kallianiotis, A. and Machias, A. (2012) Discards of the purse seine fishery targeting small pelagic fish in the Eastern Mediterranean Sea. *Scientia Marina*, 76, 561-572.
- Tsiaras K. P., Kourafalou, A. Davidov and J. Staneva, 2007. A three dimensional coupled model of the western Black Sea plankton dynamics: seasonal variability and comparison to SEAWIFS data. *JGR 113 (C7): 2156-2202*.
- Tsimplis MN, Josey SA, Rixen M, Stanev EV (2004) On the forcing of sea level in the Black Sea. *J Geophys Res* 109:C08015. doi:10.1029/2003JC002185
- Tugores, M.P., Giannoulaki, M., Iglesias, M., Bonanno, A., Ticina, V., Leonori, I., Machias, A., Tsagarakis, K., Díaz, N., Giráldez, A., Patti, B., De Felice, A., Basilone, G. and Valavanis, V. (2011) Habitat suitability modelling for sardine *Sardina pilchardus* in a highly diverse ecosystem: the Mediterranean Sea. *Marine Ecology Progress Series*, 443, 181-205.
- Ulanowicz, R. E., and Puccia, C. J. 1990. Mixed trophic impacts in ecosystems. *Coenoses*, 5: 7-16.
- Ulanowicz, R.E., 1999. *NETWRK 4.2a: A Package of Computer Algorithms to Analyze Ecological Flow Networks*. University of Maryland.
- Unluata, U., T. Oguz, M.A. Latif and E. Ozsoy, 1989. On the physical oceanography of Turkish straits. In: *The physical oceanography of sea straits*, L.J. Pratt, eds. NATO ASI Series, Kluwer, The Netherlands.
- Vrgoc N., Arneri E., Jukic-Peladic S., Krstulovic Šifner S., Mannini P., Marceta B., Osmani K., Piccinetti C., Ungaro N., 2004. Review of current knowledge on shared demersal stocks of the Adriatic Sea. GCP/RER/010/ITA/TD-12. *AdriaMed Technical Documents*, 12: 91pp.
- Walling, D.E., and Fang, D.: Recent trends in the suspended sediment loads of the world's rivers, *GPC* 39(1–2), 111–126, 2003
- Walters C, Christensen V, Pauly D (1997) Structuring dynamic models of exploited ecosystems from trophic mass-balance assessments. *Reviews in Fish Biology and Fisheries* 7: 139-172.
- Walters C, Pauly D, Christensen V, Kitchell JF (2000) Representing Density Dependent Consequences of Life History Strategies in Aquatic Ecosystems: EcoSim II. *Ecosystems* 3: 70-83.
- Yakubenko V.G., 2002b. Mesoscale eddies and related processes in the northeastern Black Sea. *J. Mar. Syst.*, 32, 71–90.
- Zaitsev, Yu., and V., Mamaev. 1997. *Marine biological diversity in the Black Sea: A study of change and decline*. UN Publications, New York.
- Zavatarelli, M., Baretta, J.W., Baretta-Bekker, J.G. and Pinardi, N., 2000. The dynamics of the Adriatic Sea ecosystem. An idealized model study. *Deep-Sea Research I*, 47:937-970.
- Zavatarelli, M., Raicich, F., Bregant, D., Russo, A., Artegiani, A. 1998. Climatological biogeochemical



PERSEUS Deliverable Nr. 4.4

characteristics of the Adriatic Sea. *Journal of Marine Systems*, 18: 227-263.

